

Minimally-invasive biomarker discovery and functional analyses in Atopic Dermatitis

Dissertation

zur Erlangung des Doktorgrades

der Mathematisch-Naturwissenschaftlichen Fakultät

der Christian-Albrechts-Universität zu Kiel

Vorgelegt von

Melina Fonfara

Kiel, 2024

Erste Gutachterin:

Dr. Hila Emmert

Zweite Gutachterin:

Prof. Dr. Manuela Dittmar

Tag der mündlichen Prüfung:

06.05.2024

Declaration

Herewith, I confirm that apart from my supervisor's guidance and the stated sources and means, the complete submitted thesis is the result of my own work. This thesis has not been submitted to another examining body neither partially nor wholly as part of a doctoral degree. No academic degree has ever been withdrawn. Parts of this thesis have been published as research articles in scientific journals. This thesis has been carried out in strict accordance with the rules of Good Scientific Practice of the German Research Foundation.

Kiel, 11.03.2024

Melina Fonfara

Summary

Atopic dermatitis (AD) is the most common chronic inflammatory skin disease and characterized by a great heterogeneity including eczematous lesions, intense pruritus and a chronic or relapsing disease course. AD pathology involves a dysfunctional epidermal barrier, skin microbiome abnormalities, immune dysregulation and oxidative stress. Despite increasingly complex and high-quality studies and analyses have advanced our understanding of disease pathology and led to the development of accurate targeted therapies, various questions regarding the pathogenesis and the triggering factors contributing to disease manifestation remain unclear.

This thesis demonstrates that keratinocytes present one major source of reactive oxygen species (ROS) underlining their substantial contribution to skin inflammation. Given the understanding that the generation of ROS can trigger pro-inflammatory processes, my thesis further highlights the interplay between oxidative stress in keratinocytes and skin inflammation. I further aimed to assess whether elevated ROS levels and following oxidative stress arise from increased intrinsic ROS production or from impaired antioxidant capacity. Therefore, I performed both, pan and specific, NADPH oxidase (NOX) inhibition and revealed that the inhibition of NOX seems to be effective in lowering oxidative stress and improving survival in AD-model keratinocytes.

Moreover, I have used tape strips, a tool to perform minimally invasive biosampling, from children at high risk for developing AD in order to characterize the pro-inflammatory environment in the epidermis. The analysis revealed that several pro-inflammatory proteins including innate immunity markers but also Th1, Th2, Th17, and Th22 mediators are highly abundant in the *stratum corneum* of children at AD onset or even precede disease manifestation. This study further underlines the feasibility of tape strips for characterization of the inflammatory environment in the skin which would notably improve biosamples quantity which is required for biomarker identification.

In a third and fourth study, 3-dimensional (3D) skin models were applied and refined. These studies demonstrated that keratinocytes secrete pro-inflammatory mediators capable of directly impairing epidermal organization. Additionally, I have proposed that these factors act independently of IL-4/IL-13 signalling, thereby highlighting the involvement of other innate and adaptive immunity players in AD pathology. Furthermore, I have incorporated T cells and *Staphylococcus aureus* into the 3D skin model to better mimicking an *in vivo* scenario. This resulted in improved model complexity that is essential to conduct functional experiments related to AD pathology.

Zusammenfassung

Atopische Dermatitis (AD) ist die häufigste chronisch-entzündliche Hauterkrankung und zeichnet sich durch eine große Heterogenität aus, welche ekzematöse Läsionen, starken Juckreiz und einen chronischen oder schubweisen Krankheitsverlauf umfasst. Die Pathologie der AD umfasst eine gestörte epidermale Barriere, Änderungen des Hautmikrobioms, eine Dysregulation des Immunsystems und erhöhten oxidativen Stress. Obwohl zunehmend komplexe und qualitativ hochwertige Studien und Analysen unser Verständnis der Krankheitspathologie verbessert und zur Entwicklung zielgerichteter Therapien geführt haben, bleiben verschiedene Fragen zur Pathogenese und zu den auslösenden Faktoren, die zur Manifestation der Krankheit beitragen, offen.

In dieser Arbeit wird gezeigt, dass Keratinozyten eine Hauptquelle für reaktive Sauerstoffspezies (ROS) darstellen, was ihren wesentlichen Beitrag zu Hautentzündungen unterstreicht. Da bekannt ist, dass die Bildung von ROS entzündungsfördernde Prozesse auslösen kann, beleuchtet meine Arbeit die Interaktion zwischen oxidativem Stress in Keratinozyten und Entzündung der Haut. Außerdem wurde untersucht, ob erhöhte ROS Werte und der daraus resultierende oxidative Stress auf eine erhöhte intrinsische ROS Produktion oder auf eine beeinträchtigte antioxidative Kapazität zurückzuführen sind. Daher wurden gezielt NADPH-Oxidasen (NOX) inhibiert. Dabei hat sich herausgestellt, dass die Hemmung von NOX den oxidativen Stress zu verringern und das Überleben von Keratinozyten im AD Modell zu verbessern scheint. Zudem habe ich bei Kindern mit hohem Risiko für die Entwicklung einer AD Tape Strips, Klebestreifen zur minimalinvasiven Entnahme von Bioproben, verwendet, um das proinflammatorische Umfeld in der Epidermis zu charakterisieren. Die Analyse ergab, dass mehrere proinflammatorische Proteine, darunter Marker der angeborenen Immunität, aber auch Th1-, Th2-, Th17- und Th22 Marker, im *Stratum corneum* von Kindern zum Zeitpunkt des Ausbruchs der AD oder bereits vor der Manifestation der Krankheit in großer Menge vorhanden sind. Diese Studie unterstreicht die Eignung von Tape Strips für die Verwendung zur Charakterisierung des entzündlichen Milieus in der Haut, wodurch sich die für die Identifizierung von Biomarkern erforderliche Menge an Bioproben deutlich verbessern würde. In einer dritten und vierten Studie wurden 3-dimensionale (3D) Hautmodelle verwendet und verfeinert. Diese Studien zeigten, dass Keratinozyten pro-inflammatorische Proteine abgeben, welche die epidermale Organisation direkt beeinträchtigen können. Außerdem wurde gezeigt, dass diese Faktoren unabhängig des IL-4/IL-13 Signalweges wirken, wodurch die Beteiligung anderer Teile der angeborenen und adaptiven Immunität an der AD-Pathologie hervorgehoben wird. Zudem habe ich T Zellen und *Staphylococcus aureus* in das 3D-Hautmodell integriert, mit dem Ziel, das tatsächliche *in vivo* Szenario besser abzubilden. Dies führte zu einer erhöhten Komplexität des Modells, die für die Durchführung funktioneller Experimente im Zusammenhang mit der AD-Pathologie notwendig ist.

Table of contents

1	Objectives	1
2	Introduction	3
2.1	Atopic Dermatitis	3
2.2	Molecular mechanisms of Atopic Dermatitis	5
2.3	Methods to study Atopic Dermatitis pathology	13
3	Outline of the thesis.....	17
3.1	Summary of article I	18
3.2	Summary of article II	18
3.3	Summary of article III	19
3.4	Summary of article IV	20
4	Methods	21
4.1	Cell Culture	21
4.2	2-dimensional <i>in vitro</i> models	22
4.3	3-dimensional <i>in vitro</i> models	25
4.4	Molecular methods	28
4.5	Skin histology	31
4.6	<i>Ex vivo</i> methods	33
4.7	Cohorts	35
4.8	Statistics.....	36
5	Results	37
5.1	Article I	37
5.2	Article II	47
5.3	Article III	63
5.4	Article IV.....	72
6	General Discussion and Outlook	98
7	References.....	110
8	Acknowledgements	123

List of abbreviations

AD	Atopic dermatitis
AHR	Aryl hydrocarbon receptor
AMP	Antimicrobial peptide
ARNT	AHR nuclear translocator
ASV	Amplicon sequence variant
BCA	Bicinchoninic acid
BSA	Bovine serum albumin
CaCl ₂	Calcium chloride
CCL	Chemokine (C-C motif) ligand
CD	Cluster of differentiation
cDNA	Complementary DNA
CO ₂	Carbon dioxide
CoNS	Coagulase-negative staphylococci
CXCL	Chemokine (C-X-C motif) ligand
Cytb558	Flavocytochrome b 558
DAPI	4',6-diamidino-2-phenylindole
DCF	2',7'-dichlorofluorescein
DCFDA	2', 7', -Dichloridihydrofluorescein-diacetat
DMSO	Dimethyl sulfoxide
DNA	Desoxyribonucleic acid
DPI	Diphenyleneiodonium
Dpl	Dupilumab
DTT	Dithiothreitol
EASI	Eczema area and severity index
ELISA	Enzyme-linked immunosorbent assay
FCS	Fetal calf serum
FLG	Filaggrin
gDNA	Genomic DNA
GWAS	Genome-wide association studies
H&E	Hematoxylin & eosin
H1R	Histamine receptor 1
H ₂ O ₂	Hydrogenperoxide
H4R	Histamine receptor 4
HaCat	Immortalized human keratinocytes
HBSS	Hanks' balanced salt solution
HSE	Full thickness human equivalent

IFN	Interferon
IgE	Immunoglobulin E
IL	Interleukin
IL-4R	Interleukin-4 receptor
iNOS	Inducible nitric oxide synthase
IVL	Involucrin
JAK	Janus kinase
KGM	Keratinocyte growth medium
LOR	Loricrin
MAP	Mitogen-activated protein
NADPH	Nicotinamide adenine dinucleotide phosphate hydrogen
MDA	Malondialdehyde
MFI	Mean fluorescence intensity
MHC	Major histocompatibility complex
MPO	Myeloidperoxidase
mRNA	Messenger ribonucleic acid
NEAA	Nonessential amino acids
NFκB	Nuclear factor kappa-light-chain-enhancer of activated B cells
NHEK	Normal human epiderma keratinocytes
NK cells	Natural killer cells
NO	Nitric oxide
NOS	Nitric oxide synthase
NOX	NADPH oxidase
Nrf2	NF-E2-related factor 2
OS	Oxidative stress
PBMC	Peripheral blood mononuclear cells
PBS	Phosphate buffered saline
PMA	Phorbol 12-myristate 13-acetate
PMSF	Phenylmethysulfonyl fluoride
PON-1	Paraoxonase 1
qPCR	Quantitative polymerase chain reaction
RHE	Reconstructed human epidermis
RIPA	Radioimmunoprecipitation assay buffer
RNA	Ribonucleic acid
ROI	Region of interest
ROS	Reactive oxygen species
RPMI	Roswell Park Memorial Institute

<i>S. aureus</i>	<i>Staphylococcus aureus</i>
<i>S. epidermidis</i>	<i>Staphylococcus epidermidis</i>
SKDM	Supplemented keratinocyte defined medium
STAT	Signal transducer and activator of transcription
TARC	Thymus and activation-regulated chemokine
TBS	Tris-buffered saline
TBS/T	Tris-buffered saline + Tween20
TEWL	Transepidermal water loss
Th	T helper
TNF	Tumor necrosis factor
TSB	Tryptic soy broth
TSLP	Thymic stromal lymphopoietin
UV	Ultraviolet
VEGF	Vascular endothelial growth factor

1 Objectives

Atopic dermatitis (AD) is characterized by persistent inflammation involving a Th2-skewed immune dysregulation coupled with skin barrier disruption. Both features are partly driven by and contribute to generation of reactive oxygen species (ROS) causing direct damage to cellular components of the skin. Despite substantial evidence exists emphasizing the involvement of ROS in AD, comprehensive studies assessing the underlying molecular mechanisms are rare. To better recapitulate AD pathology, monitor treatment responses and identify new potential therapeutic targets, *ex vivo* analyses are essential. However, comprehensive clinical research demands substantial biomaterial, often obtained through invasive methods such as skin punch biopsies. As these procedures present a very invasive tool and due to pain, scarring and risk of infections, many patients reject to donate skin biopsies. This reluctance is even more pronounced in children, where atopic dermatitis is most prevalent. Still, patient biomaterial remains crucial for clinical research, thereby driving the development of minimally invasive biopsampling techniques such as skin tape stripping. Biomarkers and innovative treatment approaches that have been identified require functional characterization and validation in appropriate disease models. Three-dimensional (3D) skin models provide a stratified epidermis, allowing for the evaluation of skin barrier function and cell-cell interactions. Therefore, the objectives of my thesis were as follows:

- **To conduct an initial characterization of the oxidative and inflammatory environment in AD using 2D *in vitro* models.** The oxidative response of keratinocytes towards treatment with cytokines characteristic of AD will be assessed and NADPH oxidase (NOX) inhibitors are systematically tested in keratinocyte monoculture. This aims to emphasize the importance of NOX inhibition in AD treatment strategies.
- **To enhance the molecular analysis of biomaterial obtained through minimally-invasive methods such as skin tape stripping.** This method is then employed to characterize the inflammatory milieu of atopic dermatitis *in vivo*. Protein extraction and respective analysis will be applied to tape strips, enabling the characterization of epidermal protein levels during the initial manifestation of atopic dermatitis in infants.

Objectives

- **To apply and refine 3D skin models and utilize them for the functional validation of research hypotheses.** My experiments concentrate on assessing alterations in skin barrier function and epidermal organization following manipulation and treatment with cytokines, immune cells, cell supernatants, bacteria, or antibodies. Additionally, I develop an immunocompetent 3D skin model incorporating T cells and *Staphylococcus aureus* to elevate model complexity and more accurately mimic atopic dermatitis *in vivo* conditions.

2 Introduction

2.1 Atopic Dermatitis

Atopic dermatitis (AD) is the most common chronic inflammatory skin diseases affecting around 20% of children and 10% of adults in Western countries ¹.

AD is characterized by a great heterogeneity regarding its clinical features. In order to ensure correct diagnosis, the Hanifin and Rajka criteria are most often used. Based on these criteria, AD diagnosis requires presence of essential features like eczematous lesions, intense pruritus and a chronic or relapsing disease course ¹⁻³.

Additional features often observed in AD patients include skin dryness, early disease onset, and a positive family history of AD ⁴. Further assessment of disease severity is required for treatment effectiveness. The eczema area and severity index (EASI) is commonly used in order to define disease severity ⁵. It integrates affected body surface area and intensity of lesions into one score and is used in clinical trials in order to quantify disease improvement and effectiveness of therapies ^{6,7}.

Different comorbidities are frequently observed in AD patients ⁸. Food allergies, allergic rhinitis and asthma are the most common comorbidities ⁹. The manifestation of AD and food allergies in infants followed by a development of allergic asthma and allergic rhinitis later in life is also known as atopic march ¹⁰. Different studies have shown that AD increases the risk of developing the atopic march ¹¹. Frequently observed non-atopic comorbidities include mental health disorders like depression, anxiety and attention-deficit disorder as well as other autoimmune mediated diseases ¹².

The causes for AD manifestation are multifactorial and involve a complex interplay between dysfunctional epidermal barrier, skin microbiome abnormalities including *Staphylococcus aureus* (*S. aureus*) overgrowth together with reduction of resident skin commensals, a type 2 shifted immune dysregulation mediated by the key cytokines IL-4 and IL-13, a genetic susceptibility and several environmental factors presented by the urban-rural gradient, a reduced prevalence in farming households, and low AD prevalence in areas with high humidity, temperature and ultraviolet exposure ¹.

Treatment of AD strongly depends on disease severity ¹³. Whereas mild forms are treated topically with skin moisturizing creams, more severe forms often require additional systemic immunomodulatory therapy ¹⁴. This includes calcineurin inhibitors and immunomodulating biologics like monoclonal antibodies. Calcineurin inhibitors decrease T cell activity via inhibiting

IL-2 synthesis which is required for T cell activation and proliferation ¹⁵. For a long time, immunosuppressant medication, for example the calcineurin inhibitor cyclosporine, was primarily used for severe AD treatment but potential toxic side effects such as hypertension and nephrotoxicity and an increased risk for malignancy only allow short-term use ^{13,16,17}. Since 2017, dupilumab (dpl), a fully monoclonal antibody against the shared α -chain subunit of the IL-4 and IL-13 receptors (IL-4R) has been approved ^{18–20}. The IL-4R complex is a heterodimeric structure composed of a common subunit (IL-4R α). IL-4R α forms a dimer with the γ c chain forming IL-4R type I which binds IL-4. It can further form a second dimer via binding with IL-13R α 1 forming IL-4R II which binds IL-4 and IL-13. Binding of IL-4 or IL-13 to IL-4R leads to phosphorylation and activation of janus kinase (JAK) followed by recruitment of signal transducer and activator of transcription proteins (STAT) leading to transcription of different pro-inflammatory proteins that amplify Th 2 inflammation (**Figure 1**). Dpl blocks IL-4R α and therefore inhibits both, IL-4 and IL-13 signaling ²¹. Due to its specificity, dpl avoids broad immunosuppression and several studies have shown a good response with less side effects ²². Tralokinumab, another fully monoclonal antibody specifically neutralizing IL-13 has also been approved for treatment of moderate to severe AD in adults and was shown to be clinically efficacious ²³.

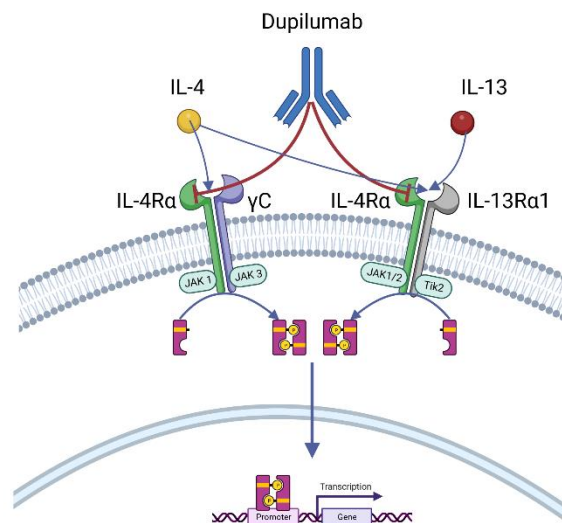


Figure 1: Mode of action of the monoclonal antibody dupilumab. Dupilumab binds to and blocks the IL-4Rα subunit of the IL-4 receptor thereby preventing IL-4 and IL-13 from binding. This prevents the activation and phosphorylation of the JAK/STAT signalling pathway which induces Th2 inflammation. Figure adapted from *Pelaia et al.* (Vaccines 2022). JAK: janus kinase; STAT: signal transducer and activator of transcription. Created with Biorender.com

2.2 Molecular mechanisms of Atopic Dermatitis

Pathology in AD involves a complex interplay between dysfunctional epidermal barrier, skin microbiome abnormalities and immune dysregulation (**Figure 2**). Until now it is not clear which of these mechanisms are consequences of AD and which processes initially cause AD manifestation, as all drivers promote and interact with each other ¹.

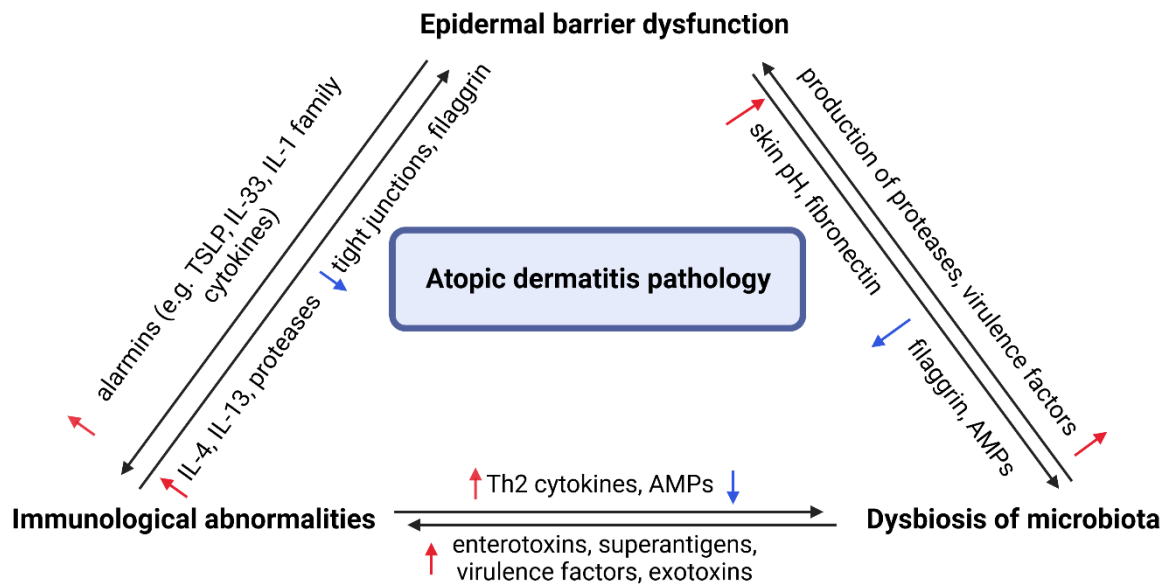


Figure 2: Overview about major molecular mechanisms in atopic dermatitis pathology. Barrier disruption leads to increased alarmin release by keratinocytes which in turn promote Th2 cell activation. Th2 cells themselves and cytokines released by them were shown to impair skin barrier by e.g. affecting tight junctions and barrier proteins such as filaggrin. In addition, immunological changes and epidermal barrier dysfunction both lead to decreased AMP production. This favours, together with other epidermal and immunological changes including increased skin pH, redistribution of fibronectin and increased levels of Th2 cytokines, *S. aureus* colonization. *S. aureus* in turn secretes enterotoxins, superantigens, virulence factors and proteases which all lead to epidermal barrier dysfunction and immunological abnormalities. Figure adapted from Nomura, Honda and Kabashima (International immunology, 2018). AMP = antimicrobial peptides. Created with BioRender.com

2.2.1 Genetic susceptibility

A positive family history of AD is one of the major risk factors for AD manifestation ¹. Different family studies have shown that AD in mother or father is significantly associated with AD manifestation in their offspring with strongest association when both parents reported AD underlining the important role of genetics in AD development ²⁴. These results were further strengthened by several twin studies that have shown a high concordance rate of AD in monozygotic twins ²⁵. Genome wide association studies (GWAS) have identified several risk loci for AD development including genes for type 2 immunity cytokines and structural proteins ^{26,27}. Until

now, the strongest genetic risk factor identified for AD manifestation is a loss of function mutation in the filaggrin (FLG) gene encoding pro-filaggrin leading to a reduction in FLG expression. FLG is a structural protein found in the epidermis and contributes to healthy skin barrier. Reduced FLG expression promotes skin barrier deficiency which presents an important player in AD pathology ²⁸. FLG loss of function mutation leads to a 3-5 times higher risk of developing AD and is carried by 9% of the European population ²⁹.

However, although the estimated heritability for AD is very high (up to 90% in Europeans), there is a missing heritability gap as the sum of the genetic loci identified so far only accounts for less than 20% of heritability. This missing gap could possibly be explained by the high heterogeneity of AD, rare variants, structural variations as well as by epigenetic mechanisms ³⁰.

2.2.2 Skin barrier

The human skin functions as a barrier against the environment and protects from mechanical insults, microorganisms, diffusion of molecules, chemical exposure, ultraviolet (UV) radiation and allergens. Moreover, it helps to prevent the passage of water and electrolytes which is important to protect the body from dehydration ³¹. Healthy skin provides its barrier function mainly through the formation of terminally differentiated keratinocytes. During the differentiation process of keratinocytes, four different layers of the epidermis called *stratum basale*, *stratum spinosum*, *stratum granulosum* and *stratum corneum* are formed with the latter playing a major role in skin barrier formation (**Figure 3**). The *stratum corneum* consists of 15-20 layers of differentiated keratinocytes called corneocytes embedded in a matrix of intercellular lipid lamellae (cholesterol, free fatty acids, ceramides) ³². Corneocytes are surrounded by a corneocyte envelope consisting of structural proteins like loricrin (LOR) and involucrin (IVL) ^{33,34}. FLG, a structural protein which is crucial for skin barrier homeostasis, and also part of the corneocyte envelope, is formed and stored as pro-filaggrin polymers in the granules of the *stratum granulosum* and cleaved and degraded via proteases at the interphase between *stratum granulosum* and *stratum corneum* leading to the formation of FLG monomers ^{28,35}. FLG is needed to maintain physical strength of the *stratum corneum* and to minimize entry of foreign antigens ³. FLG further helps to minimize transepidermal water loss (TEWL) and to maintain an acidic pH in the skin ³⁶. Moreover, at the outer part of the *stratum corneum*, FLG is degraded into amino acids necessary for natural moisturizing factor formation ²⁸. FLG mutations resulting in truncated protein products were shown to be major predisposing factors for AD manifestation ^{29,37}. Truncated FLG proteins or FLG deficiency lead to disorganized keratin filaments,

impaired skin lipid profiles and abnormal bilayer architecture. It was shown that FLG mutations increase skin TEWL and affect skin hydration³⁸. Moreover, studies have revealed that FLG mutations additionally work on immune system as patients with FLG mutations present increased epidermal IL-1 expression compared to those without mutations³⁹.

In addition to the *stratum corneum* and structural proteins, tight junctions present an important part of the skin barrier as they tightly regulate paracellular water and solute transport. Claudin-1 is the most important adhesion protein in tight junctions and reduced claudin-1 expression with consequently tight junction abnormalities have been reported in AD patients⁴⁰.

Antimicrobial peptides like defensins and S100 proteins, an intact skin microbiome and skin-resident immune cells further contribute to a healthy and stable skin barrier³³.

Several studies have highlighted the role of an impaired skin barrier in affected (lesional) and unaffected (non lesional) skin of AD patients³¹. Skin barrier dysfunction is characterized by increased TEWL and skin pH, increased permeability, reduced water redemption and altered lipid composition^{41,42}. Main factors driving skin barrier impairment include decreased levels of structural proteins (epidermal differentiation-related), ceramides, and antimicrobial peptides with concurrent increase of serine protease and disordered tight junctions⁴³. Skin barrier impairment additionally enables pathogens to infiltrate skin promoting inflammatory processes (**Figure 3**).

Studies have shown a tight crosstalk between skin barrier and immune system in AD as immune cells and cytokines can signal on skin barrier protein expression and function leading to increased skin permeability and further amplification of skin inflammation⁴⁴. The main Th2 cytokines IL-4 and IL-13 were shown to decrease LOR, IVL and FLG expression promoting skin barrier impairment and following inflammation⁴⁵.

Another contributor to AD pathogenesis is itch as it promotes scratching leading to skin barrier damage which then promotes cutaneous inflammation⁴⁶. This process is also known as itch-scratch cycle and can be induced by different mediators, called pruritogens (i.e. antigens, interleukins, histamine). The most important pruritogen in AD is histamine which binds to H1R and H4R on sensory neurons leading to their activation. In addition to histamine, type 2 cytokines like IL-4, IL-13 and IL-31 can also directly bind to receptors that lead to stimulation of neurons^{47,48}. Thus, immune function and itch may further impair skin barrier, which in turn leads to scratching and further mechanical weakening of the skin barrier leading to a vicious cycle.

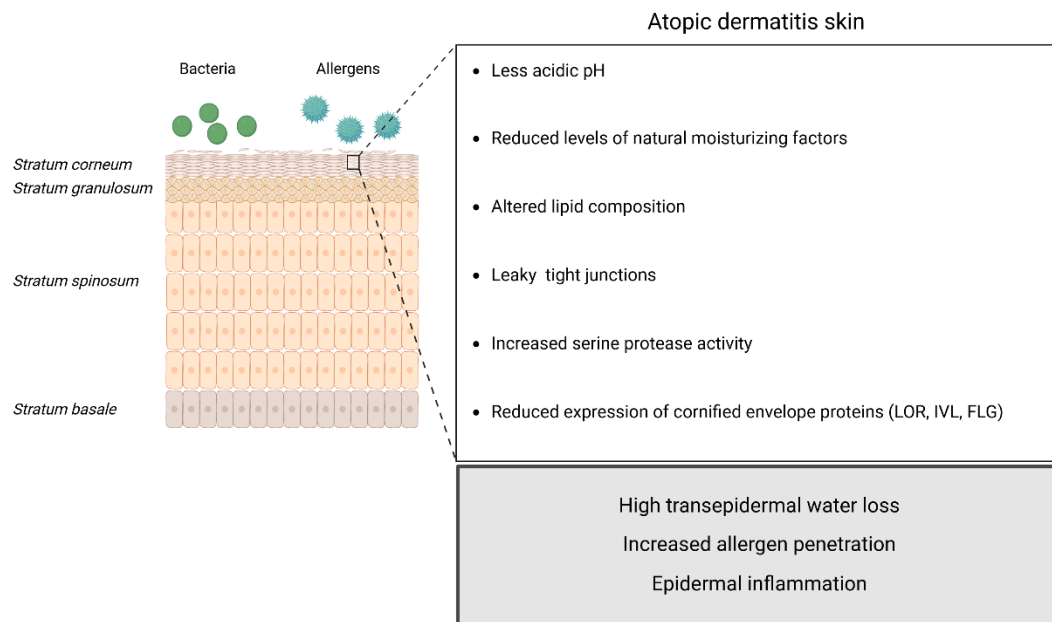


Figure 3: Simplified representation of the human epidermis. Keratinocytes differentiate and form the 4 different layers of the skin (*Stratum basale*, *Stratum spinosum*, *Stratum granulosum*, *Stratum corneum*). Main characteristics of healthy and diseased skin are indicated in the boxes. Several factors such as decreased expression of loricrin, involucrin and filaggrin, reduced levels of natural moisturizing factors, altered lipid composition, and leaky tight junctions contribute to skin barrier deficiency and result in increased transepidermal water loss, penetration of pathogens and allergens and skin inflammation. Figure adapted from *Rerknimitr et al.* (Current Dermatology Reports, 2018). AD: atopic dermatitis; LOR: loricrin; IVL: involucrin; FLG: filaggrin. Created with BioRender.com

2.2.3 Immune system dysregulation and inflammation

A further hallmark of AD is increased activation of Th2 immune response with a cytokine milieu characterized by Th2 cytokines such as IL-4 and IL-13. Due to impaired skin barrier and pathogen infiltration, keratinocytes in AD skin release alarmins (e.g. TARC, TSLP, CCL22; IL-1b, IL-33) that lead to attraction and activation of different immune cells like dendritic cells, innate lymphoid cells and Th2 cells ⁴⁹. It has been postulated that activated Th2 cells release IL-4 and IL-13 that promote IgE class switching in B-cells leading to production of antigen-specific IgE. IgE binds to basophils and mast cells and results in increased release of histamine which promotes itch ⁵⁰. Activated innate lymphoid cells also release IL-13 and IL-5 which amplify type 2 immunity and IgE production ⁵¹. TSLP additionally induces OX40 ligand (OX40L) expression by dendritic cells which binds to OX40L receptor on naïve T cells stimulating IL-4, IL-5 and IL-13 production ⁵².

Both, lesional and non lesional, skin of AD patients is characterized by spongiosis (abnormal accumulation of intercellular fluid) and immune cell infiltration ⁵³.

Acute lesions are characterized by increased levels of Th2 and Th22 (i.e. IL-22, S100A proteins) cytokines which can downregulate terminal differentiation genes and tight junction products promoting skin barrier damage ^{3,54}. Moreover, lesional skin shows dysregulated expression of genes related to keratinocyte activity and T cell infiltration ⁵⁵. Non lesional skin is characterized by type 2 immune response with high levels of innate immunity and angiogenesis markers ⁵⁶. Studies have further shown reduced natural killer cell mediated immunomodulation with decreased concentration and altered composition of peripheral natural killer (NK) blood cells and increased levels of activated NK cells in lesional skin in AD patients ⁵⁷.

2.2.4 Role of the skin microbiome

Skin microbiome dysbiosis presents a further key characteristic in AD pathogenesis. In healthy skin, the skin microbiome is stable and commensal skin microbiota play an important role in maintaining skin homeostasis via protection against pathogens and education of the host immune response ⁵⁸. Skin of AD patients presents several microbial abnormalities and it remains unclear whether these alterations are causative of AD manifestation or a consequence of epidermal alterations and immune dysregulation ⁵⁹. AD skin is characterized by a microbial dysbiosis with reduction of microbial diversity and overrepresentation of the pathogen *Staphylococcus aureus* (*S. aureus*) ⁶⁰. Different studies have shown that *S. aureus* colonization is correlated with disease severity ⁶¹. It is known that an impaired skin barrier is more prone towards *S. aureus* colonization due to increased skin pH and redistribution of fibronectin ^{62,63}, whereas *S. aureus* products themselves can damage skin barrier (e.g. via secretion of ceramidase) and promote skin inflammation ⁶⁴. The observed microbial dysbiosis in AD is further characterized by loss of potential beneficial species ⁶⁵. Coagulase-negative Staphylococci (CoNS) such as *Staphylococcus epidermidis* and *Staphylococcus hominis* were found to produce proteins possessing antimicrobial activity against *S. aureus* but not affecting growth of other commensals ^{66,67}. The relative abundance of CoNS was shown to be reduced in acute and chronic lesional skin compared to non lesional skin ^{41,68}. Moreover, significant differences in alpha- and beta-diversity across AD severity scores have been identified pointing out that bacterial diversity seems to be reduced in more severe AD forms ⁶⁹. Different therapies are available aiming to restore a healthy skin microbiome and reducing overgrowth of *S. aureus* which would in turn promote growth of commensals ⁵⁹.

2.2.5 Reactive oxygen species and the role of oxidative stress in Atopic Dermatitis

Advancing T cell infiltration, cytokine release, *S. aureus* colonization, and skin barrier disruption foster the generation of reactive oxygen species (ROS) in the skin ⁷⁰. ROS are short-lived, reactive oxygen-derived compounds like superoxide and peroxide and can irreversibly alter and destroy the function of other molecules. Examples for induced alterations are lipid peroxidation, protein oxidation and DNA damage ⁷¹. Excessive ROS can lead to a disruption of the balance between oxidants and antioxidants resulting in oxidative stress (OS). In AD, OS amplifies skin inflammation and promotes disease chronicity via different mechanisms. Protein and lipid peroxidation in the *stratum corneum* impair barrier function and OS additionally leads to the dermal expression of IL-6, IL-8, IL-9 and IL-33 that in turn amplify skin inflammation ⁷². Moreover, OS directly acts on keratinocytes via DNA damage and damages cell membrane structures via lipid oxidation leading to spongiosis and a disrupted *stratum corneum* ^{72,73}. So far, different OS markers in AD were identified in serum of AD patients including the Aryl hydrocarbon receptor/AHR translocator (AHR/ARNT) system, NF-E2-related factor 2 (Nrf2), myeloperoxidase (MPO) level and Paraoxonase-1 (PON-1) activity. The AHR/ARNT system is expressed in the skin and induces expression of different structural proteins like FLG, IVL and LOR ^{74,75}. Oxidation metabolites can be quantitatively measured as several markers for different ROS-induced alterations are available. Serum malondialdehyde (MDA) indicates lipid oxidation, urine or serum nitrate shows nitric oxide levels and urinary 8-hydroxy-2'-deoxyguanosine (8OHdG) is measured to maintain information about DNA oxidation. AD studies have shown increased levels of systemic markers of OS like 8OHdG in AD patients with a significant positive correlation between 8OHdG excretion and AD severity suggesting that impaired homeostasis of oxygen/nitrogen radicals and enhanced OS are involved in the pathophysiology of AD ⁷⁴. Additionally, increased MDA levels and less blood antioxidant capacity were observed in children with AD compared to a control group ⁷⁶.

Acute ROS production is regulated by nicotinamide adenine dinucleotide phosphate hydrogen (NADPH) oxidases (NOX) leading to the elimination of microorganisms in macrophages and neutrophils. Six homologs of the cytochrome subunit of the phagocyte NADPH oxidase (NOX2) exist and constitute the NOX family of NADPH oxidases which play an important role in anti-microbial defense and stress signaling (NOX1-5, Duox1 + 2) ⁷⁷. They consist of different subunits that interact and form an active enzyme complex which is responsible for the production of superoxide. The first characterized and best described isoform of NOX is NOX2 which consists of cytosolic and membrane components. The two integral membrane proteins gp91phox and p22phox comprise the large heterodimeric subunit flavocytochrome b 558 (cytb558). Under unstimulated conditions the multidomain regulatory subunits p40phox, p47phox and p67phox are present in the cytosol as a complex, but upon stimulation p47phox gets

phosphorylated and the entire complex translocates to the membrane and associates with cytb558 forming the active oxidase ⁷⁸. The biological function of NADPH oxidases is the generation of ROS via the oxidative burst. The active oxidase transfers electrons from the substrate to oxygen through a prosthetic and a heme group which carries oxygen leading to its reduction into superoxide and other downstream ROS. Via the generation of ROS, NOX play a key role in normal cellular homeostasis by mediating diverse functions like host defense and inflammation, posttranslational processing of proteins, cellular signaling and regulation of gene expression. However, NADPH oxidases also contribute to a wide range of diseases as a deficiency can lead to immunosuppression and increased activity will lead to excess ROS which are associated with cardiovascular changes, neurodegeneration and inflammatory skin diseases ⁷⁹. The subcellular distribution of NOX varies among different cell types and localization ranges from plasma membrane to intracellular compartments ⁷⁸. In keratinocytes, NOX1, NOX4 and NOX2 are present and generate ROS in response to ultraviolet light ⁷⁹. NOX4 is the major producer of ROS leading to caspase 1 induction and IL-1 β production. Moreover, NOX4 induces the formation of the inflammasome resulting in inflammation demonstrating the involvement of NOX derived ROS in the pathogenesis of inflammatory diseases. The production of ROS can be blocked by NADPH oxidase inhibitors. Several inhibitors are available blocking signal transduction, NOX assembly or work via Rac inhibition ⁷⁸. NOX inhibitors provide promising treatment options for diseases associated with OS. Several inhibitors are available, however, most of them target upstream signaling pathways or function as ROS scavengers and only a few target specific inhibitors exist. In most publications, Diphenyleneiodonium (DPI) was assessed, which presents a nonspecific flavin binder abstracting an electron from an electron transporter forming a radical which then acts as an inhibitor of the respective electron transporter through a covalent binding step ^{79–81}. In addition, novel specific NOX1 and NOX1/4 inhibitors are available. The specific inhibition of respective NOX would lower off target effects and would make the treatment more effective ⁸².

2.3 Methods to study Atopic Dermatitis pathology

2.3.1 Minimally invasive biomarker discovery

In order to monitor treatments, identify new potential disease biomarkers or to improve disease diagnosis, skin biosamples are needed. Currently, biopsies present the gold standard for skin biosampling and allow for several -omic analyses⁸³. However, biopsies are invasive and painful, cause scars and therefore many patients do not consent to give biopsies. Especially in young children there is limited access to biopsies and substitution with biosamples obtained from adults is not possible as childhood AD presents a different disease subtype⁸⁴. Therefore, there is need for minimally invasive biosampling methods that would increase biosample quantity or even replace skin biopsies. Tape strips are plastic strips with one adhesive side that are applied to the skin surface. When removing the tape strip, one epidermal layer is removed from the *stratum corneum*^{85–87}. Sequential tape stripping removes several layers of *stratum corneum* that can be used for transcriptomic and proteomic analyses⁸⁸. The advantage of the method is that tape stripping is only minimally invasive and does not lead to scarring. Several dermatological diseases can be assessed using tape strips including atopic dermatitis, psoriasis, melanoma, and different carcinomas⁸⁸.

Especially biosampling in infant AD studies benefits from the use of tape strips and they could additionally help to provide a minimally invasive tool for prediction of AD development^{89–91}. Researchers are currently working on the establishment of pipelines and methods for proteomic and transcriptomic profiling by using tape strips. Different components can be extracted from tape strips including soluble proteins, FLG breakdown products and RNA^{83,92–95}. By using tape strips, researchers have identified elevated expression in nitric oxide synthase (NOS) 2 and inducible NOS (iNOS) from lesional psoriasis and could therefore differentiate psoriasis from AD with 100% accuracy⁹⁶. Moreover, IL-36 γ expression could differentiate psoriasis from AD with a sensitivity of 94% and specificity of 100%⁹⁷. Studies assessing correlation of gene expression between biopsies and tape strips have shown that terminal differentiation gene expression in tape strips and biopsies is positively correlated⁸³. Currently, there is rising interest in further establishing and improving molecular analyses from tape strips as the use of minimally invasive methods for biosampling could lead to a higher likelihood of biomaterial being donated willingly.

2.3.2 *In vitro* models for functional Atopic Dermatitis analyses

In order to mechanistically study AD pathology, perform downstream analyses, and characterize potential new disease biomarkers, different AD models are available. Mouse models and *in vitro* models such as two-dimensional (2D) cell culture and three-dimensional (3D) skin models present the most common models in AD research (**Figure 4**).

For translational research, *in vivo* mouse models are frequently utilized. Advantages include low costs, easy handling and the presence of several anatomical, physiological and immunological similarities. However, different studies have shown major differences between mouse and human skin⁹⁸. Human skin is thicker, made by more keratinocyte layers, and contains less hair follicles. Importantly, mouse skin shows decreased barrier function compared to human skin and there is only 30% identity overlap between human and mouse skin associated genes⁹⁹. Moreover, different T cell populations and differences in presence and absence of antimicrobial peptides can be observed between mouse and human skin^{100,101}. For these reasons, mice models are often not suitable to analyse the causes underlying AD pathology and results from mice studies therefore often fail to be translatable to human studies⁹⁸.

2D culture systems present the simplest available *in vitro* models. Skin cells such as fibroblasts and keratinocytes are cultivated as one single layer without contact to other cells. They are straight forward and easy to reproduce. In AD research, disease models can be obtained via treatment of keratinocytes with Th2 cytokines or via isolation and cultivation of keratinocytes from AD patients^{102,103}. However, they do not consider complex structures and skin layer stratification. In addition, skin barrier analyses cannot be performed with two-dimensional culture systems as they lack stratified keratinocytes resembling a functional skin barrier.

3D skin models grown from human keratinocytes offer a human *in vitro* system for cells to grow and interact with their environment¹⁰⁴. 3D models are physiologically more relevant compared to 2D cell culture as they allow researchers to monitor skin viability, morphology, proliferation, differentiation and response to stimuli^{98,105–107}. Models presenting proper stratification and skin barrier function are valuable to study different treatments or effects of different cytokines on disease pathogenesis and skin barrier^{108,109}. In skin research the two most common 3D skin models include reconstructed human epidermis (RHE) and full-thickness human skin equivalent (HSE). RHEs are composed of keratinocytes that are grown on polycarbonate filters at an air-liquid interface whereas HSEs are keratinocytes that are grown on a dermis-like matrix that is made by fibroblasts seeded in extracellular matrix components. Both models mimic human epidermis in regard to differentiation, histology and barrier function whereas HSEs present even more complex models as they additionally mimic human dermis^{105,106}. Further important advantages of 3D skin models include greater stability as well as a longer lifespan compared

to 2D models. However, they are technically challenging, time-consuming and show low-reproducibility compared to 2D models. 3D skin models can be cultured for up to 4 weeks and are therefore suited for long term studies and survival analyses ^{107,110–112}.

Functional 3D models mimicking AD skin can be produced via incubation with interleukin cocktails ^{113–115}, use of patient-derived keratinocytes ¹¹⁵, introduction of immune cells ¹¹⁶ or gene silencing in keratinocytes ^{117,118}. AD like phenotypes are characterized by spongiosis and alteration of expression and localization of skin differentiation and barrier markers ^{37,108,119,120}. Few researchers produce 3D skin models containing lymphocytes which improves the comparability to *in vivo* situations. Cultivation of HaCat cells together with lymphocytes in a 3D skin model caused AD like features including spongiosis, keratinocyte apoptosis and elevated levels of pro-inflammatory cytokines ¹¹⁶. Other major features of AD pathology like microbiome dysbiosis and FLG mutation can be additionally included into 3D skin models ^{37,118,121–123}. Studies assessing skin microbiome in 3D skin models have shown that reduced FLG expression leads to increased epidermal *S. aureus* colonization ¹²². Moreover, 3D skin models offer the opportunity to significantly improve personalized medicine. Via construction of 3D skin models from patient-derived keratinocytes, including patient-derived lymphocytes and usage of skin rinses for the transfer of skin microbiota patient-specific models could be built ⁹⁸.

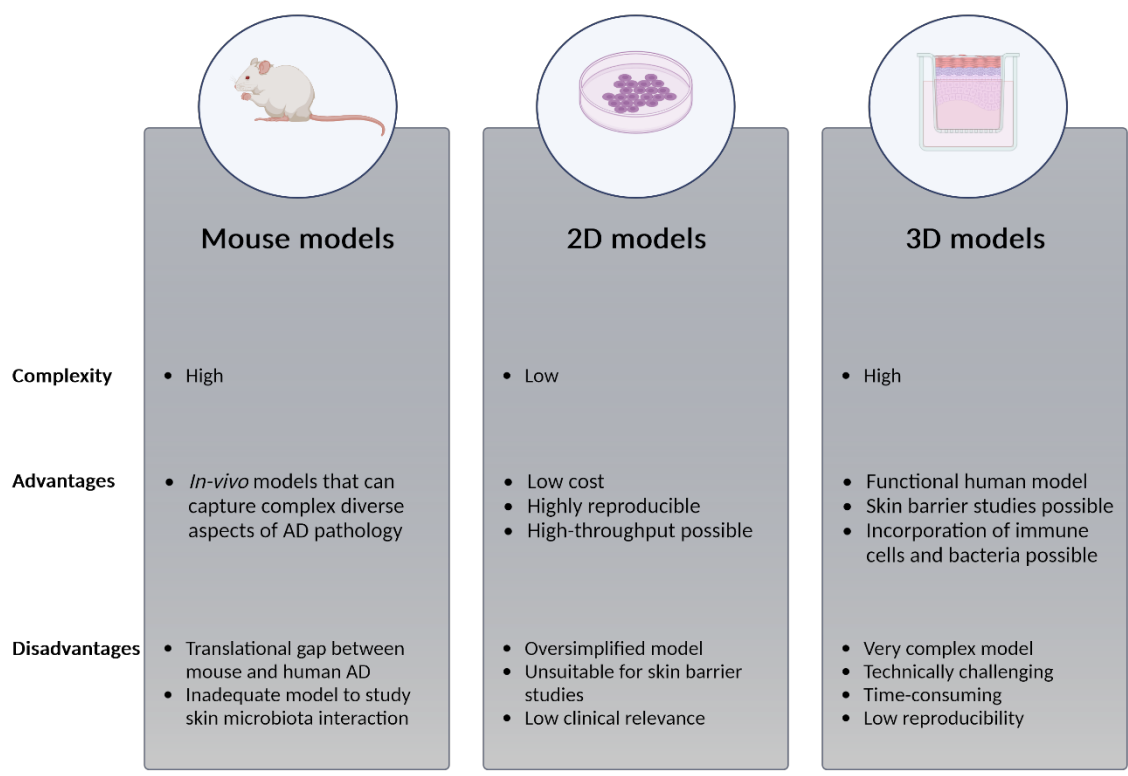


Figure 4: Overview about major models used in atopic dermatitis research. Model complexity and major advantages and disadvantages are listed. Created with BioRender.com

3 Outline of the thesis

In advancing atopic dermatitis research and therapy, the identification of disease and treatment biomarkers have become crucial. These biomarkers are required for developing novel treatment methodologies, monitoring ongoing therapies, and potentially predicting and preventing disease manifestation. Yet, the discovery of potential new biomarkers is constrained by the limitations of obtaining sufficient amounts of patient biomaterial, primarily because of the invasiveness associated with traditional skin biosampling methods. Furthermore, a comprehensive characterization of the pathological milieu in atopic dermatitis is important to enhance our understanding of the disease and concurrently, the development and refinement of suitable disease models are essential for researchers to test and validate hypothesized concepts. To address these objectives, I conducted an in-depth characterization of the oxidative and inflammatory environment in atopic dermatitis skin *in vitro* (detailed in chapters 5.1 and 5.3). Additionally, I focused on applying molecular analyses using minimally invasive biosampling methods, aiming to improve biosampling practices in atopic dermatitis research. This method was applied to samples from a prospective study involving infants at high risk for developing atopic dermatitis (chapter 5.2) resulting in the characterisation of the epidermal inflammatory environment in children during the initial manifestation of disease.

Finally, I have used and enhanced 3D skin models mimicking atopic dermatitis (chapter 5.3 and 5.4). These models were employed to illustrate the impact of molecular factors derived from keratinocytes and fibroblasts on the skin barrier and epidermal organization (highlighted in chapter 5.3). Additionally, T cells and *Staphylococcus aureus* were incorporated into 3D skin equivalents to better mimic the holistic *in vivo* environment and therefore improving model complexity (chapter 5.4).

Cumulatively, the findings of this thesis aim to enhance the process of discovering and validating biomarkers in atopic dermatitis. The overarching objective is to unravel the heterogeneity of the disease, to pinpoint early onset molecular risk predictors and to identify novel therapeutic targets to enhance future medical treatment options.

3.1 Summary of article I

H. Emmert, **M. Fonfara**, E. Rodriguez, S. Weidinger: „NADPH oxidase inhibition rescues keratinocytes from elevated oxidative stress in a 2D Atopic Dermatitis- and Psoriasis-model” in: *Experimental Dermatology* (2020). DOI: 10.1111/exd.14148

In this publication we established *in vitro* models of atopic dermatitis and psoriasis using keratinocyte monoculture. We characterized these models in terms of their oxidative stress state. Our findings reveal elevated intracellular reactive oxygen species (ROS) levels and increased DNA damage in the disease model keratinocytes following exposure to H₂O₂ compared to control cells. Notably, inhibiting NADPH oxidase (NOX), particularly NOX1, mitigated intracellular ROS levels, reduced DNA damage and improved cell viability presented by enhanced cell survival and abrogation of stress-related signaling cascades. We therefore highlight the involvement of NOX in atopic dermatitis and psoriasis pathogenesis.

3.2 Summary of article II

M. Fonfara, J. Hartmann, D. Stölzl, N. Sander, I. Harder, E. Rodriguez, M. Hübenthal, C. Mazur, S. Kerzel, M. Kabesch, J. Schmitt, H. Emmert, I. Suhrkamp, S. Weidinger: “Stratum corneum and microbial biomarkers precede and characterize childhood atopic dermatitis” in: *Journal of the European Academy of Dermatology and Venereology* (2024). DOI: 10.1111/jdv.19932

We here used minimally invasive methods to analyse epidermal biomarker levels and microbial profiles in a cohort of 50 neonates at high risk for developing AD. By performing protein extraction from tape strips, we could show that children with later AD have increased levels of epidermal IL-1Ra, TNF β , IL-8, IL-18, IL-22, CCL2, TARC, TSLP, and VEGFa levels prior to disease manifestation. Regarding the microbiome, our analyses revealed that children with later AD displayed a delayed maturation and differentially composed skin microbiome prior to AD manifestation. At time of disease manifestation, levels of multiple Th2, Th17/22 and Th1-associated proteins as well as innate immunity markers were elevated and abundances of commensal *Streptococcus* species were reduced in favour of *Staphylococcus epidermidis*. Our results therefore indicate that elevations of different pro-inflammatory *stratum corneum* biomarkers and alterations of the skin microbiome can precede childhood AD and characterize disease at its onset.

3.3 Summary of article III

M. Fonfara, C. Brodersen, I. Suhrkamp, E. Rodriguez, S. Weidinger, H. Emmert: „Effects of cultured keratinocyte- and fibroblast- derived mediators on three-dimensional skin models”. In: *Clinical & Experimental Allergy* (2023). DOI: 10.1111/cea.14420

In this work we aimed to investigate the effects of fibroblasts and keratinocytes on 3D skin models and their role in mediating skin barrier disruption. Dermal fibroblast and keratinocyte cell supernatants were analyzed regarding their cytokine profile using multiplex ELISA and the impact of keratinocyte- and fibroblast-derived cytokines on skin barrier was evaluated using 3D skin models. Our data reveals the pro-inflammatory potential of keratinocyte-derived mediators on 3D skin models resulting in skin barrier disruption comparable to established AD-skin models that can only partly be reverted by IL-4R α blocking.

We conclude that especially keratinocytes play an important role in AD pathogenesis via increased secretion of pro-inflammatory cytokines in response to external stimuli as they secrete sufficient pro-inflammatory factors to cause disease-associated patterns in 3D skin models. Moreover, we highlight the role of Th2-independent factors such as IL-1 family cytokines in AD pathology.

3.4 Summary of article IV

I. Suhrkamp, **M. Fonfara**, Magdalena, J. Hartmann, E. Rodriguez, H. Emmert, S. Weidinger:

„3D skin model to study crosstalk between T cells and *Staphylococcus aureus* in atopic dermatitis *in vitro*” (in preparation for submission)

In this study we fabricated novel *in vitro* 3D skin models including Th2 cells and topical *S. aureus* cultivation. We have assessed changes in skin barrier integrity, inflammatory environment and topical *S. aureus* load of our 3D skin models after cultivation with different T cell populations and have used the monoclonal anti IL-4R α antibody dupilumab to validate our model. We could show that integration of Th2 cells into 3D skin models leads to impairment of epidermal barrier structure and increased topical *S. aureus* growth. Moreover, treatment of immunocompetent 3D skin models with dupilumab abolished Th2 induced *S. aureus* load and additionally improved epidermal organisation. 3D skin models stimulated only with key AD cytokines IL-4 and IL-13 therefore omitting immune cells could not display significant increased *S. aureus* growth when compared to control 3D skin models. Further, dupilumab failed to rescue *S. aureus* treatment in simple 3D skin models. We conclude that immunocompetent 3D skin models are required to adequately capture physiological *S. aureus* growth *in vitro* and have provided a robust platform for *in vitro* AD research.

4 Methods

4.1 Cell Culture

4.1.1 Cultivation of keratinocytes and fibroblasts

Primary normal human keratinocytes (NHEKs) (PromoCell, Lot Number 470Z031 + 470Z001) were cultured in Keratinocyte Growth Medium (KGM) (PromoCell) + supplements + CaCl_2 at 37°C and 5% CO_2 . For 3D skin models, cells were used at passage 5 and for 2D cell culture cells were used at passage 4-10. Neonatal human dermal fibroblasts (fibroblasts) (Invitrogen, Thermo Fisher Scientific, Lot Number 1998537) were cultured in DMEM (Lonza, Köln, Germany) + 10% fetal calf serum (FCS) (Gibco) and 1% L-Glutamine. Cells were used at passages 4-30.

4.1.2 Isolation and cultivation of T cells

Peripheral blood was taken by venepuncture from healthy volunteers. Informed consent was obtained. Peripheral mononuclear blood cells (PBMCs) were isolated from peripheral blood diluted 1:3 in phosphate buffered saline (PBS) (Life technologies) by a Polysucrose 400 gradient. First, PBMCs were incubated with FITC-conjugated anti-CD45RO antibodies (Bio-Legend), and memory T cells were removed from the PBMC population by means of magnetic isolation using microbead-coupled anti-FITC antibodies (Miltenyi Biotec). Naïve T helper cells were isolated by positive magnetic selection using anti-CD4 microbeads (Miltenyi Biotec). Purity of naïve T helper cells was confirmed by flow cytometry. Naïve T cells with a purity of >90% were used for the experiments.

$0,5 \times 10^6$ cells/ml were seeded in Roswell Park Memorial Institute Medium (RPMI) (Gibco) + 10% FCS (Gibco) + non-essential amino acids solution (NEAA) (Thermo Fisher Scientific) + 55 μM β -mercaptoethanol in a 24-well plate. T cell were pan-stimulated with 2 $\mu\text{g/ml}$ anti-CD3 (Miltenyi Biotec), 0.5 $\mu\text{g/ml}$ anti-CD28 (Miltenyi Biotec), and 5ng/ml IL-2 (Miltenyi Biotec) for 7 days in a 5% CO_2 incubator at 37°C.

4.1.3 Cultivation of *Staphylococcus aureus*

Staphylococcus aureus SA 8325-4 was used. Bacteria were grown on blood agar plates for 24 h and then inoculated into tryptic soy broth (TSB) medium. Bacteria were grown for further 12 h, transferred into new TSB medium and grown again for 3 h to reach exponential growth.

4.2 2-dimensional *in vitro* models

4.2.1 Induction of 2D AD and PSO cell culture models

In order to obtain 2D AD cell culture models, NHEKs and fibroblasts were grown until 80% confluency and stimulated with cytokines known to be involved in respective disease pathology (AD: 40ng/ml IL-22, 40ng/ml IL-4, 40ng/ml IL-13 and 10ng/ml TNF α (all Peprotech), PSO: 40ng/ml IL-22, 40ng/ml IL-17a and 10ng/ml TNF α (all Peprotech)) for 24 h.

4.2.2 Inhibition of NADPH oxidases

Inhibition of NADPH oxidases was performed as previously reported ¹²⁴. In experiments where diphenyleneiodonium (DPI) was used, DPI was added at a final concentration of 10 μ mol/L for 24 h (Santa Cruz sc-202584) prior to hydrogen peroxide (H₂O₂) treatment. In experiments where NOX1 inhibitor (Nox1i) was used, ML171 was added at a final concentration of 10 μ mol/L for 24 h (ML171-CAS 6631-94-3-Calbiochem) prior to H₂O₂ treatment, and in experiments where NOX1/4 inhibitor (Nox1/4i) was used, GKT136901 was added at a final concentration of 10 μ mol/L for 24 h (GKT136901-CAS 955272-06-7-Calbiochem) prior to H₂O₂ treatment. All inhibitors were dissolved in dimethylsulfoxide (DMSO). Control cells were treated accordingly with 10 μ mol/L DMSO.

4.2.3 Induction of oxidative stress

Induction of oxidative stress was performed as previously reported ¹²⁴. To induce oxidative stress, cells were treated with H₂O₂ (Merck). For H₂O₂ treatment, media were replaced with freshly prepared media containing 250 μ mol/L H₂O₂. In control cells, the media were switched

to fresh media without H₂O₂. For 2',7'-dichlorofluorescein (DCF) assays, H₂O₂ was added for 10 min, and for immunofluorescence and Western blotting, H₂O₂ was added for 1 h.

4.2.4 DCFDA assay

Intracellular ROS levels were measured using the 2', 7', -Dichloridihydrofluorescein-diacetat (DCFDA) assay (Abcam) according to the manufacturer's instructions. Briefly, cells were seeded in a 96-well plate until 80% confluency. Cells were incubated with 10µmol/L 2',7'-dichlorofluorescein (DCF) and then washed twice. Oxidative stress was induced by treatment of cells with 250µmol/L H₂O₂. Cells were washed twice with PBS, and intracellular ROS levels were detected using a Tecan Reader (TECAN).

4.2.5 Immunofluorescence

Immunofluorescence was performed as previously reported¹²⁵. Cells grown on coverslips were fixed with 3.7% paraformaldehyde solution (PFA) for 30 min and washed three times with PBS. To permeabilize the cells, a 0.1% Triton X-100 in PBS (Life technologies) solution was added for 15 min and followed by 30 min of blocking with blocking solution (1% BSA in combination with 10% goat serum in PBS). The incubation with primary antibodies was performed at room temperature for 1 h in blocking buffer. All primary antibodies were used at a 1:200 final concentration. Cells were washed twice with PBS and incubated with the secondary antibodies at a 1:400 concentration for 90 min at room temperature in blocking buffer. After a final washing step with PBS, mounting medium with DAPI was added to the cells. Images were captured using a Zeiss microscope (serial number: 551 095) using a 40-x or 63-x objective. For each biological replicate, at least three images were taken and a total of at least 30 cells each per condition were analysed. For quantification of pH2AX, cell nuclei were manually selected via the DAPI staining in ImageJ to create a mask. The mask was then used to measure fluorescence intensity of both the DAPI and the 488 channels. pH2AX intensity was normalized to the DAPI signal for each image. For fluorescence quantification of NOX1, NOX4 and p22phox, the fluorescence intensity of the total 488 channel signal per image normalized to a blank region of interest (ROI) was measured and then normalized to the total DAPI channel signal normalized to a blank ROI. Antibodies and working concentrations are presented in **Table 2**.

4.2.6 Cell type specific secretion of cytokines

NHEKs and fibroblasts were grown until 80% confluency. An AD specific stimulation was performed using 40ng/ml IL-22, 40ng/ml IL-4, 40ng/ml IL-13 and 10ng/ml TNF α (all Peprotech) for 24 h. After stimulation, cells were washed twice with PBS (Life technologies) and serum-free keratinocyte differentiation medium was added for one hour (**Figure 5**). Afterwards, cell supernatants were collected and stored at -20°C until used for further experiments.

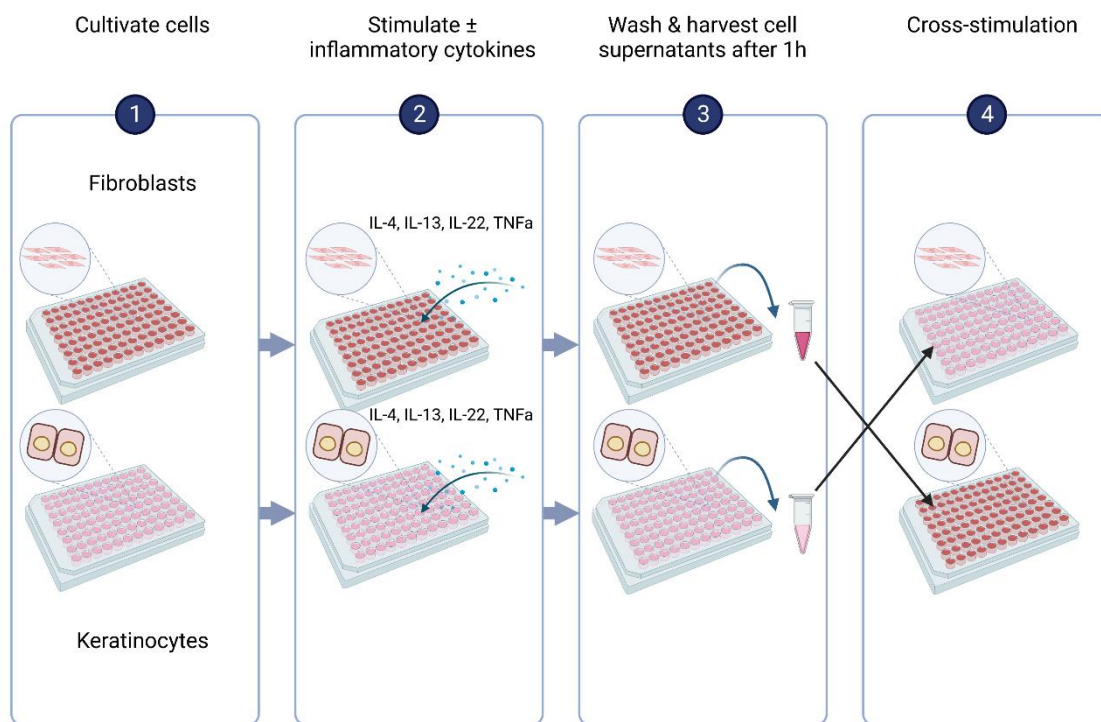


Figure 5: Experimental setup of crosstalk experiments. Keratinocytes or fibroblasts were seeded into 96-well plates and grown until 80% confluency. Afterwards, cells were stimulated with or without pro-inflammatory cytokines (TNF α , IL-4, IL-13, IL-22) for 24 h. After 24 h, the supernatants were collected and transferred to the respective other, untreated cell type. Created with BioRender.com

4.3 3-dimensional *in vitro* models

4.3.1 *Fabrication of 3D in vitro models*

Human 3-dimensional skin models were generated using a fibroblasts-collagen matrix seeded with 0.5×10^6 keratinocytes. The protocol was adapted from Mildner et al ¹¹⁷. Briefly, 0.5×10^6 fibroblasts in 250 μ l FCS were mixed with 2.5ml of 0.4% collagen G type I (Biochrom) mixed with Hank's Balanced Salt Solution (HBSS 10x, Gibco) and seeded onto filter inserts (3 μ m pore size, BD Bioscience) integrated into a 6 well deep well cell culture plate (BD Bio Coat, Corning, Wiesbaden). After 2 h at 37°C w/o CO₂ the collagen solution was gelled and KGM medium with supplements was added to the surrounding external well and to the insert containing the gelled collagen matrix. After overnight incubation at 37°C and 5% CO₂, 0.5×10^6 keratinocytes were seeded on top of the matrix. After 48 h, the keratinocyte layer was raised to an air-liquid interface by removing the apical media which initiates skin growth and differentiation (day 1). Skin models were grown for 7 days in supplemented keratinocyte defined medium (SKDM) consisting of KGM + 0.125ng/ml epidermal growth factor (recombinant human) + 5 μ g/ml insulin + 0.39 μ g/ml hydrocortisone + 10 μ g/ml transferrin (recombinant human) + 0.06mM CaCl₂ supplemented with 1.3mM calcium, 50 μ g/ml ascorbic acid (Sigma-Aldrich) and 0.1% bovine serum albumin (fatty acid-free, Roth). Medium was changed every second day. After 10 days biosampling was performed in order to conduct a multi-parameter readout analysis. Punch biopsies for total RNA isolation, histological analysis (H&E staining, immunohistochemistry) and microbial DNA isolation and basolateral media were collected (**Figure 6**).

4.3.2 *Stimulation with cell supernatants, cytokines, and antibodies*

1.5ml cell supernatants obtained from 2D cell culture were added to 3D skin for 48 h after 5 days of growth. In order to fabricate AD 3D skin models, the two Th2 cytokines IL-4 and IL-13 were added to the medium of 3D skin models after 5 days of growth for 48 h in a concentration of 5ng/ μ l and 13ng/ μ l respectively.

4.3.3 Immunocompetent 3D skin models

Freshly isolated CD4⁺ T cells were incubated for one week either with 2µg/ml anti-CD3 (Miltenyi Biotec), 0.5µg/ml anti-CD28 (Miltenyi Biotec), and 5ng/ml IL-2 (Miltenyi Biotec) (referred to as pan T cells) or additionally with 3µg/ml anti-IFN-γ and 20ng/ml IL-4 (referred to as Th2 cells). After 7 days of incubation, CD4⁺ T cells were activated with 10ng/ml phorbol 12-myristate 13-acetate (PMA) and 1ng/ml ionomycin for 2 h. Cells were collected and washed with PBS twice. 250.000 cells were pipetted into the trans well under the 3D skin equivalents (day 8). 3D skin equivalents were incubated together with CD4⁺ T cells for another 48 h (**Figure 6**).

4.3.4 Cutaneous cultivation with bacteria

Bacteria grown in TSB medium were adjusted to an optical density (OD) 600nm of 0.25 in TSB medium. 20µl of bacteria solution was added to filter paper (diameter: 8mm). Filter paper soaked with bacteria solution was administered to 3D skin equivalents for 1 h (at day 9) in order to allow bacteria to settle down on 3D skin equivalents (**Figure 6**). Filter paper was then removed and bacteria were grown on the skin for 24 h. For control conditions, 3D skin equivalents were treated with filter paper + 20µl TSB medium for 1 h.

4.3.5 Treatment with antibodies

Dupilumab (Dupixent, Sanofi) was added to media of 3D skin models at day 5 for 48 h in a concentration of 1mg/ml.

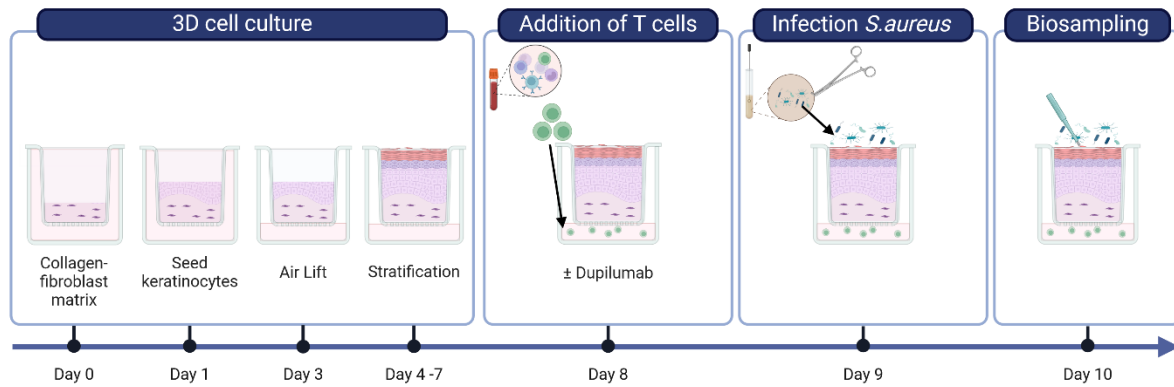


Figure 6: Workflow of 3-dimensional skin models. Keratinocytes were seeded on a collagen-fibroblasts matrix. Apical media was removed in order to initiate skin differentiation (air lift). 3D skin models were then grown for a total of 7 days (day 4 – day 10). Different treatments or manipulation was performed 48 h or 24 h prior to biosampling. Biosampling included collection of different skin punch biopsies for RNA isolation, bacterial DNA isolation, histology as well as collection of basal media for analysis of inflammatory milieu. Created with BioRender.com

4.4 Molecular methods

4.4.1 Protein extraction

For protein extraction for following western blot analysis using WES system, NHEKs were cultivated in 10cm cell culture dish. Induction of AD- and PSO-like cell culture and H₂O₂ treatment was performed as previously described. After incubation, media was removed and cells were washed twice using PBS. Cells were then removed from the culture dish using a cell scraper. The cell suspension was centrifuged at 1000xg at 4°C for 5 min. Supernatant was removed and cells were lysed using 100µl radioimmunoprecipitation assay buffer (RIPA) buffer + phenylmethylsulfonyl fluoride (PMSF). Cells + lysis buffer were kept on ice for 20 min. The lysate was then centrifuged at 14.000xg at 4°C for 20 min. Lysate was analysed using western blot.

4.4.2 Pierce™ 660nm protein assay

Assay was performed according to the manufacturer's instructions (ThermoFisher Scientific). Briefly, 150µl protein assay reagent and 10µl of each replicate and standard was added into a microplate well. The plate was then shaken at medium speed for 1 min and incubated at room temperature for 5 min. After 5 min absorbance of standards and samples was measured at 660nm. Background corrected absorbance of standards was plotted against the corresponding concentration in µg/ml and the resulting standard curve was used to calculate unknown protein concentration of samples.

4.4.3 Western Blot

Western Blotting was performed using WES™ (Bio-technique) according to the manufacturer's instructions. In brief, 5x fluorescent master mix was combined with 20µl dithiothreitol (DTT) solution. Chemiluminescence mix was prepared by mixing luminol-S and peroxidase in equal parts. Proteins were combined with the fluorescent master mix and filled into lanes of the WES™ plate. All proteins and antibodies were used in a concentration of 0.8mg/ml. Antibodies used for western blotting are shown in **Table 2**.

4.4.4 Enzyme-linked immunosorbent assay (ELISA)

For quantitative analysis of selected soluble proteins in cell supernatants, human IL-4 and IL-13 DuoSet ELISA (Bio-techne) was used according to the manufacture's instruction. Background corrected absorbance of standards was plotted against the corresponding concentration in $\mu\text{g/ml}$ using a four-parameter logistic (4-PL) curve fit and the resulting standard curve was used to calculate unknown protein concentration of samples

4.4.5 Multiplex ELISA

Cell supernatants and media of 3D skin models were analysed via multiplex ELISA (Luminex 200). Customized assays targeting proteins involved in innate and adaptive immune response as well as keratinocyte signalling was performed according to the manufacturer's instructions (ThermoFisher Scientific). Standard curves for each of the cytokines was used on each plate. Fluorescence was detected as background corrected median fluorescence intensity without standardization (net MFI) or as raw median fluorescence intensity (MFI) without standardization (indicated in respective figure legends).

Targeted proteins included: IL-1Ra, IL-1 α , IL-1 β , IL-6, IL-8, IL-16, IL-17a, IL-18, IL-22, IL-23, IL-31, CCL2/MCP-1, CCL13/MCP-4, CCL17/TARC, CCL22/MDC, CXCL10/IP-10, IFN- γ , TNF α , TNF β , VEGF α , TSLP, IL4 and IL-13.

4.4.6 RNA isolation

RNA isolation was performed as previously reported¹²⁶. Total RNA of each 3D skin equivalent was isolated using the reagent Crystal RNAmagic according to the manufacturer's protocol (BioLabproducts). In brief, the biopsy was transferred into a tube containing 500 μl Crystal RNAmagic (BioLab Products) and a monophasic, homogenic solution was created via vortexing. For separation of protein and DNA 100 μl of chloroform was added. The upper aqueous phase containing RNA was transferred in a new tube and 250 μl isopropanol was used for RNA precipitation. The pellet was washed with 500 μl 75% ethanol two times and RNA was finally solubilized in 30 μl nuclease-free water. RNA concentration was determined using Multiscan SkyHigh (ThermoFisher Scientific).

4.4.7 Reverse transcription

0.5µg of the isolated RNA was digested and reverse transcribed to cDNA (PrimeScript RT Reagent Kit with gDNA Eraser (Perfect Real Time); TaKaRa Bio). Briefly, cDNA corresponding to 10ng total RNA was used as the template in a real-time (RT) polymerase-chain-reaction (PCR).

4.4.8 Isolation of bacterial DNA

Total bacterial DNA was isolated from each skin equivalent (3mm punch biopsy) using QIAamp DNA Microbiome Kit (Qiagen). The biopsy was homogenized using innuspeed lysis tubes (IST Innuscreen AG) and a speedmill (Analytik Jena). 3 runs of 1 min duration were performed with 1 min breaks between the runs. During the break, samples were cooled on ice.

4.4.9 Real time PCR

Real-time PCR was performed with the QuantStudio 3 System (BD Biosciences) using SYBR Premix Ex Taq II mix (TaKaRa Bio). Amplification condition was performed in a 10µl reaction volume consisting of 1µl template cDNA, 5.2µl SYBR Premix EX TaqII, 3µl H₂O, 0.4µl forward primer, 0.4µl reverse primer. The primer sequences and corresponding PCR programs are shown in **Table 1**.

PCR program 1: Thermal cycle was programmed for 30 s at 95.0°C as initial denaturation, followed by 6 cycles of 95.0°C (5 s), 4.14°C/s for denaturation and 66.0°C (30 s), 3.17°C/s for annealing followed by 40 cycles of 95.0°C (15 s) for denaturation and 60.0°C (1 min) for annealing.

PCR program 2: Thermal cycle was programmed for 30 s at 95.0°C as initial denaturation, followed by 6 cycles of 95.0°C (5 s), 4.14°C/s for denaturation and 66.0°C (30 s), 3.17°C/s for annealing followed by 40 cycles of 95°C (5 s), 4.14°C/s for denaturation and 60.0°C (30 s), 3.17°C/s for annealing.

Table 1: List of genes and primer sequences used for real time PCR analysis. For each target gene, forward and reverse primer sequence is listed together with respective PCR program. All primers were obtained from bio-mers.

Gene	Primer sequence	PCR program
<i>RPL38</i>	Forward: TCAAGGACTTCCTGCTCACA	1
	Reverse: AAAGGTATCTGCTGCATCGAA	
<i>Filaggrin</i>	Forward: GGCAAATCCTGAAGAATCCAGATG	1
	Reverse: GGTAATTCTCTTTTCTGGTAGACTC	
<i>Involucrin</i>	Forward: CTGCCTCAGCCTTACTGTGA	1
	Reverse: GGAGGAGGAACAGTCTTGAGG	
<i>Loricrin</i>	Forward: CTCTCCTCACTCACCCCTTCCT	1
	Reverse: AGGTCTTCACGCAGTCCAC	
<i>Keratin 1</i>	Forward: CTTCTTCAGCCCCTCAATGT	1
	Reverse: GTACCTGGTTCTGCTGCTCC	
<i>Keratin 10</i>	Forward: TGAAAAGCATGGCAACTCAC	1
	Reverse: TGTCCGATCTGAAGCAGGATG	
<i>Keratin 14</i>	Forward: GGCCTGCTGAGATCAAAGAC	1
	Reverse: TCTGCAGAAGGACATTGGC	
<i>femSA</i>	Forward: TCA TTT TGC CGG AAG TTA TGC	2
	Reverse: AAC GGT CAA TGC CAT GAT TTA AT	

4.5 Skin histology

4.5.1 H&E staining

Hematoxylin and eosin (H&E) staining was performed as previously reported ¹²⁷ starting with deparaffinization using xylene followed by hydration steps (100% ethanol, 96% ethanol, 70% ethanol, H₂O). Hematoxylin staining was performed using Shandon Gill 3 Gematoxylin (Thermo Fisher Scientific). Glacial acid was used for differentiation and eosin staining was performed using Shandon Eosin Y (Thermo Fisher Scientific). Finally, dehydration was performed (70% ethanol, 96% ethanol, 100% ethanol) and slides were placed into xylene providing compatible solvent for the mounting medium (Thermo Fisher Scientific).

4.5.2 Immunohistochemistry

Immunohistochemistry was performed as previously reported ¹²⁸. The organotypic 3D skin equivalents were fixed by formalin and embedded in paraffin. Used antibodies and respective concentrations are shown in **Table 2**. Blocking was performed with TBS/12% BSA. For development, the Vectastain Elite ABC Komplex (PK-6100) followed by the Vector Nova Red-

Substrate (SK-4800; both Vector Laboratories, USA) was used. Slides were counterstained with hematoxylin and mounted using Cytoseal XYL (ThermoFisher Scientific).

Table 2: Overview of antibodies used for WES, immunohistochemistry or immunofluorescence. Antibody name, company, host species, working dilution and corresponding application of each antibody is listed.

Antibody	Source	Host Species	Working Concentration	Application
Actin	Cell Signaling Technology (#8457)	Rabbit	1:30	WES
Alexa Fluor anti-rabbit 488	Invitrogen (A21206)	Donkey	1:400	Immunofluorescence
Biotinylated swine anti-rabbit	Dako	Swine	1:300	Immunohistochemistry
ERK	Cell Signaling Technology (#9102)	Rabbit	1:30	WES
Filaggrin	Santa Cruz (#sc66192)	Mouse	1:50	Immunohistochemistry
Involucrin	Abcam (#ab53112)	Rabbit	1:300	Immunohistochemistry
Loricrin	Invitrogen (#PA5-30583)	Rabbit	1:500	Immunohistochemistry
NOX1	Santa Cruz (sc-518023)	Mouse	1:200	Immunofluorescence
NOX1	Santa Cruz (sc-518023)	Mouse	1:30	WES
NOX4	Abcam (133303)	Rabbit	1:200	Immunofluorescence
NOX4	Abcam (133303)	Rabbit	1:30	WES
P22phox	Santa Cruz (sc-271968)	Mouse	1:200	Immunofluorescence
P22phox	Santa Cruz (sc-271968)	Mouse	1:30	WES
p38	Cell Signaling Technology (#9212)	Rabbit	1:30	WES
pERK	Cell Signaling Technology (#9101)	Rabbit	1:30	WES
pH2AX	Cell Signaling Technology (#2577)	Rabbit	1:200	Immunofluorescence
pHsp27	Cell Signaling Technology (#2406)	Rabbit	1:30	WES
pP38	Cell Signaling Technology (#9216)	Mouse	1:30	WES
<i>Staphylococcus aureus</i>	Abcam (ab20920)	Rabbit	1:500	Immunohistochemistry

4.5.3 Spongiosis Scoring

Spongiosis scoring was performed on different skin models using H&E stained histological slides. 5 different reviewers trained in skin histology interpretation visually evaluated severity of spongiosis and scored spongiosis in a range from 0-3 (steps of 0.5 possible). Representative images of each severity score are shown in **Figure 7**.

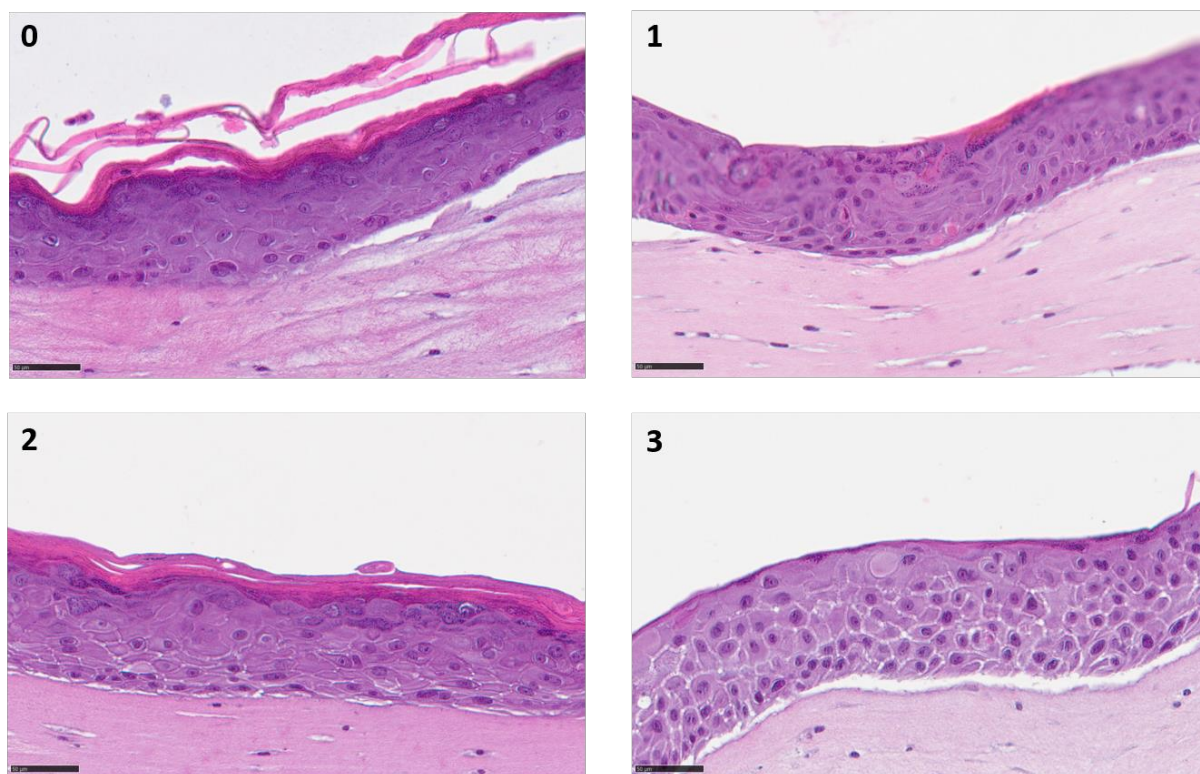


Figure 7: Representative images of spongiosis score 0-3. 0= no lines between cells; 1= faint white lines between some cells; 2= pronounced white lines between cells, 3= strongly pronounced white lines between all cells.

4.6 Ex vivo methods

4.6.1 Tape strips collection

For the analysis of proteins from the epidermis, tape strips were collected. Consecutive D-Squame Standard Sampling Discs (\varnothing 22mm) were applied on the skin for 5 s using the D-Squame pressure instrument (Clinical & Derm) to ensure standardized pressure (Pressure Applied: 225g/cm²; Pressure Area: 7/8in (22.24mm)). The first tape strip was discarded to

eliminate possible contaminants. Tape strips were stored at -80°C until analysis and tape strip 2–4 were used for further protein extraction and analysis.

4.6.2 Protein extraction from tape strips

Tape strips 2–4 were pooled for protein extraction. 500µl PBS + 0.005% Tween 20™ (Roth) were used as lysis buffer and added to a 2ml tube containing tape strip 2. The tube containing the tape strip and the lysis buffer was sonicated for 15 min in iced water to extract soluble proteins from tape strips. The tube was then briefly centrifugated and the supernatant was transferred into the next tube containing tape strip 3. The whole process was repeated for tape strip 3 and 4. The last tube was centrifugated 20 min at 13,000xg at 4°C. The supernatant was transferred into a new tube and the protein lysates were stored at -80°C until further analysis.

4.6.3 Micro BCA assay

Measurement of total soluble proteins extracted from tape strips was performed using Micro BCA™ assay (ThermoFisher Scientific) according to the manufacturer's instruction. In brief, albumin standards and working reagent were prepared and diluted according to the manual. Samples were diluted 1:10 in lysis buffer and the assay was performed in a 96 microplate. After pipetting standards, diluted samples and working reagent into the wells, the plate was covered and solutions were mixed using a plate shaker at 300rpm for 30 s. Afterwards, the plate was incubated at 37°C for 2 h and absorbance at 562nm was detected using a tecan reader (Tecan). A standard curve using a four-parameter logistic (4-PL) curve fit was prepared by plotting the net absorbance of each albumin standard against its concentration (Graphpad PRISM).

4.6.4 Skin swab sampling

Sampling collection was performed as previously reported^{129,130}. Participants were asked to avoid bathing/showering and application of any topical agents 24 h prior to sampling visits. Topical and systemic antibiotic use was recorded and samples with positive indication were removed from analysis. An area with the size of 4cm² from the antecubital fossa and volar forearm was swabbed for at least 30 s. Prior to collection, swabs (BD BBL Culture Swab EZ,

Becton, Dickinson and Company) were soaked in specimen collection fluid. Sampling negative controls were swabs that were exposed to ambient air for 5 s.

4.6.5 Microbial DNA extraction

DNA was isolated from samples with QIAmp UCP Pathogen Mini Kit on an automated QIAcube system (Qiagen).

4.6.6 Microbial profiling

The V1 and V2 variable regions of the 16S rRNA gene were amplified by PCR with the universal primer pair 27F and 338R. Sequencing was performed with MiSeq Reagent Kit v3 on the Illumina MiSeq (Illumina Inc.). The raw data was processed using the well-established amplicon pipeline (Version 2.1.0) pipeline^{131,132} integrated the nf-core framework¹³³. Briefly, the pipeline uses cutadapt for primer trimming, FastQC for quality evaluation, DADA2 to dereplicate, remove bimeras and infer ASVs using the SILVA reference (Version 132)¹³⁴.

4.7 Cohorts

4.7.1 Early Emollient cohort

Data and samples from 50 children from a parallel group, assessor-blind, randomized open-label prospective study of emollient use in neonates at high risk for AD were used in this study¹³⁰. The trial was approved by the ethics committees of the Medical Faculty at the Cristian-Albrechts-University in Kiel and the University of Regensburg and registered at ClinicalTrials.gov (NCT03376243). The newborns were included between 1 and 21 days after birth and assigned randomly (1:1) to an intervention or control group. High risk of developing AD was defined as having at least one first-degree relative with physician-diagnosed asthma, AD or allergic rhinitis. Data about skin health and care were collected during five face-to-face visits (baseline, month 1, month 6, month 12, month 24) and two telephone interviews (month 3 and month 18) (**Figure 8**). Skin examinations were performed by trained physicians. Moreover, skin physiological measures including TEWL (Tewameter TM300), *stratum corneum* hydration (Corneometer CM 825) and skin pH (pH-Meter PH 905) were performed and biosamples were

collected. Biosamples included skin swabs for skin microbiota sampling (cheek, volar forearm, antecubital fossa) and tape strips for epidermal protein extraction (volar forearm, antecubital fossa).

All parents of the participants received a structured information that included best-practice advice on infant skin care in accordance to the German Arbeitsgemeinschaft der Wissenschaftlichen Medizinischen Fachgesellschaften (AWMF) S3 guidelines for prevention¹³⁵ and the German Federal Centre of Health Education, Cologne. The parents of the children that were assigned to the intervention group were further provided by an emollient (Lipikar) and instructed to apply it at least once daily to the child's entire body surface for the first year of life.

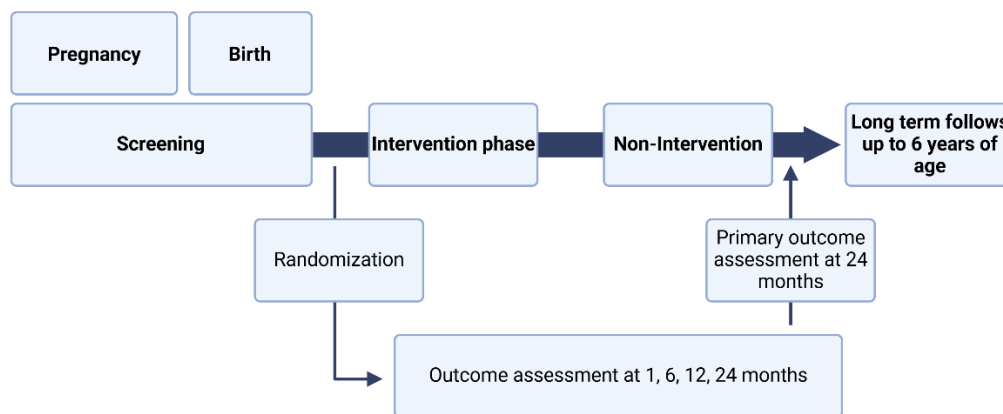


Figure 8: Overview of study design. Study participants were screened prior to birth and then randomized to control or intervention group. During the study, five face-to-face visits and two telephone interviews were performed (adapted from: *Harder et al.*, 2023 *Acta Derm Venereol.*).

4.8 Statistics

Statistical tests were performed using GraphPad PRISM 9 software (GraphPad Software, La Jolla, CA) or R (R version 4.1.3 <https://www.R-project.org/>). Data was checked for normal distribution using Shapiro-Wilk test. Respective sample size and statistical tests are indicated in each method section of the different publications and in the figure legends. A standard threshold of 0.05 was used to determine statistical significance for all tests.

5 Results**5.1 Article I**

This article was published in Experimental Dermatology, Vol. 29(8), Hila Emmert, Melina Fonfara, Elke Rodriguez, Stephan Weidinger, NADPH oxidase inhibition rescues keratinocytes from elevated oxidative stress in a 2D atopic dermatitis and psoriasis model, 749-758. DOI: 10.1111/exd.14148.

NADPH oxidase inhibition rescues keratinocytes from elevated oxidative stress in a 2D atopic dermatitis and psoriasis model

Hila Emmert  | Melina Fonfara | Elke Rodriguez | Stephan Weidinger

Department of Dermatology, Allergology and Venereology, University Hospital Schleswig-Holstein, Kiel, Germany

Correspondence

Hila Emmert, Department of Dermatology, Venereology and Allergy, University Hospital Schleswig-Holstein, Campus Kiel, Rosalind-Franklin Str. 7, 24105 Kiel, Germany.
Email: hemmert@dermatology.uni-kiel.de

Abstract

Emerging evidence suggests oxidative stress plays a role in the pathophysiology of both atopic dermatitis (AD) and psoriasis (PSO). We established in vitro models of AD and PSO skin, and characterized these models in regard to their oxidative stress state. Both AD and PSO model keratinocytes exhibited elevated reactive oxygen species (ROS) levels and accumulated more DNA damage than control cells after oxidative stress induced by 250 $\mu\text{mol/L}$ H_2O_2 . Elevated ROS levels and DNA damage accumulation could be inhibited by the NADPH oxidase (NOX) inhibitor diphenyleneiodonium (DPI). Further, immunofluorescence analysis revealed the presence of both NOX1 and NOX4 in keratinocytes. By inhibiting NOX1, stress-related signalling cascades and elevated ROS levels could be abrogated, and survival of AD and PSO cells improved. Taken together, this study reveals that inhibition of NOX inhibition could abrogate elevated oxidative stress in a 2D model of AD and PSO.

KEYWORDS

atopic dermatitis (AD), diphenyleneiodonium (DPI), NADPH oxidase (NOX), NOX1, NOX4, oxidative stress, psoriasis (PSO), reactive oxygen species (ROS)

1 | INTRODUCTION

Atopic dermatitis (AD) and psoriasis (PSO) are common chronic inflammatory skin disorders. The data from the WHO Global Burden of Diseases initiative indicate that at least 230 and 125 million people worldwide have AD and PSO (lifetime prevalences of 10%-15% and 2%-3%, respectively), with AD being the leading cause of the non-fatal disease burden conferred by skin conditions on a global level.^[1,2] Both diseases result from the complex interaction of genetic and environmental factors leading to epidermal dysfunction as well as cutaneous inflammation, which is driven by excessive T-cell activation of, however, differing polarity.^[3,4] While PSO is largely driven by type 17 responses,^[5] AD has a strong Th2 and Th22 component, but appears to be more heterogeneous with the involvement

of multiple immune pathways, potentially with different disease features.^[6] Further, in both diseases, prolonged presence of oxidative stress and a redox imbalance are postulated to promote inflammatory processes.^[7] Oxidative stress not only enhances inflammation through upregulation of inflammatory genes, but can also damage cellular structures of the skin and weaken the skin barrier function.^[8]

Redox imbalance in the skin can arise from excessive formation of reactive oxygen species (ROS) through pro-inflammatory stimuli such as pro-inflammatory cytokines, H_2O_2 or UV irradiation. Oxidative stress can lead to lipid peroxidation, protein oxidation and DNA damage, thus inducing several physiological dysfunctions.^[9-11] Cells have therefore developed various antioxidative mechanisms. Antioxidative responses include activation of signalling pathways that depend on the strength of and damage induced by the stress

This is an open access article under the terms of the Creative Commons Attribution License, which permits use, distribution and reproduction in any medium, provided the original work is properly cited.

© 2020 The Authors. *Experimental Dermatology* published by John Wiley & Sons Ltd

to initialize either pro-survival gene expression programmes for continuous ROS detoxification (eg Nrf2, pHsp27, pERK) and DNA damage repair (eg ATM and p53) or cell-death-inducing programs (eg NF- κ B, p53, p38).^[12,13] However, ROS can also lead to the activation of NADPH oxidase (NOX), which themselves generate ROS and therefore reinforce the initial ROS production. The family of NOX comprises of several members (NOX1, NOX2, NOX3, NOX4, NOX5, DUOX1, DUOX2). NOX catalyses the production of superoxide through reduction in NADPH. Via the generation of ROS, NOX mediates diverse functions such as host defense and inflammation, posttranslational processing of proteins, cellular signalling and regulation of gene expression. However, NOX also contributes to a wide range of diseases as a deficiency can lead to immunosuppression and increased activity will lead to excess ROS which is associated with cardiovascular changes, neurodegeneration and inflammatory skin diseases.^[29]

More evidence for an association between oxidative stress and AD and PSO has been provided by studies which have analysed oxidative stress markers and which have shown that in both AD and PSO malondialdehyde levels are increased,^[14-21] and antioxidant enzymes such as superoxide dismutase, catalase and GSH peroxidase are decreased.^[16,21-25]

Although extensive evidence exists suggesting an important role of oxidative stress in the pathology of inflammatory skin diseases, no comprehensive study into the molecular mechanisms has been conducted and data on the oxidative state of the skin remain sparse. Furthermore, the mechanism by which oxidative stress might influence pathophysiology has not been discovered yet. The association of oxidative stress with both AD and PSO leads to the question whether ROS play a role in the pathophysiology of both diseases and if yes, whether there are disease-specific differences in redox regulation.

2 | MATERIALS AND METHODS

2.1 | Cell culture

Normal human epidermal keratinocytes (NHEKs) (PromoCell, Lot number 407Z001) were cultured in Keratinocyte Growth Medium (KGM) + supplements + CaCl₂ + penicillin/streptomycin at 37°C and 5% CO₂. Cells were used at passages 4-10.

2.2 | Induction of a 2-D PSO and AD cell culture model

2D models of AD and PSO were induced by adding respective cytokine mixes to the culture dishes for 24 hours prior to experiments. We used neonatal human keratinocytes and adapted a protocol to stimulate with either an AD cytokine or a PSO cytokine mix as described previously.^[26] For PSO induction, 40 ng/mL IL-22, 40 ng/mL IL-17a and 10 ng/mL TNF- α were added. For AD induction, 40 ng/

mL IL-22, 40 ng/mL IL-4, 40 ng/mL IL-13 and 10 ng/mL TNF- α were added.

2.3 | Inhibition of NADPH oxidases

In experiments where diphenyleneiodonium (DPI) was used, DPI was added at a final concentration of 10 μ mol/L for 24 hours (Santa Cruz sc-202584) prior to H₂O₂ treatment. In experiments where NOX1 inhibitor (Nox1i) was used, ML171 was added at a final concentration of 10 μ mol/L for 24 hours (ML171-CAS 6631-94-3-Calbiochem) prior to H₂O₂ treatment, and in experiments where NOX1/4 inhibitor (Nox1/4i) was used, GKT136901 was added at a final concentration of 10 μ mol/L for 24 hours (GKT136901-CAS 955272-06-7-Calbiochem) prior to H₂O₂ treatment. All inhibitors were dissolved in DMSO. Control cells were treated accordingly with 10 μ mol/L DMSO.

2.4 | Induction of oxidative stress

To induce oxidative stress, cells were treated with hydrogen peroxide (H₂O₂) (Merck, 31642). For H₂O₂ treatment, media were replaced with freshly prepared media containing 250 μ mol/L H₂O₂. In control cells, the media were switched to fresh media without H₂O₂. For DCF assays, H₂O₂ was added for 10 minutes, and for immunofluorescence and Western blotting, H₂O₂ was added for 1 hour.

2.5 | DCFDA assay

Intracellular ROS levels were measured using the DCFDA assay (Abcam, AB113851) according to the manufacturer's instructions. Briefly, cells were seeded in a 96-well plate until ~80% confluency. Cells were incubated with 10 μ mol/L 2',7'-dichlorofluorescein (DCF) and then washed twice. Oxidative stress was induced by treatment of cells with 250 μ mol/L H₂O₂. Cells were washed twice with PBS, and ROS levels were quantified by measuring fluorescence at excitation/emission of 495 nm/520 nm.

2.6 | Western blotting

For Western blot analysis, cells were lysed in RIPA buffer (50 mmol/L Tris pH 8.0, 150 mmol/L NaCl, 1% Triton X-100, 0.5% natriumdeoxycholate, 0.1% SDS) plus protease and phosphatase inhibitors (Roche, 04906845001 and 04693124001, respectively). The determination of the protein concentration was performed by using the Pierce 600 nm Assay and the Tecan Reader according to the manufacturer's instructions. Western blotting was performed using WEST[™] according to the manufacturer's instructions. Antibodies used were as follows: Actin (CST #8457), ERK (CST #9102), pERK (CST #9101), p38 (CST #9212), pP38 (CST #9216), NOX1 (Santa Cruz sc-518023), NOX4 (Abcam 133303), pHsp27 (CST #2406) and p22phox (Santa

Cruz sc-271968). All primary antibodies were used at a concentration of 1:30. WES-supplied secondary antibodies were used according to the manufacturer's instruction at a final concentration of 1:1.

2.7 | Immunofluorescence

Cells grown on coverslips were fixed with 3.7% paraformaldehyde solution (PFA) for 30 minutes and washed three times with PBS. To permeabilize the cells, a 0.1% Triton X-100 in PBS solution was added for 15 minutes and followed by 30 minutes of blocking with blocking solution (1% BSA in combination with 10% goat serum in PBS). The incubation with primary antibodies (pH2AX, CST #2577; NOX1 Santa Cruz sc-518023, NOX4 Abcam 133303, p22phox Santa Cruz sc-271) was at room temperature for 1 hour in blocking buffer. All primary antibodies were used at a 1:200 final concentration. Cells were washed twice with PBS and incubated with the secondary antibodies (Alexa Fluor anti-rabbit 488, Thermo Fischer) at a 1:400 concentration for 90 minutes at room temperature in blocking buffer. Secondary antibodies were used at a final concentration of 1:400. After a final washing step with PBS, mounting medium with DAPI was added to the cells. Images were captured using a Zeiss microscope (serial number: 551 095) using a 40-x or 63-x objective. For each biological replicate, at least three images were taken and a total of at least 30 cells each per condition were analysed.

For quantification of pH2AX, cell nuclei were manually selected via the DAPI staining in ImageJ to create a mask. The mask was then used to measure fluorescence intensity of both the DAPI and the 488 channels. pH2AX intensity was normalized to the DAPI signal for each image. For fluorescence quantification of NOX1, NOX4 and p22phox, the fluorescence intensity of the total 488 channel signal per image normalized to a blank ROI was measured and then normalized to the total DAPI channel signal normalized to a blank ROI.

3 | RESULTS

3.1 | Treatment of a 2D atopic dermatitis and psoriasis skin model with pro-inflammatory cytokines leads to increased oxidative stress

In order to determine the role of oxidative stress in atopic dermatitis (AD) and psoriasis (PSO), we established an adapted 2D in vitro model of AD and PSO keratinocytes.^[26] AD, PSO and unstimulated control (Ctrl) keratinocytes were treated with a disease-specific cytokine mix for 24 hours to stimulate the Th1 or Th2 environment, respectively. Treatment with the cytokine mixes had no impact on proliferation or viability (data not shown). To find out whether oxidative stress plays a role in the pathogenesis of inflammatory skin diseases, we first investigated whether stimulation of cells with inflammatory cytokines leads to increased oxidative stress. We induced oxidative stress by treating the cells with 250 $\mu\text{mol/L}$ H_2O_2 and measured intracellular reactive oxygen species (ROS) using a H2DCFDA

assay. Treatment with H_2O_2 led to an increase in ROS production in all three models, which, however, were significantly greater in the AD and PSO models compared with the control (Figure 1A; *P* Value (Ctrl with H_2O_2 vs AD with H_2O_2) < .0001; *P* Value (Ctrl with H_2O_2 vs PSO with H_2O_2) = .0001). The data show that both the AD and PSO models are characterized by an increased oxidative state. To unravel whether the differences in oxidative capacity translate into downstream detrimental biological processes, we analysed DNA damage, as ROS are well-recognized mediators of DNA damage.^[27,28] The results showed that H_2O_2 induced increased DNA damage in the control, as well as in the cytokine-stimulated cells (Figure 1B, Figure S1; *P* Value (Ctrl without H_2O_2 vs Ctrl with H_2O_2) = .0582; *P* Value (AD without H_2O_2 vs AD with H_2O_2) < .05; *P* Value (PSO without H_2O_2 vs PSO with H_2O_2) not significant). Interestingly, DNA damage was highest in the AD model (Figure 1B, Figure S1; *P* Value (Ctrl with H_2O_2 vs AD with H_2O_2) < .05; *P* Value (Ctrl with H_2O_2 vs PSO with H_2O_2) not significant). These data recapitulate the finding that the AD-like stimulation leads to increased ROS levels, which translate into more DNA damage.

3.2 | Inhibition of NADPH oxidase activity leads to abrogation of elevated oxidative stress levels in the AD and PSO models

In order to find out whether the elevated ROS levels in the AD and PSO models are due to increased ROS production or impaired ROS clearance, we measured intracellular ROS after inhibition of NADPH oxidase activity. DPI addition successfully reduced ROS levels after stress induction in all three models (Figure 2A; *P* Value (Ctrl with H_2O_2 without DPI vs Ctrl with H_2O_2 with DPI) = .1681; *P* Value (AD with H_2O_2 without DPI vs AD with H_2O_2 with DPI) < .001, *P* Value (PSO with H_2O_2 without DPI vs PSO with H_2O_2 with DPI) < .001), but inhibition of ROS production was significantly greater in the AD model compared with the Ctrl (Figure 2A; *P* Value (Ctrl with H_2O_2 without DPI/Ctrl with H_2O_2 with DPI vs AD with H_2O_2 without DPI/AD with H_2O_2 with DPI) < 0.05). Inhibition of NOX activity also rescued AD cells from increased DNA damage accumulation (Figure 2B). Analysis of DNA damage accumulation showed that the inhibition of NOX activity significantly reduced DNA damage accumulation after stress in AD and PSO, but reduction in DNA damage accumulation was not significant in control cells.

3.3 | Increased oxidative stress in the AD and PSO models is mainly due to NADPH oxidase 1 activity

To further characterize the molecular mechanisms involved in increased oxidative stress sensitivity in the AD and PSO models, we analysed NOX family member expression and localization in keratinocytes. Western blot analysis revealed that only NOX1 and NOX4 can be detected in keratinocytes (Figure 3A). There was no difference in the expression of NOX1 and NOX4 between AD- and

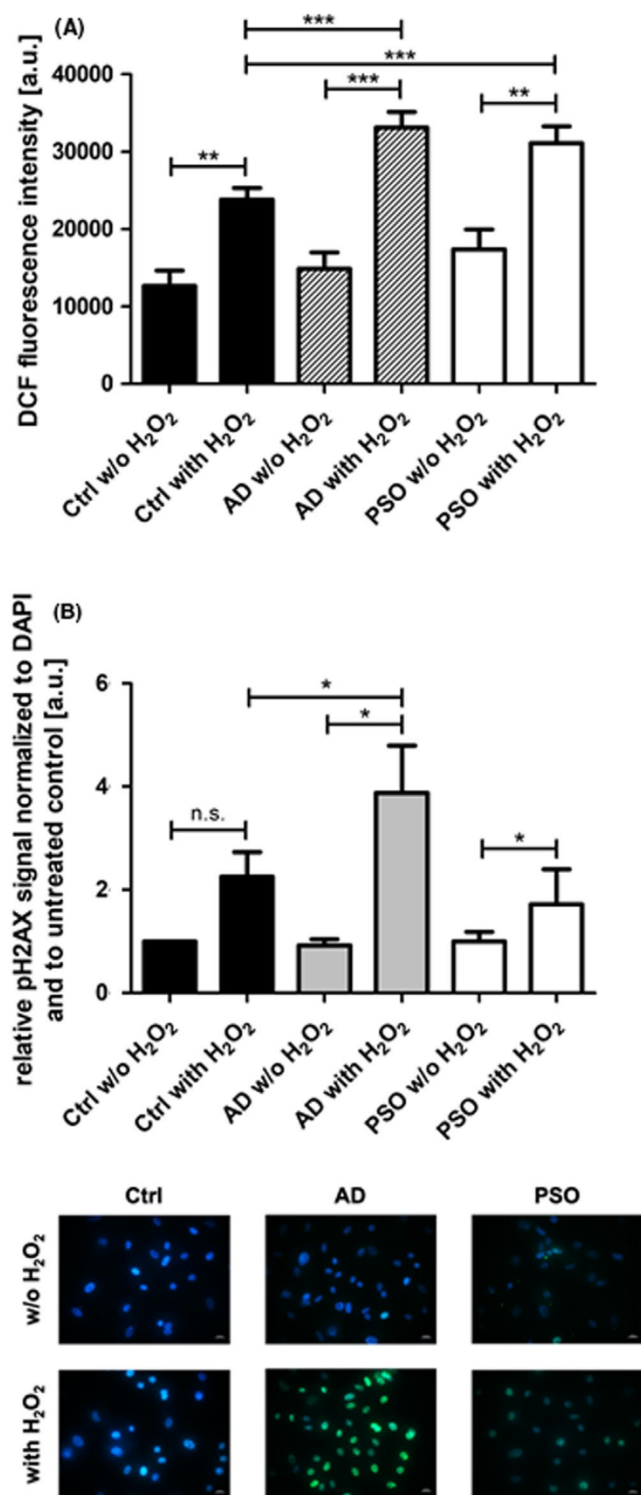


FIGURE 1 Atopic dermatitis (AD) and psoriasis (PSO) model keratinocytes react more sensitive to oxidative stress. A, Cells were treated with H₂O₂ to induce oxidative stress, and reactive oxygen species (ROS) were measured by using a DCFDA assay. AD model keratinocytes exhibit significantly more ROS than untreated control cells. B, DNA damage in the AD and PSO models. Cells were stressed with H₂O₂, and DNA damage was measured by analysing levels of pH2AX via immunofluorescence staining (IF). B, shows representative images as well as the quantification of nuclear pH2AX fluorescence intensity normalized to nuclear DAPI. Results represent the means and s.e.m. from more than five independent experiments. **P* < .05: statistically significant difference from control value after paired Student *t* test

we used the selective NOX1 and NOX4 inhibitors, respectively, to find out which NOX family member is responsible for induction of elevated ROS levels in the AD and PSO models. DCFDA analysis revealed that the inhibition of NOX1 and NOX4 by NOX1/4 inhibitor (Nox1/4i) (GKT136901) led to a significant but slight decrease in ROS levels in H₂O₂-stressed AD model keratinocytes, but had no effect on control or PSO model keratinocytes (Figure 3B; *P* Value (Ctrl with H₂O₂ without Nox1/4i vs Ctrl with H₂O₂ with Nox1/4i) = *n.s.*; *P* Value (AD with H₂O₂ without Nox1/4i vs AD with H₂O₂ with Nox1/4i) < .05; *P* Value (PSO with H₂O₂ without Nox1/4i vs PSO with H₂O₂ with Nox1/4i) = *n.s.*). Inhibition of NOX1 with the NOX1 inhibitor (NOX1i) ML171 on the other hand completely abolished increased ROS production after oxidative stress in AD model keratinocytes and led to a significant reduction in ROS in control cells, but not in PSO model keratinocytes (Figure 3B, *P* Value (Ctrl with H₂O₂ without NOX1i vs Ctrl with H₂O₂ with NOX1i) < .01; *P* Value (AD with H₂O₂ without NOX1i vs AD with H₂O₂ with NOX1i) < .01; *P* Value (PSO with H₂O₂ without NOX1i vs PSO with H₂O₂ with NOX1i) = *n.s.*).

3.4 | Inhibition of NADPH oxidase activity rescues elevated stress signalling in keratinocytes in the AD and PSO models and promotes survival

For the identification of signalling cascades involved in redox balance in the AD and PSO models, we analysed the stress-related signalling cascades via Western blot. Treatment with H₂O₂ led to an activation of well-known stress-related signalling cascades such as pERK, pP38 and pHsp27 in all three cell models (Figure 4). While P38 signalling is considered to be a pro-apoptosis signal,^[10,29] activation of ERK signalling and of the heat shock response via phosphorylation of Hsp27 are considered to be survival-related signalling pathways.^[9,10,30,31] Our Western blot analysis revealed activation of both pro-apoptotic and pro-survival signalling pathways. This is not surprising, as we used a non-lethal H₂O₂ concentration.^[32,33] Analysis of cell viability and caspase cleavage showed no significant differences between Ctrl, AD, PSO or H₂O₂ treatment (data not shown).

We investigated whether stress induction impacts long-term survival by conducting a colony formation assay (CFA). For the CFA, cells were plated very sparsely on a 10-cm cell culture dish, stimulated

PSO-stimulated cells. DPI treatment reduced NOX1 but not NOX4 expression after DPI and H₂O₂ treatment in control, and AD and PSO model keratinocytes. Detailed immunofluorescence analysis showed that as expected, there is no difference in expression or localization of either NOX1 or NOX4 in the AD and PSO models (Figures S2 and S3), and that neither expression nor localization of the regulatory p22phox subunit of NOX family members is altered, indicating that DPI reduced NOX activity, but not its abundance (Figure S4). Next,

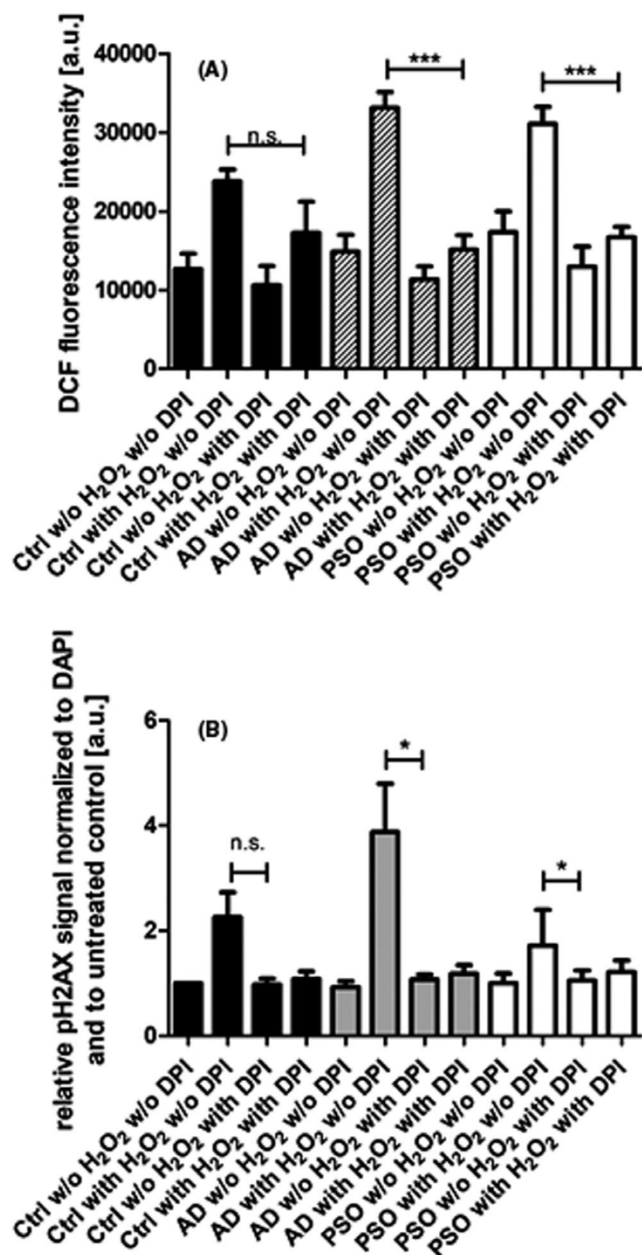


FIGURE 2 Abrogation of increased oxidative stress in atopic dermatitis (AD) model and psoriasis (PSO) model keratinocytes by NADPH oxidase inhibitor. AD and PSO model keratinocytes were treated with H₂O₂ and with diphenyleneiodonium chloride (DPI). A, Reactive oxygen species (ROS) production was measured via DCFDA assay. Increased ROS levels in H₂O₂-treated AD and PSO model keratinocytes were abrogated when adding DPI. B, DNA damage in the AD and PSO model after H₂O₂ stress and treatment with DPI. DNA damage was measured by analysing levels of pH2AX via immunofluorescence staining (IF). B, shows the quantification of nuclear pH2AX fluorescence intensity normalized to nuclear DAPI and to the untreated control cells. Results represent the means and s.e.m. from more than five independent experiments. **P* < .05, ***P* < .01; ****P* < .001: statistically significant difference after paired Student *t* test

with the AD or PSO mix for 24 hours, respectively, and then stressed by addition of 250 μmol/L H₂O₂ for 24 hours. Colony formation was

measured after 14 days, thus indicating long-term survival of colonies. Figure 5 shows that treatment of Ctrl, AD and PSO keratinocytes with H₂O₂ led to a reduction in colony-forming units (CFUs). Inhibition of NOX activity only led to a better survival rate after oxidative stress in AD and PSO cells models (Figure 5; *P* Value (Ctrl with H₂O₂ without DPI vs Ctrl with H₂O₂ with DPI) = n.s.; *P* Value (AD with H₂O₂ without DPI vs AD with H₂O₂ with DPI) < .05; *P* Value (PSO with H₂O₂ without DPI vs PSO with H₂O₂ with DPI) < .05).

4 | DISCUSSION

Both AD and PSO are common inflammatory skin diseases characterized by epidermal barrier dysfunction and excessive T-cell activation of, however, differing polarity. While AD is driven by the type 2 cytokines, PSO is a Th17-mediated disease.^[34-36] In both diseases, the increased release of other pro-inflammatory cytokines such as TNF-α and IL-1 in both AD and PSO may cause chronic low-grade systemic inflammation.^[34] Our results indicate that the different cytokine milieu associated with AD and PSO have different effects on NOX activity, which might explain why our study revealed differences in the oxidative stress sensitivity of the AD and PSO models in vitro. It is well known that oxidative stress promotes tissue inflammation through upregulation of genes that code pro-inflammatory cytokines, and thus that inflammatory signalling is closely linked to oxidative stress.^[37,38] Inflammatory cells in turn release free radicals when activated. Given its prominent inflammatory component, it is conceivable that oxidative stress may play a role in the pathogenesis of inflammatory skin diseases.

As both AD and PSO are inflammatory diseases, inflammatory cells such as T cells and dendritic cells could be the source of elevated oxidative stress marker, but pro-inflammatory signalling in keratinocytes has also been discussed as a possible cause.^[8] Our study reveals for the first time that in fact keratinocytes are characterized by high intracellular levels of ROS after treatment with previously described AD and PSO signature cytokines,^[26] with IL-4 and IL-13 having a greater effect than IL-17. These differences in oxidative burden translate into downstream detrimental biological processes, such as accumulation of DNA damage and reduced survival rate in the AD and PSO models.

Another important question when regarding impaired redox homeostasis mechanisms that might contribute to disease pathology is whether elevated oxidative stress is due to increased ROS production or due to reduced antioxidative capacity. By utilizing the pan-NADPH oxidase inhibitor DPI, which inhibits the intracellular production of ROS due to environmental stress induction, we were able to show that elevated oxidative stress in the AD and PSO models arises from increased intrinsic ROS production and not impaired antioxidant capacity as hypothesized previously elsewhere.^[20,22-25] The results indicate a beneficial effect of NOX inhibition on reducing ROS in an AD and PSO models, however, whether these findings translate to in vivo remain to be investigated. Given the multifactorial nature of both AD and PSO, and the high level of complexity of

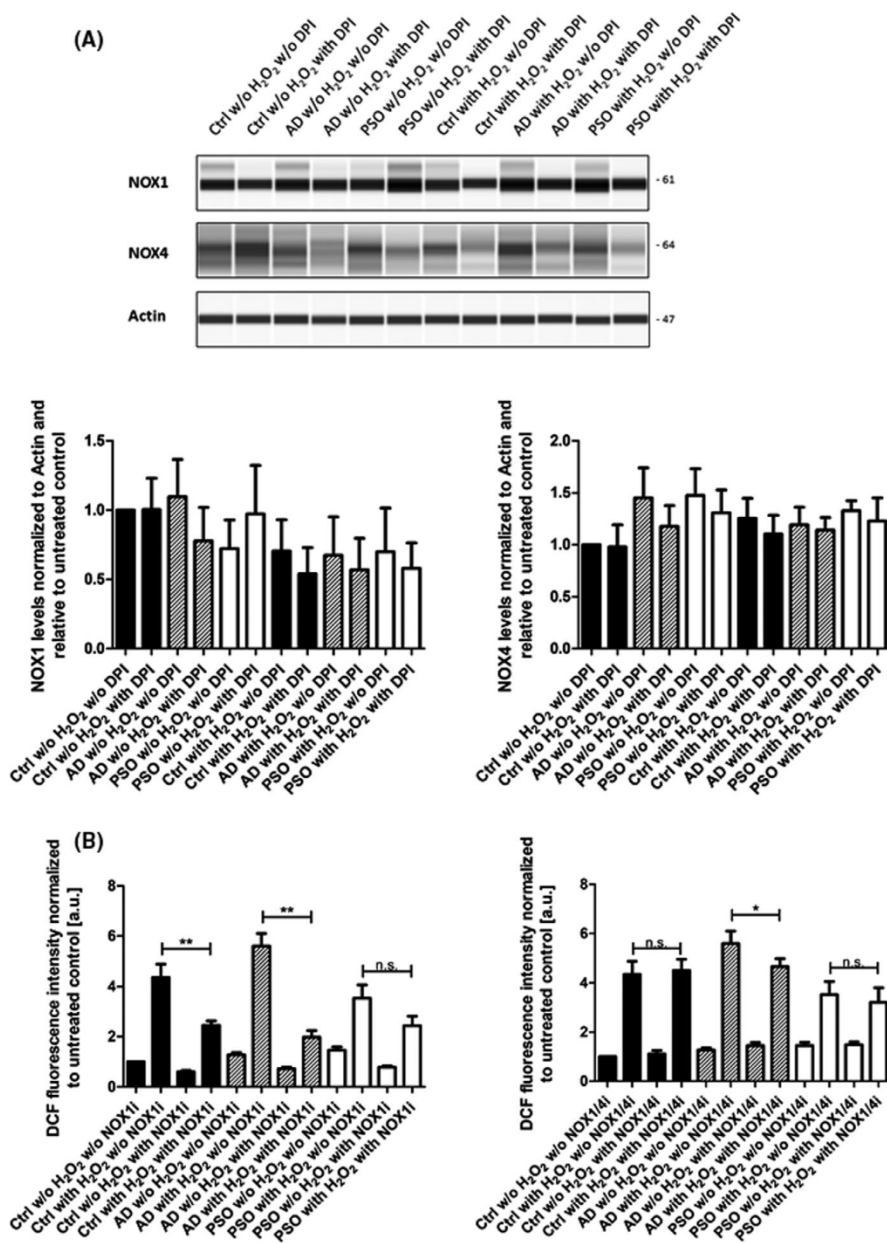


FIGURE 3 Inhibition of NADPH oxidase (NOX) 1 leads to abrogation of elevated oxidative stress levels in the atopic dermatitis (AD) and psoriasis (PSO) models. AD and PSO model keratinocytes were treated with H₂O₂ and with either DPI, NOX1i (ML171) or Nox1/4i (GKT136901). A, NOX1 and NOX4 protein levels as determined by Western blotting. Figure A shows a representative Western blot as well as quantification of protein levels normalized to actin and to the untreated control keratinocytes. NOX4 levels remain unchanged, while NOX1 levels were reduced after H₂O₂ stress and treatment with DPI. Results represent the means and s.e.m. from three independent experiments. B, Reactive oxygen species (ROS) production was measured via DCFDA assay. Increased ROS levels in H₂O₂-treated control and AD model keratinocytes were abrogated when adding NOX1i and in AD model keratinocytes when adding Nox1/4i, respectively. Results represent the means and s.e.m. from more than five independent experiments. **P* < .05; ***P* < .01; ****P* < .001; n.s. *P* > .05: statistically significant difference after paired Student *t* test

the underlying disease mechanisms, counteracting oxidative stress *in vivo* might not lead to similarly reduced cell damage as observed *in vitro*.

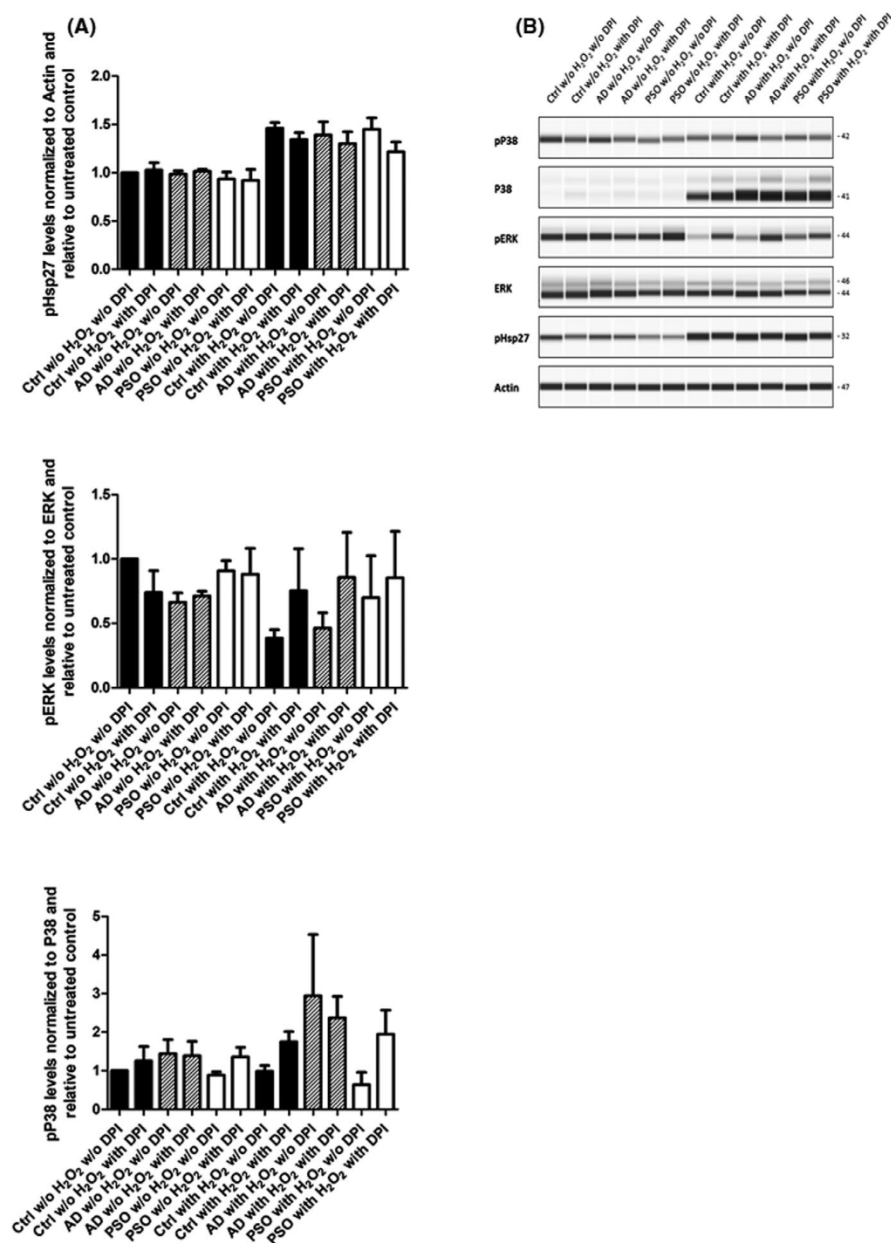
Interestingly, AD model keratinocytes reacted more sensitive to mild H₂O₂ stimulation than PSO model keratinocytes and had better responsiveness to treatment with NOX inhibitors. This is in line with the observation that while AD skin lesions are characterized by apoptosis of keratinocytes,^[39] PSO lesions are characterized by hyperproliferation of keratinocytes.^[40,41] It is tempting to speculate that the disease-specific cytokine profile leads to elevated ROS levels in both AD and PSO, but the unique concentration of the key cytokine mediators leads to alternate stress-induced outcomes of cell fate.

As oxidative stress resulting from excess ROS plays an important role in several diseases including AD, PSO, urticaria and allergic diseases,^[7] there is a strong need to find strategies lowering ROS in

keratinocytes. Possible strategies could include the use of antioxidants or the inhibition of ROS production. Despite many antioxidant therapies that have been evaluated in clinical trials involving tens of thousands of patients, most clinical trial results failed to show effectiveness.^[42,43] One of the possible reasons is that in many clinical trials, antioxidants were not chosen because they proved to be the most effective antioxidants, but rather because of their easy availability. This led to the use of antioxidants that were unspecific, ineffective at the doses given or simply also had pro-oxidative effects (eg vitamin E).^[42] Due to the clinical fail of many trials dealing with antioxidants, NOX inhibitors are more promising for diseases associated with excess oxidative stress, as NADPH oxidases are the only enzymes solely dedicated to ROS generation and thus prove to be a selective target.^[44]

Diphenyleneiodonium is a non-specific flavin binder abstracting an electron from an electron transporter forming a radical which

FIGURE 4 Inhibition of NADPH oxidase (NOX) activity alters stress signalling. Atopic dermatitis (AD) and psoriasis (PSO) model keratinocytes were treated with H_2O_2 and with diphenyleneiodonium chloride (DPI). Oxidative stress signalling was characterized by analysing phosphorylation of extracellular signal-regulated kinase (ERK), p38 and heat shock protein (Hsp) 27 via Western blotting. A, shows quantification of pHsp27 levels normalized to actin, pERK levels normalized to total ERK and pP38 levels normalized to total p38 from three independent experiments. B, Representative Western blots



then acts as an inhibitor of the respective electron transporter through a covalent binding step.^[45] It is commonly used as a NOX inhibitor not only in chronic inflammatory skin diseases as excess ROS production is associated with many different diseases. A major advantage of DPI is the incomplete suppression of ROS production maintaining a basal ROS level which is needed for physiological processes.^[44] DPI has been shown to be a potent and reliable NOX inhibitor; however, DPI has several drawbacks. As it is a flavoprotein inhibitor, it also inhibits CYP450, NO synthase and the mitochondrial electron chain, thus representing an unspecific and toxic inhibitor.^[46] In this study, the possible toxic effect of DPI on survival has been addressed via a colony formation assay. We observed reduced colony formation in cells treated with DPI, however, and most importantly, we showed that the combined treatment with H_2O_2 and DPI leads to increased colony formation as compared to H_2O_2 alone and thus rescues cells from oxidative damage. Due to the lack of specificity

and its toxicity, DPI remains a problematic candidate for drug usage, but is useful as a reference compound for NOX inhibition in vitro.^[46] Studies have showed NOX1 and NOX4 KO mice have no significant spontaneous pathologies making the respective selective inhibition of NOX1 and NOX4 more feasible. In addition to the unspecific NOX inhibitor DPI, novel selective NOX1 and NOX4 inhibitors are currently tested in clinical trials. The specific inhibition of respective NOX would lower off-target effects and would make the treatment more effective. The novel inhibitors ML171 and GKT136901 selectively inhibit NOX1 and NOX1/NOX4, respectively.^[46-50] Clinical trials with 170 patients have demonstrated that the novel inhibitors are well-tolerated and non-toxic, and thus provide a good alternative for DPI.^[50] In this study, we controlled for the possible unspecific effects of DPI by additionally analysing intracellular ROS levels after inhibition of NOX1 and NOX1/4 by the selective inhibitors. Both ML171 and GKT136901 significantly reduced ROS production in AD

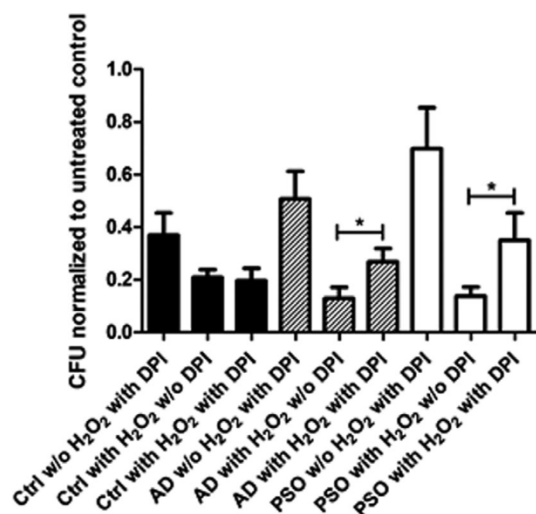


FIGURE 5 NADPH oxidase (NOX) inhibition promotes long-term cell survival after oxidative stress in the atopic dermatitis (AD) and psoriasis (PSO) models. Colony formation (CFU) assay in AD and PSO model keratinocytes treated with H₂O₂ and diphenyleneiodonium chloride (DPI). CFU was normalized to the untreated control. In AD and PSO model keratinocytes, additional treatment with DPI and H₂O₂ leads to more CFUs as compared to treatment with H₂O₂ alone. Results represent the means and s.e.m. from more than five independent experiments. **P* < .05: statistically significant difference after paired Student *t* test

keratinocytes, but of note the effect was stronger in ML171-treated cells. This indicates that NOX1 is possibly a more important NOX family member in regulating oxidative stress in AD than NOX4, and that a combined inhibition of NOX1 and NOX4 is not as effective as inhibition of NOX1 alone, but further experiments are necessary to elucidate these findings.

Other studies, supporting the important role of NOX inhibitors in the treatment of chronic inflammatory skin diseases, have demonstrated the reduction in AD severity by using the antimicrobial agent gentian violet. Gentian violet is a NOX inhibitor originally used for the treatment of bacterial infections, but studies have proven that the topical administration of gentian violet leads to a reduction in AD severity.^[51] Gentian violet is an approved drug and thus might represent a good candidate for further clinical studies.

To our knowledge, there are no *in vivo* data available regarding NOX inhibition in an AD mouse model. However, there is a study showing a benefit of the antioxidative compound rosmarinic acid in the treatment of NC/Nga mice.^[52] Although the study does not mention NADPH oxidases, rosmarinic acid has been described to inhibit NOX2/4 and the effects observed in the above-mentioned study could be due to NOX inhibitory effects.^[53]

This is the first study to show that keratinocytes treated with AD and PSO signature cytokines elicit an oxidative response, which leads to reduced keratinocyte survival and may contribute to the formation of lesions especially in AD. ROS generation and downstream deleterious effects can be rescued by inhibition of NOX. In the case of AD, where a hallmark of the formation of lesions is the

increased apoptosis of keratinocytes,^[39,40] the results of this study directly support a link between increased oxidative stress and reduced survival of keratinocytes and lesion formation in patients. In PSO, lesions are characterized by hyperproliferation of keratinocytes instead of apoptosis, but apoptotic features as determined by TUNEL method are still prominent in lesions despite PSO being a hyperproliferative disorder.^[54,55]

Taken together, the data of this study demonstrate the possible use of NOX inhibitors to counteract detrimental effects of high levels of AD and PSO signature cytokines, but further *in vivo* experiments are warranted to further elucidate whether NOX inhibition may represent a promising treatment strategy for inflammatory skin diseases. In conclusion, it is important to focus further research on this field in order to characterize the mechanisms of NOX enzymes as major producer of ROS and in order to develop a safe and effective approach to attenuate the ROS production in AD and PSO.

ACKNOWLEDGEMENTS

HE designed the experiments; HE, MF, Anke Rose and Steffen Bachmann acquired the data. HE and MF analysed the data, and HE and SW interpreted the data. HE, ER and SW drafted the article and revised it critically. All authors approved the final version.

CONFLICT OF INTEREST

The authors have declared no conflicting interests.

ORCID

Hila Emmert  <https://orcid.org/0000-0002-7051-7350>

REFERENCES

- [1] T. Vos, A. D. Flaxman, M. Naghavi, R. Lozano, C. Michaud, M. Ezzati, K. Shibuya, J. A. Salomon, S. Abdalla, V. Aboyans, J. Abraham, I. Ackerman, R. Aggarwal, S. Y. Ahn, M. K. Ali, M. A. AlMazroa, M. Alvarado, H. R. Anderson, L. M. Anderson, K. G. Andrews, C. Atkinson, L. M. Baddour, A. N. Bahalim, S. Barker-Collo, L. H. Barrero, D. H. Bartels, M. G. Basáñez, A. Baxter, M. L. Bell, E. J. Benjamin, D. Bennett, E. Bernabé, K. Bhalla, B. Bhandari, B. Bikbov, A. B. Abdulhak, G. Birbeck, J. A. Black, H. Blencowe, J. D. Blore, F. Blyth, I. Bolliger, A. Bonaventure, S. Boufous, R. Bourne, M. Boussinesq, T. Braithwaite, C. Brayne, L. Bridgett, S. Brooker, P. Brooks, T. S. Brugha, C. Bryan-Hancock, C. Bucello, R. Buchbinder, G. Buckle, C. M. Budke, M. Burch, P. Burney, R. Burstein, B. Calabria, B. Campbell, C. E. Canter, H. Carabin, J. Carapetis, L. Carmona, C. Cella, F. Charlson, H. Chen, A. T. A. Cheng, D. Chou, S. S. Chugh, L. E. Coffeng, S. D. Colan, S. Colquhoun, K. E. Colson, J. Condon, M. D. Connor, L. T. Cooper, M. Corriere, M. Cortinovis, K. C. de Vaccaro, W. Couser, B. C. Cowie, M. H. Criqui, M. Cross, K. C. Dabhadkar, M. Dahiya, N. Dahodwala, J. Damsere-Derry, G. Danaei, A. Davis, D. De Leo, L. Degenhardt, R. Dellavalle, A. Delossantos, J. Denenberg, S. Derrett, D. C. Des Jarlais, S. D. Dharmaratne, M. Dherani, C. Diaz-Torne, H. Dolk, E. R. Dorsey, T. Driscoll, H. Duber, B. Ebel, K. Edmond, A. Elbaz, S. E. Ali, H. Erskine, P. J. Erwin, P. Espindola, S. E. Ewoigbokhan, F. Farzadfar, V. Feigin, D. T. Felson, A. Ferrari, C. P. Ferri, E. M. Fèvre, M. M. Finucane, S. Flaxman, L. Flood, K. Foreman, M. H. Forouzanfar, F. G. R. Fowkes, R. Franklin, M. Fransen, M. K. Freeman, B. J. Gabbe, S. E. Gabriel, E. Gakidou, H. A. Ganatra, B. Garcia, F. Gaspari, R. F. Gillum, G. Gmel, R. Gosselin, R. Grainger, J. Groeger, F. Guillemin,

- D. Gunnell, R. Gupta, J. Haagsma, H. Hagan, Y. A. Halasa, W. Hall, D. Haring, J. M. Haro, J. E. Harrison, R. Havmoeller, R. J. Hay, H. Higashi, C. Hill, B. Hoen, H. Hoffman, P. J. Hotez, D. Hoy, J. J. Huang, S. E. Ibeanusi, K. H. Jacobsen, S. L. James, D. Jarvis, R. Jasrasaria, S. Jayaraman, N. Johns, J. B. Jonas, G. Karthikeyan, N. Kassebaum, N. Kawakami, A. Keren, J. P. Khoo, C. H. King, L. M. Knowlton, O. Kobusingye, A. Koranteng, R. Krishnamurthi, R. Laloo, L. L. Laslett, T. Lathlean, J. L. Leasher, Y. Y. Lee, J. Leigh, S. S. Lim, E. Limb, J. K. Lin, M. Lipnick, S. E. Lipshultz, W. Liu, M. Loane, S. L. Ohno, R. Lyons, J. Ma, J. Mabweijano, M. F. MacIntyre, R. Malekzadeh, L. Mallinger, S. Manivannan, W. Marcenes, L. March, D. J. Margolis, G. B. Marks, R. Marks, A. Matsumori, R. Matzopoulos, B. M. Mayosi, J. H. McNulty, M. M. McDermott, N. McGill, J. McGrath, M. E. Medina-Mora, M. Meltzer, Z. A. Memish, G. A. Mensah, T. R. Merriman, A. C. Meyer, V. Miglioli, M. Miller, T. R. Miller, P. B. Mitchell, A. O. Mocumbi, T. E. Moffitt, A. A. Mokdad, L. Monasta, M. Montico, M. Moradi-Lakeh, A. Moran, L. Morawska, R. Mori, M. E. Murdoch, M. K. Mwaniki, K. Naidoo, M. N. Nair, L. Naldi, K. M. V. Narayan, P. K. Nelson, R. G. Nelson, M. C. Nevitt, C. R. Newton, S. Nolte, P. Norman, R. Norman, M. O'Donnell, S. O'Hanlon, C. Olives, S. B. Omer, K. Ortblad, R. Osborne, D. Ozgediz, A. Page, B. Pahari, J. D. Pandian, A. P. Rivero, S. B. Patten, N. Pearce, R. P. Padilla, F. Perez-Ruiz, N. Perico, K. Pesudovs, D. Phillips, M. R. Phillips, K. Pierce, S. Pion, G. V. Polanczyk, S. Polinder, C. A. Pope, S. Popova, E. Porrini, F. Pourmalek, M. Prince, R. L. Pullan, K. D. Ramaiah, D. Ranganathan, H. Razavi, M. Regan, J. T. Rehm, D. B. Rein, G. Remuzzi, K. Richardson, F. P. Rivara, T. Roberts, C. Robinson, F. R. De Leòn, L. Ronfani, R. Room, L. C. Rosenfeld, L. Rushton, R. L. Sacco, S. Saha, U. Sampson, L. Sanchez-Riera, E. Sanman, D. C. Schwebel, J. G. Scott, M. Segui-Gomez, S. Shahraz, D. S. Shepard, H. Shin, R. Shivakoti, D. Silberberg, D. Singh, G. M. Singh, J. A. Singh, J. Singleton, D. A. Sleet, K. Sliwa, E. Smith, J. L. Smith, N. J. C. Stapelberg, A. Steer, T. Steiner, W. A. Stolk, L. J. Stovner, C. Sudfeld, S. Syed, G. Tamburlini, M. Tavakkoli, H. R. Taylor, J. A. Taylor, W. J. Taylor, B. Thomas, W. M. Thomson, G. D. Thurston, I. M. Tleyjeh, M. Tonelli, J. A. Towbin, T. Truelsen, M. K. Tsilimbaris, C. Ubeda, E. A. Undurraga, M. J. van der Werf, J. van Os, M. S. Vavilala, N. Venketasubramanian, M. Wang, W. Wang, K. Watt, D. J. Weatherall, M. A. Weinstock, R. Weintraub, M. G. Weisskopf, M. M. Weissman, R. A. White, H. Whiteford, S. T. Wiersma, J. D. Wilkinson, H. C. Williams, S. R. M. Williams, E. Witt, F. Wolfe, A. D. Woolf, S. Wulf, P. H. Yeh, A. K. M. Zaidi, Z. J. Zheng, D. Zonies, A. D. Lopez, C. J. L. Murray, *Lancet* **2012**, 380, 2163.
- [2] R. J. Hay, N. E. Johns, H. C. Williams, I. W. Bolliger, R. P. Dellavalle, D. J. Margolis, R. Marks, L. Naldi, M. A. Weinstock, S. K. Wulf, C. Michaud, C. J. L. Murray, M. Naghavi, *J. Invest. Dermatol.* **2014**, 134, 1527.
- [3] J. E. Greb, A. M. Goldminz, J. T. Elder, M. G. Lebwohl, D. D. Gladman, J. J. Wu, N. N. Mehta, A. Y. Finlay, A. B. Gottlieb, *Nat. Rev. Dis. Primers* **2016**, 2, 16082.
- [4] S. Weidinger, L. A. Beck, T. Bieber, K. Kabashima, A. D. Irvine, *Nat. Rev. Dis. Primers* **2018**, 4, 1.
- [5] B. Li, L. C. Tsoi, W. R. Swindell, J. E. Gudjonsson, T. Tejasvi, A. Johnston, J. Ding, P. E. Stuart, X. Xing, J. J. Kochkodan, J. J. Voorhees, H. M. Kang, R. P. Nair, G. R. Abecasis, J. T. Elder, *J. Invest. Dermatol.* **2014**, 134, 1828.
- [6] L. C. Tsoi, E. Rodriguez, F. Degenhardt, H. Baurecht, U. Wehkamp, N. Volks, S. Szymczak, W. R. Swindell, M. K. Sarkar, K. Raja, S. Shao, M. Patrick, Y. Gao, R. Uppala, B. E. Perez White, S. Getsios, P. W. Harms, E. Maverakis, J. T. Elder, A. Franke, J. E. Gudjonsson, S. Weidinger, *J. Invest. Dermatol.* **2019**, 139, 1480.
- [7] Y. Okayama, *Curr. Drug Targets Inflamm. Allergy* **2005**, 4, 517.
- [8] H. Ji, X. K. Li, *Oxid. Med. Cell Longev.* **2016**, 2016, 2721469.
- [9] T. Finkel, *Curr. Opin. Cell Biol.* **2003**, 15, 247.
- [10] T. Finkel, N. J. Holbrook, *Nature* **2000**, 408, 239.
- [11] H. E. Kanavy, M. R. Gerstenblith, *Semin. Cutan. Med. Surg.* **2011**, 30, 222.
- [12] J. L. Martindale, N. J. Holbrook, *J. Cell Physiol.* **2002**, 192, 1.
- [13] P. D. Ray, B. W. Huang, Y. Tsuji, *Cell Signal.* **2012**, 24, 981.
- [14] D. P. Kadam, A. N. Suryakar, R. D. Ankush, C. Y. Kadam, K. H. Deshpande, *Indian J. Clin. Biochem.* **2010**, 25, 388.
- [15] H. Nemati, K. Reza, S. Masoud, E. Ali, R. Mansour, A. Vaisi-Raygani, *Cell Biochem. Funct.* **2014**, 32, 268.
- [16] V. M. Pujari, S. Ireddy, I. Itagi, S. Kumar H, *J. Clin. Diagn. Res.* **2014**, 8, CC14.
- [17] V. Relhan, S. K. Gupta, S. Dayal, R. Pandey, H. Lal, *J. Dermatol.* **2002**, 29, 399.
- [18] N. Omata, H. Tsukahara, S. Ito, Y. Ohshima, M. Yasutomi, A. Yamada, M. Jiang, M. Hiraoka, M. Nambu, Y. Deguchi, M. Mayumi, *Life Sci.* **2001**, 69, 223.
- [19] J. Chung, S. Y. Oh, Y. K. Shin, *Clin. Chem. Lab. Med.* **2009**, 47, 1475.
- [20] N. Sivarajani, S. V. Rao, G. Rajeev, *J. Clin. Diagn. Res.* **2013**, 7, 2683.
- [21] K. Nakai, K. Yoneda, R. Maeda, A. Munehiro, N. Fujita, I. Yokoi, J. Morieue, T. Morieue, H. Kosaka, Y. Kubota, *J. Eur. Acad. Dermatol. Venereol.* **2009**, 23, 1405.
- [22] G. Drewa, E. Krzyzyska-Malinowska, A. Wozniak, F. Protas-Drozd, C. Mila-Kierzenkowska, M. Rozwodowska, B. Kowaliszyn, R. Czajkowski, *Med. Sci. Monit.* **2002**, 8, BR338.
- [23] S. A. Gabr, A. H. Al-Ghadir, *Arch. Dermatol. Res.* **2012**, 304, 451.
- [24] A. Wozniak, G. Drewa, E. Krzyzyska-Malinowska, R. Czajkowski, F. Protas-Drozd, C. Mila-Kierzenkowska, M. Rozwodowska, M. Soponska, E. Czarnecka-Zaba, *Med. Sci. Monit.* **2007**, 13, CR30.
- [25] M. Yildirim, H. S. Inaloz, V. Baysal, N. Delibas, *J. Eur. Acad. Dermatol. Venereol.* **2003**, 17, 34.
- [26] F. X. Bernard, F. Morel, M. Camus, N. Pedretti, C. Barrault, J. Garnier, J. C. Lecron, *J. Allergy (Cairo)* **2012**, 2012, 718725.
- [27] A. Sallmyr, J. Fan, F. V. Rassool, *Cancer Lett.* **2008**, 270, 1.
- [28] U. S. Srinivas, B. W. Q. Tan, B. A. Vellayappan, A. D. Jayasekharan, *Redox Biol.* **2019**, 25, 101084.
- [29] J. Kralova, M. Dvorak, M. Koc, V. Kral, *Oncogene* **2008**, 27, 3010.
- [30] P. J. Roberts, C. J. Der, *Oncogene* **2007**, 26, 3291.
- [31] B. Gibert, E. Hadchity, A. Czekalla, M. T Aloy, P. Colas, C. Rodriguez-Lafrasse, A. P. Arrigo, C. Diaz-Latoud, *Oncogene* **2011**, 30, 3672.
- [32] H. Chang, W. Oehrl, P. Elsner, J. J. Thiele, *Free Radic. Res.* **2003**, 37, 655.
- [33] T. Zuliani, V. Denis, E. Noblesse, S. Schnebert, P. Andre, M. Dumas, M. H. Ratinaud, *Free Radic. Biol. Med.* **2005**, 38, 307.
- [34] M. Furue, T. Kadono, *Inflamm. Res.* **2017**, 66, 833.
- [35] E. Guttman-Yassky, J. G. Krueger, M. G. Lebwohl, *Exp. Dermatol.* **2018**, 27, 409.
- [36] E. Guttman-Yassky, J. G. Krueger, *Curr. Opin. Immunol.* **2017**, 48, 68.
- [37] D. R. Bickers, M. Athar, *J. Invest. Dermatol.* **2006**, 126, 2565.
- [38] S. Reuter, S. C. Gupta, M. M. Chaturvedi, B. B. Aggarwal, *Free Radic. Biol. Med.* **2010**, 49, 1603.
- [39] A. Trautmann, M. Akdis, D. Kleemann, F. Altnauer, H. U. Simon, T. Graeve, M. Noll, E. B. Bröcker, K. Blaser, C. A. Akdis, *J. Clin. Invest.* **2000**, 106, 25.
- [40] T. Schwarz, *J. Clin. Invest.* **2000**, 106, 9.
- [41] H. Valdimarsson, B. S. Bake, I. Jónsdóttir, L. Fry, *Immunol. Today* **1986**, 7, 256.
- [42] S. R. Steinhilb, *Am. J. Cardiol.* **2008**, 101, 14D.
- [43] F. A. S. Addor, *An. Bras. Dermatol.* **2017**, 92, 356.
- [44] S. Altenhofer, K. A. Radermacher, P. W. M. Kleikers, K. Wingler, H. H. W. Schmidt, *Antioxid. Redox Signal.* **2015**, 23, 406.
- [45] C. Riganti, E. Gazzano, M. Polimeni, C. Costamagna, A. Bosia, D. Ghigo, *J. Biol. Chem.* **2004**, 279, 47726.
- [46] F. Augsburger, A. Filippova, D. Rasti, T. Seredenina, M. Lam, G. Maghzal, Z. Mohiout, P. Jansen-Durr, U. G. Knaus, J. Doroshow, R. Stocker, K. H. Krause, V. Jaquet, *Redox Biol.* **2019**, 26, 101272.

- [47] M. Munoz, M. P. Martínez, M. E. López-Oliva, C. Rodríguez, C. Corbacho, J. Carballido, A. García-Sacristán, M. Hernández, L. Rivera, J. Sáenz-Medina, D. Prieto, *Redox Biol.* **2018**, *19*, 92.
- [48] B. Laleu, F. Gaggini, M. Orchard, L. Fioraso-Cartier, L. Cagnon, S. Houngninou-Molango, A. Gradia, G. Duboux, C. Merlot, F. Heitz, C. Szyndralewicz, P. Page, *J. Med. Chem.* **2010**, *53*, 7715.
- [49] M. Kumar, M. Garand, S. Al Khodor, *J. Transl. Med.* **2019**, *17*, 419.
- [50] G. Teixeira, C. Szyndralewicz, S. Molango, S. Carnesecchi, F. Heitz, J. M. Wiesel, J. M. Wood, *Br. J. Pharmacol.* **2017**, *174*, 1647.
- [51] A. M. Maley, J. L. Arbiser, *Exp. Dermatol.* **2013**, *22*, 775.
- [52] A. H. Jang, T. H. Kim, G. D. Kim, J. E. Kim, H. J. Kim, S. S. Kim, Y. H. Jin, Y. S. Park, C. S. Park, *Int. Immunopharmacol.* **2011**, *11*, 1271.
- [53] S. Revoltella, G. Baraldo, B. Waltenberger, S. Schwaiger, P. Kofler, J. Moesslacher, A. Huber-Seidel, K. Pagitz, R. Kohl, P. Jansen-Duerr, H. Stuppner, *Molecules* **2018**, *23*, 653.
- [54] K. Gunduz, P. Demireli, S. Vatansever, I. Inanir, *J. Cutan. Pathol.* **2006**, *33*, 788.
- [55] K. Kawashima, H. Doi, Y. Ito, M. A. Shibata, R. Yoshinaka, Y. Otsuki, *J. Dermatol. Sci.* **2004**, *35*, 207.

SUPPORTING INFORMATION

Additional supporting information may be found online in the Supporting Information section.

Figure S1. Immunofluorescence staining of pH2AX in atopic dermatitis (AD)- and psoriasis (PSO)- model keratinocytes treated with H₂O₂ and diphenyleneiodonium chloride (DPI).

Figure S2. Immunofluorescence staining of NADPH oxidase 1 (NOX1) in atopic dermatitis (AD)- and psoriasis (PSO)- model keratinocytes treated with H₂O₂ and diphenyleneiodonium chloride (DPI).

Figure S3. Immunofluorescence staining of NADPH oxidase 4 (NOX4) in atopic dermatitis (AD)- and psoriasis (PSO)- model keratinocytes treated with H₂O₂ and diphenyleneiodonium chloride (DPI).

Figure S4. Immunofluorescence staining of p22phox in atopic dermatitis (AD)- and psoriasis (PSO)- model keratinocytes treated with H₂O₂ and diphenyleneiodonium chloride (DPI).

App S1. Supplementary figures.


How to cite this article: Emmert H, Fonfara M, Rodriguez E, Weidinger S. NADPH oxidase inhibition rescues keratinocytes from elevated oxidative stress in a 2D atopic dermatitis and psoriasis model. *Exp Dermatol.* 2020;29:749–758. <https://doi.org/10.1111/exd.14148>

5.2 Article II

This article was published in the Journal of European Academy of Dermatology & Venereology, Melina Fonfara, Jan Hartmann, Dora Stölzl, Nicole Sander, Inken Harder, Elke Rodriguez, Matthias Hübenthal, Carsten Mazur, Sebastian Kerzel, Michael Kabesch, Jochen Schmitt, Hila Emmert, Ina Suhrkamp, Stephan Weidinger, Stratum corneum and microbial biomarkers precede and characterize childhood atopic dermatitis, online ahead of print. DOI: 10.1111/jdv.19932.

SHORT REPORT

Stratum corneum and microbial biomarkers precede and characterize childhood atopic dermatitis

Melina Fonfara¹ | Jan Hartmann¹  | Dora Stölzl¹ | Nicole Sander¹ | Inken Harder¹ |
Elke Rodriguez¹ | Matthias Hübenthal¹ | Carsten Mazur¹ | Sebastian Kerzel² |
Michael Kabesch² | Jochen Schmitt³ | Hila Emmert¹ | Ina Suhrkamp¹ |
Stephan Weidinger¹

¹Department of Dermatology and Allergy, University Hospital Schleswig-Holstein, Kiel, Germany

²Department of Pediatric Pneumology and Allergy, University Children's Hospital Regensburg (KUNO), Clinic St. Hedwig, Regensburg, Germany

³Center of Evidence-based Healthcare, University Hospital and Medical Faculty Carl Gustav Carus, TU Dresden, Dresden, Germany

Correspondence

Stephan Weidinger, Department of Dermatology and Allergy, University Hospital Schleswig-Holstein, Campus Kiel, Arnold-Heller-Str. 3, 24105 Kiel, Germany.
Email: sweidinger@dermatology.uni-kiel.de

Funding information

BIOMAP; LA ROCHE-POSAY Laboratoire Pharmaceutique, France

Abstract

Background: Atopic dermatitis (AD) is the most common paediatric inflammatory skin disease. There are currently no robust biomarkers that could reliably predict its manifestation, and on the molecular level, it is less well characterized than adult AD.

Objectives: This study aimed to extend previous findings and provide evidence for distinct changes of the epidermal proteome and microbiome preceding the onset of AD as well as characterizing early AD.

Methods: We longitudinally analysed epidermal biomarker levels and microbial profiles in a cohort of 50 neonates at high risk for AD, who had participated in a randomized controlled trial on early emollient use for AD prevention.

Results: About 26% of the infants developed AD until month 24 with an average age of 10 month at disease onset. In children with later AD, IL-1Ra, TNFβ, IL-8, IL-18, IL-22, CCL2, TARC, TSLP and VEGFa showed increased levels prior to disease manifestation with levels of IL-1Ra, TNFβ and VEGFa already increased shortly after birth. Further, children with later AD displayed a delayed maturation and differentially composed skin microbiome prior to AD onset. At manifestation, levels of multiple Th2, Th17/22 and Th1-associated biomarkers as well as innate immunity markers were elevated, and abundances of commensal *Streptococcus* species were reduced in favour of *Staphylococcus epidermidis*.

Conclusions: Our results indicate that elevations of proinflammatory stratum corneum biomarkers and alterations of the skin microbiome precede paediatric AD and characterize the disease at onset.

INTRODUCTION

Atopic dermatitis (AD) is the most common paediatric inflammatory skin disease with a one-year prevalence of up to 15%.^{1,2} Its pathogenesis involves a complex interplay between type-2 dominated cutaneous inflammation, impaired skin barrier function including decreased stratum corneum

hydration and increased transepidermal water loss (TEWL), as well as skin dysbiosis.¹

Previous studies reported that an increase of epidermal levels of TARC (CCL17), TSLP, IL-8, IL-18 and IL-13³⁻⁵ as well as a reduced colonization with commensal *Staphylococci* precede AD manifestation, although exact microbial predictors of infant AD remain elusive.⁶⁻⁹ At present in the absence of

Melina Fonfara, Jan Hartmann and Dora Stölzl Shared first authorship.

This is an open access article under the terms of the [Creative Commons Attribution-NonCommercial](https://creativecommons.org/licenses/by-nc/4.0/) License, which permits use, distribution and reproduction in any medium, provided the original work is properly cited and is not used for commercial purposes.

© 2024 The Authors. *Journal of the European Academy of Dermatology and Venereology* published by John Wiley & Sons Ltd on behalf of European Academy of Dermatology and Venereology.

robust biomarkers, the development and course of AD cannot be predicted reliably, and there are no well-established primary prevention measures. Although the importance of epidermal barrier dysfunction in AD has stimulated approaches of a preventive use of basic barrier-restoring emollients, clinical studies yielded conflicting results.^{10,11} In this study, we longitudinally analysed stratum corneum expression of selected candidate biomarkers and skin microbiome composition in a cohort of 50 newborns at high risk for AD who had previously participated in a recently described randomized open-label prospective study of emollient use.¹²

METHODS

Data and samples from 50 children from a previously described parallel group, assessor-blind, randomized open-label prospective study of emollient use in neonates at high risk for atopic dermatitis (AD) were used in this study.¹² Thirty-nine of the 50 children contributed tape strip samples whereas all 50 infants contributed skin swab samples for this analysis, both of which were collected at the antecubital fossa. Briefly, proteins from tape strips and DNA from swabs was extracted and analysed using Luminex and 16S amplicon sequencing, respectively (For detailed methods, see Online Repository material). For analysis of epidermal proteins, raw median fluorescence intensity was used independently of total protein amount.¹³

RESULTS AND DISCUSSION

Across all study visits (Days 2–21 after birth/baseline, months 6, 12 and 24 and/or at interim visit due to manifestation of AD), infants who had received emollients from birth and donated tape strips ($n=17$) displayed lower levels of IL-6, TARC (CCL17), MDC (CCL22), IL-1Ra, IL-16, MCP-1 (CCL2), TNF β , TSLP, IL-18 and IL-22 than infants of the control group ($n=22$), indicating potential anti-inflammatory effects of early emollient use (Table S1).

13 (26%) of 50 the infants developed AD until month 24 with an average age at manifestation of 9.6 months and no significant difference between the two groups. For better comparability between children with and without AD, we used epidermal protein profiles of children with no later AD determined at the closest study visit to the mean age of AD manifestation, hence reducing the impact of natural variation of cytokine levels over time to the extent possible. Cytokine levels were corrected for emollient intervention as confounder.

In children with later AD, epidermal levels of IL-1Ra, TNF β and VEGFa were significantly upregulated as early as 2–21 days after birth, though significance did not withstand correction for emollient use (Table 1; Figure 1a).

Previous studies reported an association of stratum corneum levels of TSLP and TARC with later AD development as well as IL-8 and IL-18 with later moderate to severe AD

manifestation.^{3,5} In line with this, we observed significantly increased levels of TARC, IL-8 and IL-18 in children with later AD averaged across all study visits prior to disease manifestation. We also observed elevations of additional markers prior to AD manifestation such as IL-22, which can promote abnormal keratinocyte proliferation and differentiation and amplify inflammation, MCP-1 (CCL2), which regulates the migration and infiltration of memory T lymphocytes and natural killer (NK) cells, as well as VEGFa, which enhances microvascular permeability¹⁴ (Table 1; Figure 1b).

At AD onset multiple additional protein markers involved in AD pathology were upregulated, in particular markers associated with Th2 immune responses (MCP-1 (CCL2), TARC (CCL17), MDC (CCL22), IL-31, TSLP, MCP-4 (CCL13)), but also markers linked to Th1 (IP-10, IFN γ) and Th17/Th22 (IL-17a, IL-22, IL-23) immune responses, as well as key innate and adaptive immune markers (IL-1 β , IL-6, IL-8, IL-16, IL-18, IL-1Ra, TNF α , TNF β , VEGFa) (Table 1; Figure 1c). Taken together, our data extend previous observations and highlight noninvasively collected skin biomarkers that characterize paediatric AD at onset as well as markers that precede the onset of AD. Interestingly, those marker level increases could be measured at a skin site that typically displays AD lesions not before later childhood (Table S3).¹⁵

Across all infants, the diversity of the skin microbiome continuously increased over time potentially reflecting its maturation (Figure 2a).^{8,16} Interestingly, in children who later developed AD, the most abundant 14 core amplicon sequence variants (ASVs) showed significantly more variance over time ($p=0.04$) indicating that the establishment of a stable skin microbiome might be delayed (Figure 2b). In line with previous observations, children with later AD also displayed an altered skin microbiome composition at time points prior to and at manifestation of AD (Figure 2c; Table 2).^{6–8,17} Of note, already at the baseline visit of these children *Staphylococcus epidermidis*, *Streptococcus vestibularis* and *Streptococcus oralis* showed increased abundances, whereas the abundance of *Staphylococcus hominis* was decreased. At the timepoints before AD manifestation, abundances of multiple *Staphylococcus epidermidis* ASVs were increased and abundances of *Streptococcus oralis*, *Streptococcus vestibularis* and multiple *Streptococcus mitis* ASVs were decreased compared to children with no later AD. Finally, at disease onset the abundances of *Staphylococcus epidermidis* continued to be increased while *Streptococcus oralis* and *Streptococcus vestibularis* abundances showed a further reduction (Figure 2c; Table 2). Of note, at AD onset the skin microbiome was dominated by *Staphylococcus epidermidis*, while essentially no *Staphylococcus aureus* sequences were present in the samples in our cohort, even at sites typically affected by AD, which is in line with previous reports.⁶ Taken together, children with future AD appear to display early alterations and a delayed maturation of the skin microbiome with distinct features maintained from birth until disease onset.

Overall, our results confirm and extend previous findings and provide evidence for distinct changes of the epidermal

TABLE 1 Stratum corneum biomarker levels at baseline, prior to AD manifestation and at time of AD onset.

Cytokine	Baseline			Pre AD			AD onset		
	Effect size	<i>p</i> -value	<i>p</i> -adjusted	Effect size	<i>p</i> -value	<i>p</i> -adjusted	Effect size	<i>p</i> -value	<i>p</i> -adjusted
IL-1b	1.06	0.18	0.45	1.06	0.068	0.080	1.20	<0.001	<0.001
IP-10 (CXCL10)	1.06	0.36	0.72	1.13	0.003	0.010	1.16	0.003	0.004
IL-6	1.06	0.51	0.76	1.12	0.043	0.073	1.27	0.003	0.004
IL-8 (CXCL8)	1.12	0.41	0.72	1.35	<0.001	0.001	1.80	<0.001	<0.001
TARC (CCL17)	1.16	0.18	0.45	1.23	0.001	0.006	1.30	0.001	0.002
MDC (CCL22)	1.05	0.73	0.85	1.17	0.039	0.073	1.44	0.001	0.002
IL-17a	1.05	0.62	0.83	1.12	0.045	0.073	1.27	0.002	0.002
IL-31	1.03	0.87	0.93	1.05	0.692	0.726	1.84	0.001	0.002
IL-1Ra	6.07	0.05	0.35	1.23	0.818	0.818	32.70	0.001	0.002
IFN γ	1.00	0.93	0.93	1.06	0.063	0.078	1.14	0.003	0.004
TNF α	1.07	0.38	0.72	1.10	0.063	0.078	1.24	0.001	0.002
IL-16	1.04	0.63	0.83	1.12	0.057	0.078	1.22	0.02	0.02
MCP-1 (CCL2)	1.23	0.15	0.45	1.48	<0.001	0.001	1.52	0.001	0.002
TNFB	1.70	0.04	0.35	1.58	0.017	0.050	2.57	0.001	0.002
TSLP	1.06	0.48	0.76	1.13	0.028	0.063	1.21	0.01	0.01
IL-1a	55.01	0.70	0.85	448.17	0.061	0.078	17.71	0.87	0.87
IL-23	1.18	0.13	0.45	1.20	0.030	0.063	1.38	<0.001	0.002
IL-18	1.12	0.19	0.45	1.22	<0.001	0.003	1.34	<0.001	<0.001
MCP-4 (CCL13)	1.00	0.91	0.93	1.01	0.495	0.548	1.03	0.03	0.03
IL-22	1.23	0.13	0.45	1.33	0.001	0.003	1.49	<0.001	0.001
VEGFa	7.08	0.01	0.20	3.81	0.019	0.05	17.79	<0.001	<0.001

Note: Comparison of epidermal cytokine levels between healthy and diseased children was performed using analysis of variance (ANOVA). Epidermal cytokine levels of healthy children at 12 months of age were used for comparison. Effect sizes and *p*-values prior to AD manifestation and at AD onset were corrected for emollient use and multiple testing.

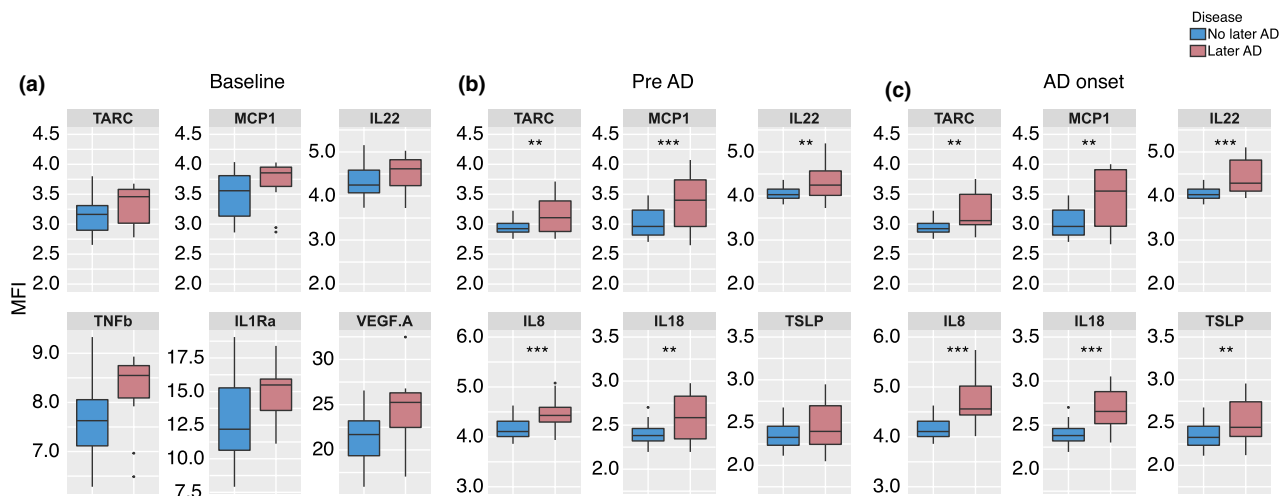


FIGURE 1 Stratum corneum biomarker levels in children with later AD as compared to children with no later AD: (a) At Baseline: Biomarker levels at baseline visit (2–21 days after birth) in children with later AD as compared to children with no later AD. (b) Prior to AD manifestation: Biomarker levels of children with later AD across timepoints prior to disease manifestation as compared to children with no later AD. (c) At AD onset: Biomarker levels at AD onset compared children with no later AD. Median fluorescence intensities were transformed using box cox transformation. For comparison between no AD and AD analysis of variance was performed and *p*-values were corrected for intervention. Significant alterations are marked by asterisks (*p*-values Benjamini–Hochberg adjusted for multiple testing, * $p_{adj} < 0.05$; ** $p_{adj} < 0.01$; *** $p_{adj} < 0.001$).

proteome and microbiome preceding the onset of AD and characterizing early AD (Table S3).

Limitations of our study are the small sample size, the exclusive analysis of children at familial risk for AD,

the lack of follow-up samples for severity analysis and the focus on volar forearm samples, which makes these findings not necessarily generalizable for paediatric AD at large.

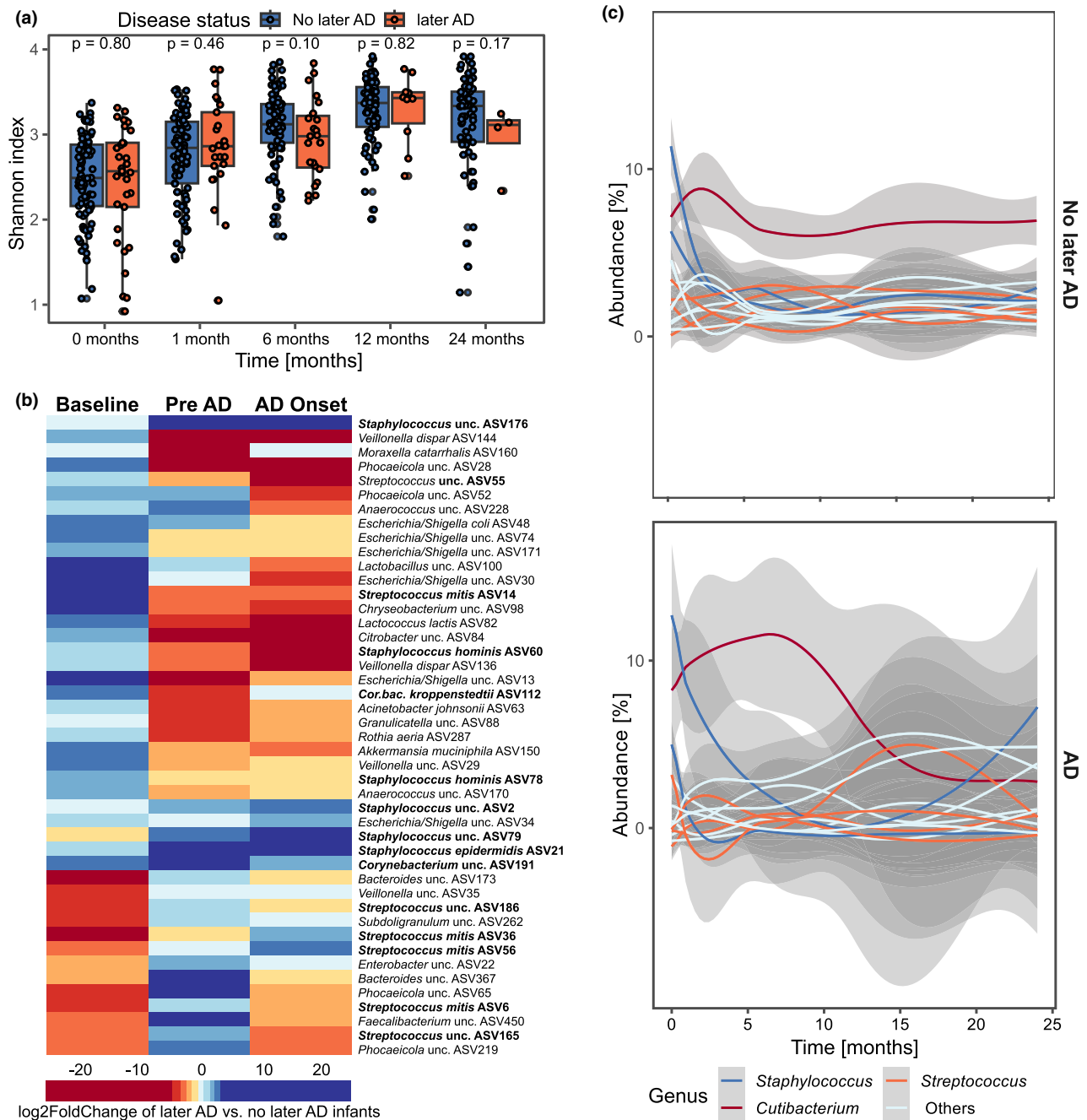


FIGURE 2 Skin microbiome. (a) Alpha diversity (Shannon Index) over the first 24 months, stratified by children with and without later AD. Wilcoxon rank-sum test p -values indicate differences between the groups at each timepoint. (b) LOESS regression displaying the relative abundance of core ASVs over time stratified by later AD and no AD. (c) Heatmap of log2FoldChanges of later AD vs no AD at baseline, averaged across time points prior to disease manifestation and at AD onset. Only ASVs which are classified at genus level, significantly differentially abundant and show a Log2FoldChange > 2 at least one timepoint are shown.

We further decided to perform analysis on raw MFI values that were not corrected for stratum corneum amount in order to minimize potential sources of error. However, an important limitation of this approach is the presence of interindividual differences due to differences in stratum corneum structure that were not considered. Finally, only selected biomarkers were measured, limiting the scope of investigation to pre-defined proteins.

Major strengths are the prospective study design and the dense and detailed follow-up.

The results of our and previous studies also imply that minimally invasive sampling methods have the potential to identify clinically useful skin biomarkers for AD. However, more studies with larger sample sizes and broader profiling are needed to work out the most conclusive and robust markers.

TABLE 2 Microbial differences of children with later AD vs. children with no later AD, determined at baseline (2–21 days after birth), prior to AD manifestation and at time of AD onset.

Microbial ASV	Baseline		Pre AD		AD onset	
	Log2FoldChange	<i>p</i> -adjusted	Log2FoldChange	<i>p</i> -adjusted	Log2FoldChange	<i>p</i> -adjusted
ASV2 Staphylococcus NA	0.62	0.49	2.66	<0.001	4.02	<0.001
ASV6 Streptococcus mitis	−2.57	0.03	2.91	0.25	0.71	0.85
ASV15 Staphylococcus hominis	−2.20	0.07	8.94	<0.001	11.39	<0.001
ASV21 Staphylococcus epidermidis	−1.06	0.35	4.69	0.02	3.56	0.16
ASV25 Streptococcus mitis	2.32	<0.001	0.05	0.99	−0.98	0.73
ASV26 Streptococcus vestibularis	4.19	<0.001	−5.08	0.01	−6.28	0.01
ASV28 Phocaeicola NA	4.15	<0.001	−7.55	0.01	−23.13	<0.001
ASV35 Veillonella NA	1.64	0.04	−2.15	0.35	4.60	0.07
ASV36 Streptococcus mitis	−3.39	0.01	−2.22	0.48	3.11	0.39
ASV41 Bacteroides uniformis	2.80	0.04	−0.90	0.78	−3.47	0.29
ASV48 Escherichia/Shigella coli	−3.36	0.001	22.85	<0.001	<0.001	NA
ASV52 Phocaeicola NA	2.28	0.02	1.30	0.78	−1.12	0.87
ASV61 Streptococcus NA	3.10	<0.001	−2.49	0.59	2.60	0.59
ASV65 Phocaeicola NA	5.82	<0.001	6.24	0.11	3.29	0.57
ASV72 Kocuria rhizophila	2.03	0.04	2.53	0.17	2.61	0.30
ASV76 Klebsiella NA	3.01	<0.001	2.03	NA	−0.86	NA
ASV79 Staphylococcus NA	−1.07	0.38	4.10	0.10	6.70	0.01
ASV93 Phocaeicola NA	1.08	0.35	7.90	0.02	4.80	0.39
ASV94 Collinsella aerofaciens	1.43	0.01	6.70	0.09	2.30	NA
ASV96 Streptococcus mitis	6.41	<0.001	−5.17	0.21	0.47	0.96
ASV99 Klebsiella NA	3.50	<0.001	−0.80	NA	0.93	NA
ASV107 Streptococcus mitis	3.62	<0.001	−1.46	NA	0.61	0.95
ASV108 Streptococcus oralis	2.94	<0.001	−2.29	0.19	−4.16	0.03
ASV135 NA NA	2.87	<0.001	−25.09	<0.001	−3.57	0.46
ASV138 Bacteroides thetaiotaomicron	5.01	<0.001	6.99	0.07	−0.28	NA
ASV139 Parabacteroides merdae	8.42	<0.001	6.46	0.10	<0.001	NA
ASV148 Streptococcus NA	3.05	0.01	−3.19	0.48	−22.98	<0.001
ASV150 Akkermansia muciniphila	2.77	0.002	−0.49	NA	0.15	NA
ASV152 Phocaeicola NA	6.43	<0.001	0.00	NA	<0.001	NA
ASV160 Moraxella catarrhalis	−0.15	0.83	−4.88	0.12	5.74	0.03
ASV161 Streptococcus mitis	3.94	<0.001	8.34	0.03	−0.05	1.00
ASV162 Roseomonas NA	3.32	<0.001	−1.46	0.49	−0.58	0.83
ASV170 Anaerococcus NA	3.56	<0.001	2.51	0.59	2.58	0.59
ASV173 Bacteroides NA	6.52	<0.001	2.61	NA	22.79	<0.001
ASV176 Staphylococcus epidermidis	3.36	0.01	25.47	<0.001	26.03	<0.001
ASV177 Escherichia/Shigella coli	2.93	<0.001	<0.001	NA	NA	NA
ASV196 Parabacteroides distasonis	3.69	<0.001	NA	NA	NA	NA

(Continues)

TABLE 2 (Continued)

Microbial ASV	Baseline		Pre AD		AD onset	
	Log2FoldChange	<i>p</i> -adjusted	Log2FoldChange	<i>p</i> -adjusted	Log2FoldChange	<i>p</i> -adjusted
ASV206 <i>Bacteroides</i> NA	4.59	<0.001	<0.001	NA	NA	NA
ASV213 <i>Bacteroides</i> uniformis	6.04	<0.001	−1.88	NA	−0.07	NA
ASV226 <i>Bacteroides</i> xylanisolvens	6.50	<0.001	<0.001	NA	<0.001	NA
ASV228 <i>Anaerococcus</i> NA	2.18	0.01	8.57	0.02	−0.95	NA
ASV231 <i>Parabacteroides</i> NA	3.80	<0.001	−4.75	NA	−0.001	1.00
ASV239 <i>Bacteroides</i> ovatus	2.70	<0.001	−0.82	NA	−0.76	NA
ASV260 <i>Faecalibacterium</i> NA	2.80	<0.001	−2.38	0.60	−1.23	0.83
ASV263 <i>Lachnospira</i> NA	7.24	<0.001	3.85	0.27	0.70	NA
ASV265 <i>Roseburia</i> intestinalis	2.24	0.03	2.36	NA	−1.22	NA
ASV272 <i>Parabacteroides</i> distasonis	4.08	<0.001	2.65	0.56	−0.97	NA
ASV294 <i>Ruminococcus</i> NA	6.16	<0.001	4.92	0.24	1.49	NA
ASV303 NA NA	2.28	<0.001	−1.19	NA	0.54	NA
ASV311 <i>Bacteroides</i> NA	4.35	<0.001	−0.81	NA	−0.76	NA
ASV327 <i>Alistipes</i> putredinis	3.10	0.002	0.79	NA	−3.60	NA
ASV338 NA NA	4.81	<0.001	−1.30	NA	−0.01	NA
ASV355 <i>Escherichia/Shigella</i> coli	2.71	<0.001	<0.001	NA	NA	NA
ASV364 <i>Parasutterella</i> NA	1.54	0.04	4.54	0.27	NA	NA
ASV367 <i>Bacteroides</i> NA	4.04	<0.001	4.38	NA	<0.001	NA
ASV378 <i>Alistipes</i> onderdonkii	2.74	<0.001	0.79	NA	0.43	NA
ASV394 <i>Eggerthella</i> lenta	2.82	<0.001	0.95	NA	0.61	NA
ASV417 <i>Flavonifractor</i> plautii	1.64	0.004	−2.34	NA	2.40	NA
ASV450 <i>Faecalibacterium</i> NA	1.67	0.04	2.81	0.54	1.13	NA

Note: Comparison of microbial ASV abundances between later AD and no later AD was performed using DESeq2 negative binomial modelling with emollient use as co-factor and including *p*-value adjustment for multiple testing using Benjamini–Hochberg correction. Log2Fold changes are presented as AD compared to no AD children.

Abbreviation: ASV, Amplicon sequence variant.

ACKNOWLEDGEMENTS

NGS analyses were carried out at the Competence Centre for Genomic Analysis (Kiel). Open Access funding enabled and organized by Projekt DEAL.

FUNDING INFORMATION

The EARLYemollient Study was financially supported by LA ROCHE-POSAY Laboratoire Pharmaceutique, France. LA ROCHE-POSAY was not involved in the study design, the collection, analysis and interpretation of data, and the writing of and the decision to submit this article for publication.

This work was also supported by the BIOMAP project. This project has received funding from the Innovative Medicines Initiative 2 Joint Undertaking (JU) under grant agreement No 821511. The JU receives support from the European Union's Horizon 2020 research and innovation programme and EFPIA. This publication reflects only the author's view, and the JU is not responsible for any use that may be made of the information it contains.

This work was further supported by the DFG Research Infrastructure NGS_CC (project 407495230) as part of the Next Generation Sequencing Competence Network (project 423957469).

CONFLICT OF INTEREST STATEMENT

S. Weidinger has received institutional research grants from Sanofi Deutschland GmbH, LEO Pharma and Pfizer, and performed consultancies and/or lectures for AbbVie, Almirall, Boehringer, Eli Lilly, Galderma, Kymab, Leo Pharma, Pfizer, Regeneron and Sanofi. J. Schmitt has received institutional grants from Novartis and Pfizer for scientifically initiated research; and has received honoraria for consulting from Sanofi, Lilly, Novartis and ALK. H. Emmert has received an institutional research grant from LEO Pharma. Matthias Hübenal has performed consulting work for Sanofi. S. Kerzel has performed consultancies and/or lectures for Regeneron and Sanofi. The other authors declare that they have no relevant conflicts of interest.

DATA AVAILABILITY STATEMENT

The data that support the findings of this study are available on request from the corresponding author. The data are not publicly available due to privacy and ethical restrictions.

ORCID

Jan Hartmann  <https://orcid.org/0000-0003-1842-8219>

REFERENCES

1. Langan SM, Irvine AD, Weidinger S. Atopic dermatitis. *Lancet*. 2020;396(10247):345–60.
2. Silverberg JI, Barbarot S, Gadkari A, Simpson EL, Weidinger S, Mina-Osorio P, et al. Atopic dermatitis in the pediatric population: a cross-sectional, international epidemiologic study. *Ann Allergy Asthma Immunol*. 2021;126(4):417–428.e2.
3. Rinnov MR, Halling AS, Gerner T, Ravn NH, Knudgaard MH, Trautner S, et al. Skin biomarkers predict development of atopic dermatitis in infancy. *Allergy*. 2023;78(3):791–802.
4. Halling AS, Rinnov MR, Ruge IF, Gerner T, Ravn NH, Knudgaard MH, et al. Skin TARC/CCL17 increase precedes the development of childhood atopic dermatitis. *J Allergy Clin Immunol*. 2023;151(6):1550–1557.e6.
5. Berdyshev E, Kim J, Kim BE, Goleva E, Lyubchenko T, Bronova I, et al. Stratum corneum lipid and cytokine biomarkers at age 2 months predict the future onset of atopic dermatitis. *J Allergy Clin Immunol*. 2023;151(5):1307–16.
6. Kennedy EA, Connolly J, Hourihane JO, Fallon PG, McLean WHI, Murray D, et al. Skin microbiome before development of atopic dermatitis: early colonization with commensal staphylococci at 2 months is associated with a lower risk of atopic dermatitis at 1 year. *J Allergy Clin Immunol*. 2017;139(1):166–72.
7. Shi B, Bangayan NJ, Curd E, Taylor PA, Gallo RL, Leung DYM, et al. The skin microbiome is different in pediatric versus adult atopic dermatitis. *J Allergy Clin Immunol*. 2016;138(4):1233–6.
8. Halling AS, Fritz BG, Gerner T, Rinnov MR, Bay L, Knudgaard MH, et al. Reduced skin microbiome diversity in infancy is associated with increased risk of atopic dermatitis in high-risk children. *J Invest Dermatol*. 2023;143(10):2030–2038.e6.
9. Rinnov MR, Gerner T, Halling AS, Liljendahl MS, Ravn NH, Knudgaard MH, et al. The association between *S. Aureus* colonization on cheek skin at 2 months and subsequent atopic dermatitis in a prospective birth cohort. *Br J Dermatol*. 2023;189:695–701.
10. Kelleher MM, Phillips R, Brown SJ, Cro S, Cornelius V, Carlsen KCL, et al. Skin care interventions in infants for preventing eczema and food allergy. *Cochrane Database Syst Rev*. 2022;11(11):CD013534.
11. Liang J, Hu F, Tang H, Jiang F, Sang Y, Hong Y, et al. Systematic review and network meta-analysis of different types of emollient for the prevention of atopic dermatitis in infants. *J Eur Acad Dermatol Venereol*. 2023;37(3):501–10.
12. Harder I, Stölzl D, Sander N, Hartmann J, Rodriguez E, Mazur C, et al. Effects of early emollient use in children at high risk of atopic dermatitis: a German pilot study. *Acta Derm Venereol*. 2023;103:adv5671.
13. Breen EJ, Tan W, Khan A. The statistical value of raw fluorescence signal in Luminex xMAP based multiplex immunoassays. *Sci Rep*. 2016;6(1):26996.
14. Bakker D, de Bruin-Weller M, Drylewicz J, van Wijk F, Thijs J. Biomarkers in atopic dermatitis. *J Allergy Clin Immunol*. 2023;151(5):1163–8.
15. Yew YW, Thyssen JP, Silverberg JI. A systematic review and meta-analysis of the regional and age-related differences in atopic dermatitis clinical characteristics. *J Am Acad Dermatol*. 2019;80(2):390–401.
16. Chu DM, Ma J, Prince AL, Antony KM, Seferovic MD, Aagaard KM. Maturation of the infant microbiome community structure and function across multiple body sites and in relation to mode of delivery. *Nat Med*. 2017;23(3):314–26.
17. Glatz M, Jo JH, Kennedy EA, Polley EC, Segre JA, Simpson EL, et al. Emollient use alters skin barrier and microbes in infants at risk for developing atopic dermatitis. Flores GE, editor. *PLoS One*. 2018;13(2):e0192443.

SUPPORTING INFORMATION

Additional supporting information can be found online in the Supporting Information section at the end of this article.

How to cite this article: Fonfara M, Hartmann J, Stölzl D, Sander N, Harder I, Rodriguez E, et al. Stratum corneum and microbial biomarkers precede and characterize childhood atopic dermatitis. *J Eur Acad Dermatol Venereol*. 2024;00:1–7. <https://doi.org/10.1111/jdv.19932>

Online Repository

Title

Stratum corneum and microbial biomarkers precede and characterize childhood atopic dermatitis

Authors

Melina Fonfara^{1*}; Jan Hartmann^{1*}; Dora Stölzl^{1*}; Nicole Sander¹; Inken Harder¹; Elke Rodriguez¹; Matthias Hübenthal¹; Carsten Mazur¹; Sebastian Kerzel²; Michael Kabesch²; Jochen Schmitt³; Hila Emmert¹; Ina Suhrkamp¹; Stephan Weidinger¹

*Shared first authorship

Online Repository

Methods

Study participants and sampling

Data and samples from 50 children from a parallel group, assessor-blind, randomized open-label prospective study of emollient use in neonates at high risk for atopic dermatitis (AD) were used in this study(1). 23 infants were female and 27 infants were male. All but 5 infants were of Caucasian ethnicity. There were no significant differences for the outcomes presented with regard to gender and ethnicity. The trial was registered at ClinicalTrials.gov (NCT03376243). Samples were collected at day 2-21 after birth/baseline (due to data protection regulations, exact birth dates could not be accessed), month 6, 12 and 24 and/or at interim visit due to manifestation of AD.

Tape stripping

For the analysis of proteins from the epidermis, tape strips were collected. Four consecutive D-Squame Standard Sampling Discs (Ø 22mm) were applied on the skin for 5 sec using the D-Squame pressure instrument (Clinical & Derm, Dallas, Texas) to ensure standardized pressure (Pressure Applied: 225g/cm²; Pressure Area: 7/8in (22.24mm)). The first tape strip was discarded to eliminate possible contaminants. Tape strips were stored at -80°C until analysis and tape strip 2–4 were used for further protein extraction and analysis.

Protein extraction

Tape strips 2–4 were pooled for protein extraction. Proteins were isolated from tape strips as previously reported(2). Briefly, 500µl PBS + 0.005% Tween 20™ were used as lysis buffer and samples were sonicated for 15 min to extract soluble proteins from tape strips. Protein lysates were stored at -80°C until further analysis.

Multiplex ELISA

A customized Luminex multiplex assay targeting 22 proteins of interest was performed (ThermoFisher Scientific). All assays and consumables were supplied by ThermoFisher. The custom Luminex assay includes immunomodulatory proteins (IL-1Ra, IL-1α, IL-1β, IL-6, IL-8, IL-16, IL-17a, IL-18, IL-22, IL-23, IL-31, CCL2/MCP-1, CCL13/MCP-4, CCL17/TARC,

CCL22/MDC, CXCL10/IP-10, IFN- γ , TNF- α , TNF- β , VEGFA, TSLP) that were previously reported to be associated with inflammation in AD skin and AD pathogenesis. The panel covers the general inflammatory response (IL-1Ra, IL-1 α , IL-1 β , IL-6, IL-8, IL-18), and important Th2 (IL-31, TSLP, CCL2, CCL13, CCL17, CCL22), Th17/Th22 (IL-17a, IL-22, IL-23) and Th1 mediators IFN- γ , CXCL10/IP-10). The assay was performed as per the manufacturer's instruction and standard curves for each of the cytokines was used on each plate. Fluorescence was detected on the Luminex 200 as median fluorescence intensity without standardization(3). To limit errors that potentially occur by incorporating further measurements especially on samples with very low protein concentrations, we chose to use raw MFI values, rather than calculated protein concentration corrected for the amount of stratum corneum in each sample. By following a standardized protocol during tape strip collecting including a pressure instrument providing equal pressure during application, set time of pressure application and equal sampling site, we aimed to reduce variation in amount of stratum corneum collected per tape strip.

Statistical analysis

For comparison of epidermal cytokine levels between intervention and control group boxplots for visualization and the Wilcoxon rank sum test were used and all statistical analyses were performed using R (R version 4.1.3, <https://www.R-project.org/>). A standard threshold of 0.05 was used to determine statistical significance for all tests.

For comparison between AD and no AD, median fluorescence intensities were transformed using Box-Cox transformation. An Analysis of variance (ANOVA) including correction for intervention was performed on box cox transformed data to calculate effect sizes and p-values.

For comparison between AD and no AD at baseline, no correction for intervention was performed.

For comparison between AD and no AD at AD onset and pre AD, epidermal cytokine levels of healthy individuals at timepoint 12 months were used.

P-values were corrected for multiple testing using Benjamini Hochberg method.

Microbiome data analysis

We used the amplicseq(4) (Version 2.1.0) pipeline with default parameters integrated in the nf-core framework(5). Briefly, the pipeline uses cutadapt for primer trimming, FastQC for quality

evaluation, DADA2 to dereplicate, remove bimeras and infer ASVs using the SILVA reference (Version 132)(6). Shannon index and Bray-Curtis dissimilarities were calculated based on rarefied data. Differential abundances were inferred from non-rarefied data using the DESeq2 package and Wald test with standard significance threshold 0.05 and Benjamini Hochberg correction for multiple testing (R package Version 1.30.1)(7). As the results on emollient use on the cutaneous microbiome have already been shown elsewhere(1), we corrected our used models for emollient use as a confounder and focused our analysis on the differences between AD and no AD infants.

Defining a core microbiome

To gain a more focused view on key ASVs in the context of infant microbiomes, we refined our analysis to include a representative core microbiome of healthy children and focus on differences in children that will develop AD from those that remain healthy. After graphical inspection, we used a cut-off prevalence of 0.2 and detection of 0.01 to obtain a core microbiome that was comprised of 14 species (**Supplement Table E2**). We used Levene test of homogeneity of variance, including Benjamini Hochberg correction for multiple testing, to check variability in abundance between groups and timepoints of core ASVs.

References

1. Harder I, Stölzl D, Sander N, Hartmann J, Rodriguez E, Mazur C, et al. Effects of Early Emollient Use in Children at High Risk of Atopic Dermatitis: A German Pilot Study. *Acta Derm Venereol*. 2023 May 29;103:adv5671.
2. Clausen ML, Slotved HC, Kroghfelt KA, Agner T. Tape Stripping Technique for Stratum Corneum Protein Analysis. *Sci Rep*. 2016 Jan 28;6:19918.
3. Breen EJ, Tan W, Khan A. The Statistical Value of Raw Fluorescence Signal in Luminex xMAP Based Multiplex Immunoassays. *Sci Rep*. 2016 May 31;6(1):26996.
4. Straub D, Blackwell N, Langanica-Fuentes A, Peltzer A, Nahnsen S, Kleindienst S. Interpretations of Environmental Microbial Community Studies Are Biased by the Selected 16S rRNA (Gene) Amplicon Sequencing Pipeline. *Frontiers in Microbiology* [Internet]. 2020 [cited 2023 Jul 13];11. Available from: <https://www.frontiersin.org/articles/10.3389/fmicb.2020.550420>
5. Ewels PA, Peltzer A, Fillinger S, Patel H, Alneberg J, Wilm A, et al. The nf-core framework for community-curated bioinformatics pipelines. *Nat Biotechnol*. 2020 Mar;38(3):276–8.
6. Quast C, Pruesse E, Yilmaz P, Gerken J, Schweer T, Yarza P, et al. The SILVA ribosomal RNA gene database project: improved data processing and web-based tools. *Nucleic Acids Research*. 2013 Jan 1;41(D1):D590–6.
7. Love MI, Huber W, Anders S. Moderated estimation of fold change and dispersion for RNA-seq data with DESeq2. *Genome Biology*. 2014 Dec 5;15(12):550.

Tables

Online Repository Table E1: Differences in cutaneous cytokine levels between control and intervention group averaged across all study visits. Statistical significance was assessed using Wilcoxon signed rank test and p values were adjusted for multiple testing using Benjamini Hochberg correction

Cytokine	Log2 foldchange	P-value	P-adjusted
IL-1b	0.58	0.18	0.21
IP-10 (CXCL10)	0.45	0.06	0.09
IL-6	0.66	0.01	0.03
IL-8 (CXCL8)	0.93	0.09	0.13
TARC (CCL17)	0.80	0.01	0.03
MDC (CCL22)	0.55	0.01	0.03
IL-17a	0.57	0.06	0.09
IL-31	0.16	0.09	0.13
IL-1Ra	0.85	0.02	0.03
IFN γ	0.36	0.49	0.52
TNF α	0.39	0.17	0.21
IL-16	0.67	<0.001	<0.001
MCP-1 (CCL2)	1.46	<0.001	<0.001
TNFb	0.38	0.004	0.02
TSLP	1.03	0.001	0.004
IL-23	0.32	0.04	0.07
IL-18	1.62	0.01	0.03
MCP-4 (CCL13)	0.13	0.13	0.17
IL-22	0.77	0.01	0.03
VEGFa	0.38	0.22	0.24
IL-1a	0.24	0.62	0.62

Online Repository Table E2: Core microbiome members. ASVs with genus level and highest confidence result for species classification.

ASV_sp	blast_result
ASV1 Cutibacterium NA	Cutibacterium acnes
ASV2 Staphylococcus NA	Staphylococcus epidermidis
ASV3 Staphylococcus NA	Staphylococcus hominis
ASV4 Enhydrobacter NA	Moraxella osloensis
ASV5 Streptococcus mitis	Streptococcus mitis
ASV7 Streptococcus NA	Streptococcus salivarius
ASV8 Gemella haemolysans	Gemella haemolysans
ASV9 Enhydrobacter aerosac-cus	Moraxella osloensis
ASV10 Corynebacterium NA	Corynebacterium tuberculostearicum/kefirresi-dentii/
ASV11 Rothia mucilaginosa	Rothia mucilaginosa
ASV12 Streptococcus NA	Uncultured Streptococcus sp.
ASV18 Streptococcus NA	Uncultured Streptococcus sp.
ASV19 Haemophilus parainflu-enzae	Haemophilus parainfluenzae
ASV20 Micrococcus NA	Micrococcus luteus

Online Repository Table E3: Summary of pediatric AD biomarkers across the timepoints of the study

	Baseline	Pre AD	AD Onset
Increased in later AD	IL-1Ra, TNF β , VEGFa, <i>Staphylococcus epidermidis</i> , <i>Streptococcus vestibularis</i> , <i>Streptococcus oralis</i>	TARC, IL-8, IL-18, IL-22, MCP-1, VEGFa, <i>Staphylococcus epidermidis</i>	MCP-1, TARC, MDC, IL-31, TSLP, MCP-4, IP-10, IFN γ , IL-17a, IL-22, IL-23, IL-1 β , IL-6, IL-8, IL-16, IL-18, IL-1Ra, TNF α , TNF β , VEGFa, <i>Staphylococcus epidermidis</i>
Decreased in later AD	<i>Staphylococcus hominis</i>	<i>Streptococcus oralis</i> , <i>Streptococcus vestibularis</i> , <i>Streptococcus mitis</i>	<i>Streptococcus oralis</i> , <i>Streptococcus vestibularis</i>

5.3 Article III

This article was published in Clinical & Experimental Allergy, Vol. 54(1), Melina Fonfara, Carina Brodersen, Ina Suhrkamp, Elke Rodriguez, Stephan Weidinger, Hila Emmert, Effects of cultured keratinocyte- and fibroblast-derived mediators on three-dimensional skin models, 74-76. DOI: 10.1111/cea.14420.

RESEARCH LETTER

WILEY

Effects of cultured keratinocyte- and fibroblast-derived mediators on three-dimensional skin models

To the Editor,

Atopic dermatitis (AD) is a complex disease involving epidermal barrier dysfunction and immunological abnormalities.¹ The communication between keratinocytes and T cells as major drivers of immune dysfunction has been studied extensively.² Still, there is data available underlining some contribution of dermal fibroblasts to AD pathogenesis.³ This study therefore aimed to investigate the pathological effects of keratinocyte- and fibroblast-derived factors on 3D skin models focusing on epidermal organization and barrier marker expression.

Primary keratinocytes and fibroblasts were cultured and stimulated with AD-relevant cytokines (IL-22, IL-4, IL-13, TNF α) for 24 h. Cells were washed and serum-free keratinocyte differentiation medium (SKDM) was added for 1 h. Supernatant was collected and used for further analyses. Multiplex ELISA (Luminex) was performed to determine protein levels in cell supernatants. For the construction of three-dimensional (3D) skin models, a well-established protocol was used.⁴ Stimulation of 3D skin models with cytokines (IL-4, IL-13) or cell supernatants was performed for 48 h. The monoclonal interleukin-4 receptor antagonist dupilumab (dpl) was additionally added for 48 h. Two punch biopsies were taken from each 3D skin and embedded in paraffin for histological analyses and used for RNA isolation and following qPCR.⁵ Detailed methods and additional results are available at <https://zenodo.org/records/10036562>.

We first performed multiplex ELISA to identify soluble factors secreted by fibroblasts and keratinocytes. Analysis revealed that both keratinocyte and fibroblast secretion was increased following cytokine stimulation. For both cell types increased secretion of innate and adaptive immunity markers as well as T cell attracting cytokines and chemokines was observed after stimulation, however, secretion by keratinocytes was higher as compared to fibroblasts.

To study the effects of keratinocyte- and fibroblast-derived factors on skin physiology and barrier properties, 3D skin models were constructed and stimulated with either IL-4, IL-13 creating AD-skin models or with supernatants obtained from unstimulated (Sup-Ctrl) or stimulated (Sup-AD) fibroblasts or keratinocytes. Decreased gene expression of the structural proteins filaggrin, involucrin and loricrin in IL-4 and IL-13 treated skin was observed, confirming the induction of an AD-like epidermis phenotype (Figure 1A–C).

Treatment with keratinocyte Sup-AD but not Sup-Ctrl caused significantly reduced gene expression of all targeted proteins when compared to control skin. When comparing the effects of K-Sup-AD on gene expression to those of K-Sup-Ctrl, no significant differences could be observed for filaggrin and loricrin expression levels. This might be explained by the high cytokine levels present in keratinocyte Sup-Ctrl. Treatment with fibroblast supernatants resulted in minor changes in gene expression with significantly decreased expression of loricrin when treated with fibroblast Sup-AD.

We performed additional H&E histological analysis of 3D skin models and checked for AD-characteristic spongiosis. AD-model skins revealed significantly higher levels of spongiosis compared to control skin (Figure 1D). Skin sections obtained from 3D skin manipulated with supernatants from keratinocytes showed comparable but non-significant changes. Treatment of 3D skin with fibroblast supernatants did not lead to spongiosis development. Taken together, our data underline the contribution of keratinocyte-derived cytokines to skin barrier dysfunction in human skin models. Keratinocytes that were pre-exposed to external stimuli secreted pro-inflammatory factors which caused pathological changes in 3D skin models mimicking AD skin with regard to their histology and structural protein expression. The amounts of pro-inflammatory mediators secreted by fibroblasts seemed to be not sufficient to lead to significant changes in skin models indicating that keratinocyte signalling is key to skin barrier regulation. It is known that IL-4 and IL-13 influence gene expression of involucrin, loricrin and filaggrin,⁶ but our data suggests that additional keratinocyte-derived cytokines could promote skin barrier disruption in AD.

We further assessed whether the observed pathological changes in 3D skin models treated with cell supernatants were primarily caused by IL-4 and IL-13 signalling. 3D skin models were incubated with Sup-AD from keratinocytes or with IL-4 and IL-13 and were additionally treated with dpl in order to block IL-4/IL-13 receptor signalling. Results demonstrated that blockade of IL-4R α led to a rescue of filaggrin, involucrin and loricrin expression in AD-skin models (Figure 1A–C). Likewise, spongiosis was significantly reduced (Figure 1D). Less pronounced effects were observed when dpl was added to skin models treated with keratinocytes Sup-AD, where spongiosis was significantly improved but only loricrin expression recovered (Figure 1C,D).

This is an open access article under the terms of the [Creative Commons Attribution-NonCommercial](https://creativecommons.org/licenses/by-nc/4.0/) License, which permits use, distribution and reproduction in any medium, provided the original work is properly cited and is not used for commercial purposes.

© 2023 The Authors. *Clinical & Experimental Allergy* published by John Wiley & Sons Ltd.

Our data showed that skin barrier dysfunction in 3D skin models treated with keratinocyte Sup-AD can in part be reverted by blocking IL-4R α signalling. However, additional factors present in keratinocyte supernatant that do not signal via IL-4R α seem to contribute to impaired expression of barrier genes comparable to effects of IL-4 and IL-13 signalling. Michaelidou et al. have previously shown that IL-1 family cytokines downregulate loricrin and pro-filaggrin expression in human explants *in vivo*⁷ which supports our findings. IL-1 family cytokines are involved in the innate immune response⁸ and can possibly amplify the inflammatory state in the skin resulting in the observed skin barrier deficiency. The relatively low secretion of IL-1 cytokines by fibroblasts could be a reason for their relatively small effects on 3D skin model physiology. Thus, our findings indicate the important role of the variety of keratinocyte-derived pro-inflammatory signalling in disrupting the skin barrier both in a Th2-dependent

Summary Box

- Keratinocytes secrete sufficient pro-inflammatory mediators to cause disease-associated patterns in 3D skin models
- IL-4R α blockade only partly improves the skin barrier highlighting Th2-independent factors' role in skin inflammation

and independent matter. Targeting of IL-1 family cytokine signalling with for example recombinant IL-1Ra (anakinra) would be of interest to further characterize the role of keratinocytes and IL-1 family cytokine signalling in AD.

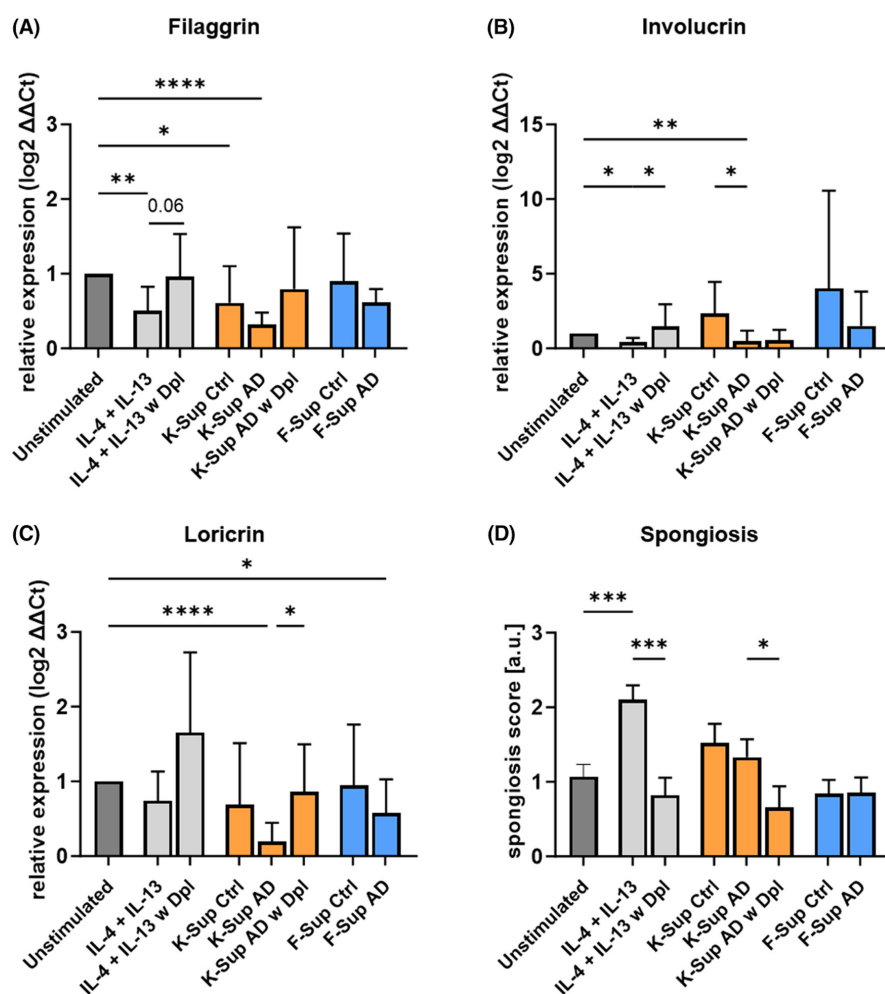


FIGURE 1 3D skin models treated with cell supernatants or cytokines and dupilumab. RNA was isolated from a 4 mm punch biopsy in order to perform real-time PCR. Gene expression of selected skin barrier proteins was assessed. $\Delta\Delta$ Ct values were calculated using RPL38 as housekeeping gene. (A) Relative gene expression of filaggrin. (B) Relative gene expression of involucrin. (C) Relative gene expression of loricrin. (D) Spongiosis scoring performed on H&E histological slides (range 0–3). Results represent the means and standard deviation from independent experiments (unstimulated [$n=10$]; IL-4 + IL-13 [$n=10$]; IL-4 + IL-13 w Dpl [$n=5$]; K-Sup Ctrl [$n=5$]; K-Sup AD [$n=10$]; K-Sup AD w Dpl [$n=5$]; F-Sup Ctrl [$n=5$]; F-Sup AD [$n=5$]). Significant comparisons are shown for * p -value < .05, ** p -value < .01, *** p -value < .001, **** p -value < .0001. Significant differences were calculated using the Kruskal–Wallis test (relative gene expression) and one-way ANOVA (spongiosis). AD, atopic dermatitis; Ctrl, control; dpl, dupilumab; F-sup, fibroblast supernatant; K-sup, keratinocyte supernatant; Sup, supernatant.

AUTHOR CONTRIBUTIONS

Hila Emmert and Melina Fonfara designed the experiments. Melina Fonfara and Carina Brodersen conducted the experiments. Melina Fonfara and Carina Brodersen analysed the data, and Melina Fonfara, Hila Emmert and Ina Suhrkamp interpreted the data. Melina Fonfara and Hila Emmert drafted the article and Hila Emmert, Elke Rodriguez, Ina Suhrkamp and Stephan Weidinger revised it critically. All authors read and approved the final version.

ACKNOWLEDGEMENTS

Open Access funding enabled and organized by Projekt DEAL.

FUNDING INFORMATION


No funders available.

CONFLICT OF INTEREST STATEMENT

S. Weidinger has received institutional research grants from Sanofi Deutschland GmbH, LEO Pharma, and Pfizer and performed consultancies and/or lectures for AbbVie, Almirall, Boehringer, Eli Lilly, Galderma, Kymab, Leo Pharma, Regeneron, Sanofi-Genzyme, and Novartis. H. Emmert has received institutional research grants from LEO Pharma. The rest of the authors declare that they have no conflicts of interest.

DATA AVAILABILITY STATEMENT

The data that support the findings of this study are available from the corresponding author upon reasonable request.

Melina Fonfara 
Carina Brodersen
Ina Suhrkamp
Elke Rodriguez
Stephan Weidinger
Hila Emmert

Department of Dermatology and Allergy, University Hospital
Schleswig-Holstein, Kiel, Germany

Correspondence

Stephan Weidinger, Department of Dermatology and
Allergy, University Hospital Schleswig-Holstein, Campus
Kiel, Rosalind-Franklin Str. 9, 24105 Kiel, Germany.
Email: sweidinger@dermatology.uni-kiel.de

ORCID

Melina Fonfara  <https://orcid.org/0009-0000-9729-0494>

REFERENCES

1. Langan SM, Irvine AD, Weidinger S. Atopic dermatitis. *The Lancet*. 2020;396:345-360.
2. Humeau M, Boniface K, Bodet C. Cytokine-mediated crosstalk between keratinocytes and T cells in atopic dermatitis. *Front Immunol*. 2022;13:801579. doi:10.3389/fimmu.2022.801579
3. Löwa A, Graff P, Kaessmeyer S, Hedtrich S. Fibroblasts from atopic dermatitis patients trigger inflammatory processes and hyperproliferation in human skin equivalents. *J Eur Acad Dermatol Venereol*. 2020;34:e262-e265.
4. Mildner M, Ballaun C, Stichenwirth M, et al. Gene silencing in a human organotypic skin model. *Biochem Biophys Res Commun*. 2006;348:76-82.
5. Stange EL, Rademacher F, Drerup KA, et al. *Staphylococcus aureus* activates the aryl hydrocarbon receptor in human keratinocytes. *J Innate Immun*. 2022;14:582-592.
6. Furue M. Regulation of filaggrin, loricrin, and involucrin by IL-4, IL-13, IL-17A, IL-22, AHR, and NRF2: pathogenic implications in atopic dermatitis. *Int J Mol Sci*. 2020;21:1-25.
7. Michaelidou M, Redhu D, Kumari V, Babina M, Worm M. IL-1 α / β and IL-18 profiles and their impact on claudin-1, loricrin and filaggrin expression in patients with atopic dermatitis. *J Eur Acad Dermatol Venereol*. 2023;37:e1141-e1143.
8. Dinarello CA. Immunological and inflammatory functions of the interleukin-1 family. *Annu Rev Immunol*. 2009;27:519-550. doi:10.1146/annurev.immunol.021908.132612

Online Repository for the article: “Effects of cultured keratinocyte- and fibroblast- derived mediators on three-dimensional skin models”

Fonfara et al., 2023

Material and methods

Cell-type specific secretion of cytokines

Normal human keratinocytes (NHEKs) (PromoCell, Heidelberg, Germany, Lot Number 470Z031 + 470Z031) were cultured in Keratinocyte Growth Medium (KGM) (PromoCell, Heidelberg, Germany) + supplements + CaCl_2 at 37°C and 5% CO_2 . For 3D skin models, cells were used at passage 5 and for 2D cell culture cells were used at passage 4-10. Neonatal human dermal fibroblasts (fibroblasts) (Invitrogen, Thermo Fisher Scientific, Dreieich, Germany, Lot Number 1998537) were cultured in DMEM (Lonza, Köln, Germany) + 10% fetal calf serum (FCS) (Gibco, Eggenstein, Germany) and 1% L-Glutamine. Cells were used at passages 4-30.

In order to induce an AD environment, the cells were stimulated with AD signature cytokines (40ng/ml IL-22, 40ng/ml IL-4, 40ng/ml IL-13 and 10ng/ml $\text{TNF}\alpha$ (all Peprotech, Hamburg, Germany)) for 24 hours prior to experiments as described previously¹⁰². After stimulation, cells were washed twice with PBS (Life technologies, Darmstadt, Germany) and serum-free keratinocyte differentiation medium (SKDM) was added for one hour. Afterwards, supernatant was collected and stored at -20°C until used for multiplex ELISA analysis and 3D skin stimulation.

3D skin models

Human 3-dimensional skin models were generated using a fibroblasts-collagen matrix seeded with 0.5×10^6 keratinocytes. The protocol was adapted from Mildner et al¹¹⁷. Briefly, 0.5×10^6 fibroblasts in 250µl FCS were mixed with 2.5ml of 0.4% collagen G type I (Biochrom, Berlin, Germany) mixed with Hank's Balanced Salt Solution (HBSS 10x, Gibco, Eggenstein, Germany) and seeded onto filter inserts (3µm pore size, BD Bioscience, Heidelberg, Germany) integrated into a 6 well deep well cell culture plate (BD Bio Coat, Corning, Wiesbaden, Germany). After 2 h at 37°C w/o CO_2 the collagen solution was gelled and KGM medium with supplements was added to the surrounding external well and to the insert containing the gelled collagen matrix. After overnight incubation at 37°C and 5 % CO_2 , 0.5×10^6 keratinocytes were

seeded on top of the matrix. After 48 hours, the keratinocyte layer was raised to an air-liquid interface by removing the apical media which initiates skin growth and differentiation (day 1). Skin models were grown for 5 days in SKDM consisting of KGM + 0.125ng/ml epidermal growth factor (recombinant human) + 5µg/ml insulin + 0.39µg/ml hydrocortisone + 10µg/ml transferrin (recombinant human) + 0.06mM CaCl₂ supplemented with 1.3 mM calcium, 50 µg/ml ascorbic acid (Sigma-Aldrich) and 0.1 % bovine serum albumin (fatty acid-free, Roth, Karlsruhe, Germany). An atopic dermatitis-like environment was created by stimulating the skin models on day 5 with 5ng/µl of IL-4 (Peprotech, Hamburg, Germany) and 50ng/µl of IL-13 (Peprotech, Hamburg, Germany) for 48h. Dupilumab (Dupixent, Sanofi, Frankfurt, Germany) was added additionally after 5 days in a concentration of 1mg/ml for 48h. Cell supernatants were added also for 48 hours. Unstimulated skin served as control. After incubation, two 4mm punch biopsies (Pfm medical, Köln, Germany) were taken from each 3D skin model. One biopsy was embedded in paraffin for histological analysis and the second biopsy was used for RNA isolation and following qPCR.

H&E Staining

Biopsies from the organotypic 3D skin model were fixed in 4,5% formalin (Geyer, Renningen, Germany), embedded in paraffin and used for further analysis. H&E staining was performed as previously reported¹³⁶ H&E staining was performed starting with deparaffinization using xylene (Geyer, Renningen, Germany) followed by hydration steps (decreasing alcohol series). Hematoxylin staining was performed using *Shandon Gill 3 Hematoxylin* (Thermo Fisher Scientific, Dreieich, Germany). Glacial acid was used for differentiation and eosin staining was performed using *Shandon Eosin Y* (Thermo Fisher Scientific, Dreieich, Germany). Finally, dehydration (increasing alcohol series, xylene) and mounting was performed (Thermo Fisher Scientific, Dreieich, Germany). Histological slides were scanned for visualization using Nano-Zoomer S60 (Hamamatsu, Herrsching, Germany).

Spongiosis scoring

Spongiosis scoring was performed on different skin models using H&E stained histological slides. 5 different reviewers trained in skin histology interpretation visually evaluated severity of spongiosis and scored spongiosis in a range from 0-3.

RNA isolation and qPCR

Total RNA of each 3D skin model was isolated using Crystal RNAmagic reagent according to the manufacturer's protocol (Biolabproducts, Hamburg, Germany) and cDNA corresponding to 10ng total RNA was used as the template in real-time PCR.

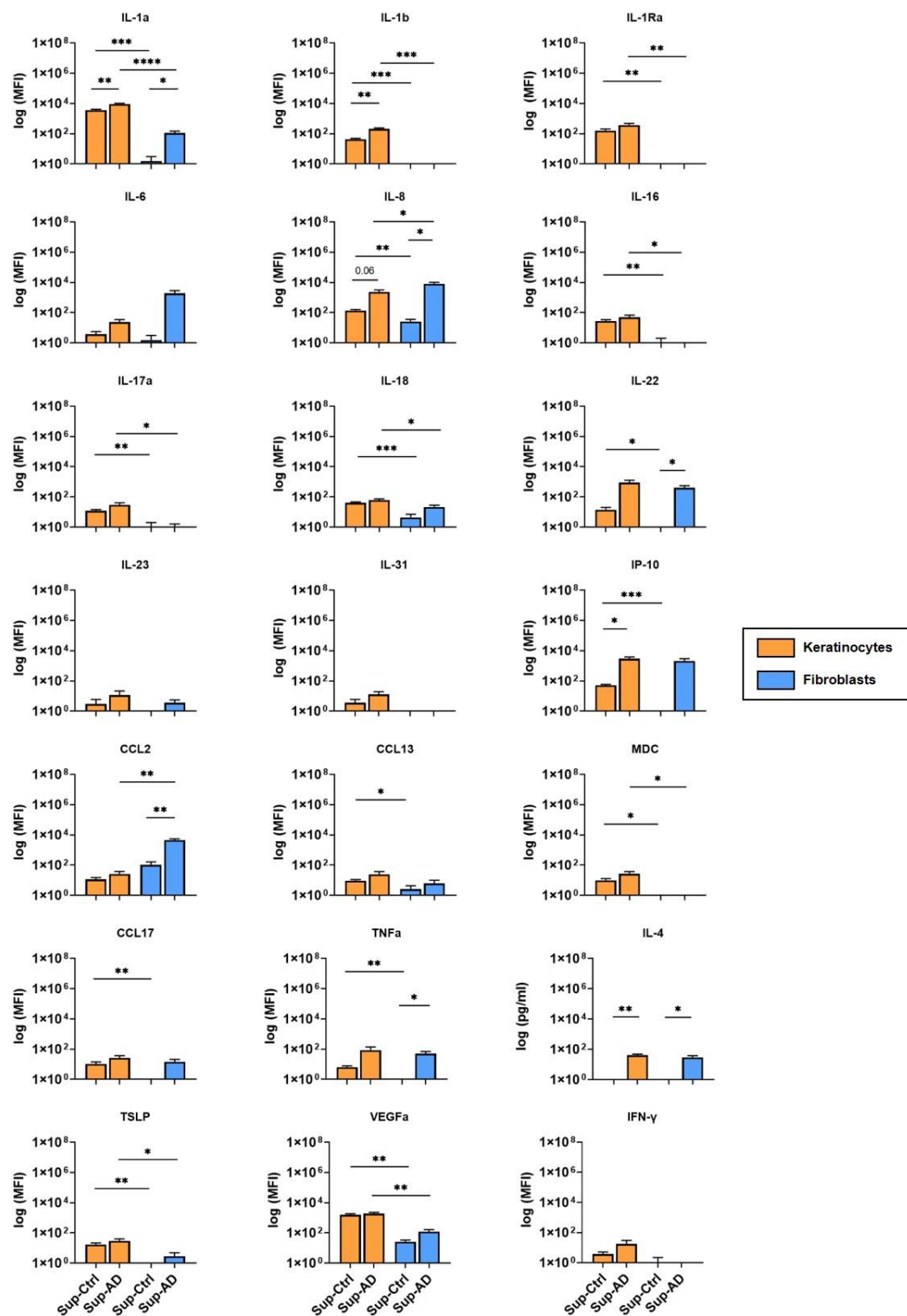
RNA quantification and A_{260}/A_{280} ratio measurement was performed using multiscan skyhigh (ThermoFisher Scientific). 0.5µg of the isolated RNA was digested and reverse transcribed to cDNA (PrimeScript RT Reagent Kit with gDNA Eraser (Perfect Real Time); TaKaRa Bio, Saint-Germain-en-Laye, France). cDNA corresponding to 10ng total RNA was used as the template in a real-time PCR. Real-time PCR was performed with the QuantStudio 3 System (BD Biosciences) using SYBR Premix Ex Taq II mix (TaKaRa Bio, Saint-Germain-en-Laye, France). The following primers were used: *filaggrin* (forward: GGCAAATCCTGAAGAATCCAGATG, reverse: GGTAATTCTCTTTTCTGGTAGACTC), *involucrin* (forward: CTGCCTCAGCCTTACTGTGA, reverse: GGAGGAGGAACAGTCTTGAGG), *loricrin* (forward: CTCTCCTCACTCACCTTCCT, reverse: AGGTCTTCACGCAGTCCAC). Amplification condition was performed in a 10µl reaction volume consisting of 1µl template cDNA, 5.2µl SYBR Premix EX TaqII, 3µl H₂O, 0.4µl forward primer, 0.4µl reverse primer. Thermal cycle was programmed for 30 sec at 95°C as initial denaturation, followed by 6 cycles of 95.0°C (5 sec), 4.14°C/s for denaturation and 66.0°C (30sec), 3.17°C/s for annealing followed by 40 cycles of 95.0°C (15 sec) for denaturation and 60.0°C (1 min) for annealing. RPL38 (forward: TCAAGGACTTCCTGCTCACA, reverse: AAAGGTATCTGCTGCATCGAA) was used as a housekeeping gene in order to calculate ΔC_t values.

Multiplex and conventional ELISA

Cell supernatants and media of 3D skin models were analysed via multiplex ELISA (Luminex 200). A customized assay targeting 22 proteins involved in epidermal-dermal communication was performed according to the manufacturer's instructions (ThermoFisher Scientific): IL-1Ra, IL-1 α , IL-1 β , IL-6, IL-8, IL-16, IL-17a, IL-18, IL-22, IL-23, IL-31, CCL2/MCP-1, CCL13/MCP-4, CCL17/TARC, CCL22/MDC, CXCL10/IP-10, IFN- γ , TNF α , TNF β , VEGFA, TSLP). Fluorescence was detected as background corrected median fluorescence intensity without standardization. The two cytokines IL-4 and IL-13 were detected using human IL-4 and IL-13 DuoSet ELISA (Bio-technique, Wiesbaden, Germany) according to the manufacturer's instruction.

Statistics

Statistical analysis was performed using GraphPad Prism software (GraphPad Software, La Jolla, CA). Shapiro-Wilk test was used to check for normal distribution of the data. For analyses of 3D skin models, ANOVA and Kruskal Wallis test were used. For analyses of cytokine levels in cell supernatants, paired and unpaired t tests were used.



Online Figure 1: Multiplex ELISA of keratinocyte and fibroblast supernatants. Keratinocytes or fibroblasts were stimulated with IL-4, IL-13, IL-22 and TNFα (Sup-AD) or cultivated without treatment (Sup-Ctrl) for 24h. Cytokine repertoire was analyzed by multiplex ELISA (Luminex 200). Background corrected median fluorescence intensities (MFI) were scaled for visualization by log₁₀ transformation. Conventional ELISA was performed assessing IL-4 levels. Results represent the means and s.e.m from 5 independent experiments. Significant comparisons are shown for p-value < 0.05 = *, p-value < 0.01 = **, p-value < 0.001 = ***. Sup = supernatant, Ctrl = control, AD = atopic dermatitis.

5.4 Article IV

3D skin model to study crosstalk between T cells and *Staphylococcus aureus* in atopic dermatitis *in vitro* (in preparation for submission)

Ina Suhrkamp^{1*}, Melina Fonfara^{1*}, Magdalena¹, Jan Hartmann¹, Elke Rodriguez¹, Jürgen Har-
der¹, Hila Emmert^{1**}, Stephan Weidinger^{**1}.

* Joint first authors

** Joint senior authors

¹Department of Dermatology and Allergy, University Hospital Schleswig-Holstein, Campus
Kiel, Kiel, Germany

Funding sources

This research received no specific grant from any funding agency in the public, commercial, or
not-for-profit sectors

Abbreviations

AD - Atopic dermatitis
Dpl - Dupilumab
IL - Interleukin
PMA - Phorbol 12-myristate 13-acetate
Th2 - T helper cells 2

Summary

Background: Atopic dermatitis (AD) is characterized by cutaneous inflammation driven by a skewed Th2 immune response and skin barrier dysfunction including a microbial dysbiosis and abundance of *Staphylococcus (S.) aureus*. The anti-IL-4R α monoclonal antibody dupilumab improves AD symptoms and reduces cutaneous *S. aureus* abundance and colonization. Due to a lack of multi-level functional models, the causality in AD remains unexplored and the contribution of microbiome dysbiosis to impaired skin barrier and altered immune response or *vice versa* remains unclear.

Methods: We introduce a novel *in vitro* model incorporating Th2 cells into 3D skin models with topical *S. aureus* colonization. We analyzed the influence of different T cell populations on skin barrier integrity, inflammatory environment, *S. aureus* load and explored the influence of dupilumab.

Results: Incorporation of Th2-differentiated but not pan T cells into the 3D skin model impaired the epidermal barrier structure. *S. aureus* colonization induced barrier defects in both models with strongest effect in a Th2 milieu. *S. aureus* growth was increased in the Th2 milieu. Dupilumab abolished Th2-induced *S. aureus* load and improved epidermal organization.

Conclusion: Hence, only complex immunocompetent 3D skin microbiome models adequately capture physiological *S. aureus* growth *in vitro*, providing a robust platform for *in vitro* AD research.

Introduction

Atopic dermatitis (AD) is characterized by type 2 immune-mediated inflammation, which is characterized by high levels of IL-4 and IL-13 along with alarmins such as TARC, TSLP, CCL22, IL-1 β and IL-33. These molecules attract and activate different immune cells, and introduce a complex skin barrier dysfunction, involving a reduced expression of epidermal structural genes and natural moisturizing factors^{1,2}, abnormalities in lipid composition and organization³, and insufficient antimicrobial peptide production⁴. Both features are closely interrelated and reinforce each other; keratinocyte-derived alarmins and chemokines stimulate inflammation, Th2 priming and activation, and type 2 cytokines amplify inflammation and in turn negatively impact skin barrier function⁵. Established AD is also characterized by a marked skin dysbiosis with reduced bacterial diversity and colonization with *Staphylococcus (S.) aureus*, the abundance of which correlates with disease activity⁶. *S. aureus* at the same time exploits and worsens skin barrier disruption, exemplarily by taking advantage of corneocyte deficiencies⁷ and insufficient AMP production⁸ while releasing proteases that degrade barrier proteins⁹. Likewise, it benefits by employing type 2 inflammation, e.g. by using plasma proteins that invade the skin through Th2 cytokine-mediated microvascular leakage which act as ligands¹⁰, and promotes T-cell-mediated inflammation by releasing superantigens which activate keratinocytes to release proinflammatory chemokines¹¹ and trigger oligoclonal T cell activation and cytokine release¹². However, it is yet unclear whether dysbiosis and colonization by *S. aureus* is a causal or secondary yet important mechanism in AD.

Three-dimensional human skin equivalents (3D skin models) mimic human skin as they provide a stratified epidermal skin barrier grown on a dermis-like matrix. Such models are helpful to study mechanisms in skin diseases including AD¹³. 3D skin models treated with interleukin cocktails¹⁴, generated with AD patient-derived keratinocytes¹⁵ or with keratinocytes with silenced filaggrin expression exhibit AD-like skin barrier abnormalities with regard to epidermal morphology, gene expression and lipid synthesis¹⁶. However, to fully recapitulate AD features and create an *in vivo*-like situation, incorporating skin resident bacteria and immune cells into 3D skin models is crucial, as both are central players in AD development and maintenance¹⁷.

Few studies have incorporated bacteria into their 3D skin models¹⁸; these studies have shown that reduced filaggrin protein expression leads to increased epidermal *S. aureus* colonization¹⁹, while co-cultivation with *S. epidermidis* reduced *S. aureus* growth²⁰. Likewise, most published studies working with 3D skin models have not incorporated immune cells. Some studies have introduced Langerhans cells to study sensitization²¹ and van den Bogaard et al. have published an inflammatory 3D skin model including CD4⁺ T cells, although AD skin could not be fully mimicked²². To our knowledge, there are no published studies so far that have used 3D skin models including both T cells and skin microbiota members. Here we established

immunocompetent 3D skin *S. aureus* models and characterized the advantages of integrating immune cells and *S. aureus*. This provided us with a powerful tool to study the complex relationship between barrier function, microbiota and immunity in the context of AD.

Material and Methods

Cell culture

Primary normal human keratinocytes from juvenile foreskin (NHEKs) (PromoCell, Lot Number 470Z031) were cultured in Keratinocyte Growth Medium (KGM) (PromoCell) + supplements + 0.06mM CaCl₂ at 37°C and 5% CO₂. Cells were used at passage 5. Neonatal human dermal fibroblasts (fibroblasts) (Invitrogen, Lot Number 1998537) were cultured in DMEM (Lonza) + 10% fetal calf serum (FCS) (Gibco) and 1% L-Glutamine. Cells were used at passages 4-12.

Isolation and polarization of T cells

Peripheral blood was taken by venepuncture from healthy volunteers. Informed consent was obtained. Peripheral blood mononuclear cells (PBMCs) were isolated from peripheral blood by a Polysucrose 400 gradient. First, PBMCs were incubated with FITC-conjugated anti-CD45RO antibodies (BioLegend), and memory T cells were removed from the PBMC population by means of magnetic isolation using microbead-coupled anti-FITC antibodies (Miltenyi Biotec). Naïve T helper cells were isolated by positive magnetic selection using anti-CD4 microbeads (Miltenyi Biotec). Purity of naïve T helper cells was confirmed by flow cytometry. Naïve T cells with a purity of >90% were used for the experiments.

0.5 x 10⁶ cells/ml were seeded in RPMI + 10% FCS + non-essential amino acids (NEAA) + 55µM β-mercaptoethanol in a 24-well plate. T cell were pan-stimulated with 2µg/ml anti-CD3, 0.5µg/ml anti-CD28, and 5ng/ml IL-2 (all Miltenyi Biotec) for 7 days in a 5% CO₂ incubator at 37°C. For Th2 differentiation cells were incubated additionally with 3µg/ml anti-IFN-γ and 20ng/ml IL-4 (both Miltenyi Biotec). After 7 days of incubation, CD4⁺ T cells were activated with 10ng/ml phorbol 12-myristate 13-acetate (PMA) and 1ng/ml ionomycin for 2 h. Cells were collected and washed with phosphate buffered saline (PBS) twice. 250,000 cells were pipetted into the trans well under the 3D skin equivalents (day 8). 3D skin equivalents were incubated together with CD4⁺ T cells for another 48 h (Figure S1).

For analysing success of *in-vitro* differentiation (Figure S2), PMA/ionomycin activated T cells were incubated for 3h with 2.5ng/ml brefeldin A. Afterwards, cells were washed and surface

stained with anti-CD4 and Zombie NIR live/dead dye (both BioLegend). Samples were fixed and permeabilized (FoxP3 Staining Buffer Set, Miltenyi Biotec) and further stained intracellularly with fluorescently labelled antibodies against GATA3, IL-13, IL-4, TNF- α , IL-2, and IL-5 (BioLegend).

Flow cytometry was conducted on a CytoFLEX flow cytometer using CytExpert software (Beckman Coulter). The resulting data were analysed using FlowJo v10 software (Becton, Dickinson & Company).

***Staphylococcus aureus* cultivation and transfer on 3D skin models**

Staphylococcus aureus SA 8325-4 (clinical isolate) was used. Bacteria were grown on blood agar plates for 24 h and then inoculated into tryptic soy broth (TSB) medium. Bacteria were grown for further 12 h, transferred into new TSB medium and grown again for 3 h. Bacteria were adjusted to an OD 600 nm of 0.25 in TSB medium. 20 μ l of bacteria solution was added to filter paper (diameter: 8mm). Filter paper soaked with bacteria solution was administered to 3D skin equivalents for 1 h (day 9) in order to allow bacteria to settle down on 3D skin equivalents (Figure S1). Filter paper was removed and bacteria were grown on the skin for 24 h. For control conditions, 3D skin equivalents were treated with filter paper + 20 μ l TSB medium for 1 h.

3D skin equivalents

Human 3-dimensional skin equivalents were generated using a fibroblasts-collagen matrix seeded with 0.5×10^6 keratinocytes using a well-established protocol²³ (Appendix S1). An atopic dermatitis like environment was created by adding Th2-polarized T cells beyond the 3D skins onto the insert. Pan-activated T cells were used as a control. Dupilumab (Dupixent, Sanofi) was additionally added at day 8 in a concentration of 1mg/ml for 48 h. *S. aureus* was added at day 9 and grown for 24 h. At day 10, the experiment was terminated and for further downstream analysis three 3mm punch biopsies were taken from each 3D skin equivalent. One biopsy was embedded in paraffin for histological analysis (Appendix S4, S5), the second biopsy was used for RNA isolation and following qPCR (Appendix S2), and the third biopsy was used for bacterial DNA isolation (Appendix S3) and following qPCR (Appendix S3).

Stimulation of simple AD models

3D skin models were constructed as mentioned above. An atopic dermatitis like environment was created by stimulating the skin equivalents on day 8 with 5ng/μl of IL-4 (Peprotech) and 50ng/μl of IL-13 (Peprotech) for 48h. 1mg/ml Dupilumab (Dupixent, Sanofi) was added at day 8 48h. *S. aureus* was added at day 9 and grown for 24h. At day 10, the experiment was terminated.

Multiplex ELISA

Soluble proteins in media of 3D skin models were analyzed via multiplex ELISA (Luminex 200). A customized assay targeting 22 proteins involved in epidermal-dermal communication and skin inflammation (IL-1Ra, IL-1α, IL-1β, IL-4, IL-6, IL-8, IL-13, IL-16, IL-17a, IL-18, IL-22, IL-23, IL-31, CCL2/MCP-1, CCL13/MCP-4, CCL22/MDC, CXCL10/IP-10, IFN-γ, TNF-α, TNF-β, VEGFα, TSLP) was performed according to the manufacturer's instructions (ThermoFisher Scientific). Fluorescence was detected as median fluorescence intensity without standardization²⁴. A standard curve for each cytokine was measured on each plate.

Statistical analysis

Statistical analysis was performed using R (R version 4.3.1 (2023-06-16)). Pairwise Wilcoxon rank-sum testing was used to find significances for comparisons of individual groups.

Additional methods are available as supplementary material and methods.

Results

***S. aureus*-induced upregulation of T cell-derived proinflammatory cytokines is facilitated in a CD4⁺ Th2 microenvironment**

To investigate the impact of *S. aureus* colonization in an AD-like setting, we introduced activated Th2 cells into the 3D skin models. Flow cytometry analysis revealed that Th2-polarized cells, just before their integration into the 3D skin models, exhibited elevated levels of Th2 cytokines IL-13, IL-4, IL-5, and IL-2, along with heightened expression of GATA3, compared to pan T cells (Figure S2), confirming successful Th2 polarization.

The inflammatory milieu within the 3D skin models was evaluated through analysis of soluble factors in the basolateral medium (Figure 1). Incorporation of activated, *in vitro* polarized Th2 cells into the 3D skin models led to a notable increase in levels of IL-4, IL-13, IL-31, and TSLP compared to unstimulated control skins, confirming the establishment and maintenance of a Th2 cytokine environment (Figure 1). Additionally, incorporation of Th2 cells alone induced the expression of further pro-inflammatory cytokines such as IL-22, IL-1 β , IL-1 α , or IL-17a. Introduction of pan T cells resulted in a significant elevation of IL-13, IL-22, IL-1 β , IL-1 α , and IL-17a compared to control skin models. No significant differences in the levels of the mentioned cytokines in basolateral media between Th2 and pan T cell models were observed. Interestingly, there was an increase in IFN- γ in both pan T cell and Th2 models when compared to control models. The addition of *S. aureus* to Th2 models led to an augmentation of all mentioned cytokines, with significant increases in TSLP, IL-22, IL-1 β , and IFN- γ levels compared to Th2 models. Notably, *S. aureus* addition also induced a significant increase in production of TSLP and IFN- γ in control models. Dupilumab treatment resulted in a significant reduction in IFN- γ levels in Th2 models. Although not statistically significant, there was a trend towards a reduction in secretion of IL-4, IL-13, IL-31, TSLP, and IL-17a in Th2 models. However, dupilumab had minimal effects in all other models.

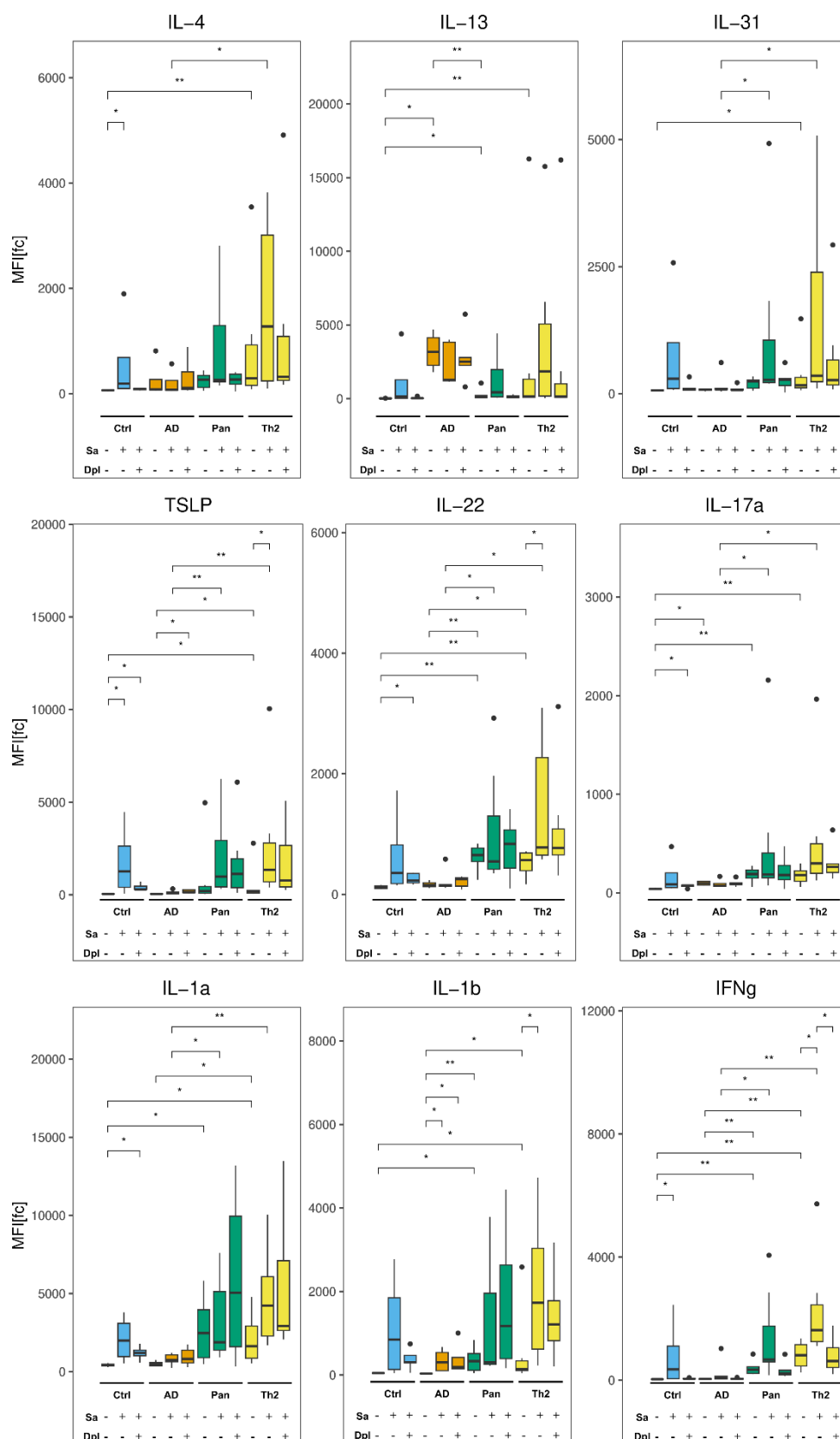


Figure 1: Multiplex ELISA of pro-inflammatory cytokines from 3D skin culture supernatants. Basolateral medium from 3D skin models was analysed by Luminex 200 multiplex ELISA. Mean fluorescence intensities (MFI) of cytokine levels were normalized to unstimulated control models (MFI [FC]). Significant comparisons are shown for p-value < 0.05 = *, p-value < 0.01 = **; (n=5). Ctrl = control; AD = atopic dermatitis (IL-4 (5ng/μl) + IL-13 (50ng/μl)); Sa = *Staphylococcus aureus*; Dpl = dupilumab; MFI = mean fluorescence intensity; FC = fold change.

***S. aureus*-induced epidermal gene expression and pathology are enhanced in a Th2 microenvironment**

H&E staining was conducted for histological assessment and to evaluate the epidermal organization of the skin equivalents. In unstimulated control skin equivalents, all epidermal layers, including the *stratum basale*, *stratum spinosum*, *stratum granulosum*, and *stratum corneum*, were observed, confirming appropriate differentiation and development of the skin model. Cultivation of *S. aureus* seem to negatively affect skin differentiation and epidermal organization in all conditions (Figure 2).

In Th2 *S. aureus* models, some spongiosis was noted, which appeared to be mitigated by dupilumab treatment (Figure 2). This spongiosis was either absent or less pronounced in the other conditions.

Furthermore, we conducted real-time PCR (Figure 3) and immunohistochemistry (Figure S3a-c) to evaluate the expression of skin barrier and differentiation-related proteins, including involucrin, loricrin, filaggrin, keratin 1, keratin 10, and keratin 14. Unstimulated control models served as control for calculating $\Delta\Delta$ ct values. Treatment of 3D skin models with IL-4 and IL-13 alone (simple AD models) resulted in reduced levels of involucrin, loricrin, and filaggrin, although this reduction was not considered as significant. Introduction of pan T cells into 3D skin models notably decreased filaggrin levels and had minor effects on loricrin and involucrin levels. Incorporation of Th2 cells led to diminished levels of filaggrin, involucrin, and loricrin, with significant reductions in loricrin and involucrin expression. The presence of *S. aureus* exacerbated the decrease in expression of all targeted barrier proteins in Th2 models, with particularly significant reductions observed in involucrin levels. Additionally, filaggrin expression significantly decreased after *S. aureus* application in control and simple AD models. Dupilumab treatment did not caused observable effects in control, AD, and pan models but did improved levels of involucrin in Th2 *S. aureus* models, with no discernible effects in other models (Figure 3, Figure S3a-c). The expression of the keratinocyte differentiation gene keratin 1 was adversely affected by IL-4 and IL-13 treatment of 3D skin models and by Th2 cell incorporation, while effects on keratin 10 and keratin 14 were negligible. Moreover, incorporation of pan T cells into 3D skin models resulted in minor alterations in the gene expression of keratins (Figure 3).

In summary, treating 3D skin models with IL-4 and IL-13, along with the integration of Th2 cells, results in a decrease in the expression of skin barrier proteins and, to some degree, adversely impacts skin differentiation, as evidenced by reduced keratin 1 expression. The introduction of *S. aureus* further disrupts epidermal organization in all conditions (Figure 2) and leads to a reduction in all skin barrier proteins in Th2 models (Figure 3, Figure S3a-c).

Results

However, dupilumab treatment did not show any visible or detectable effects in control, AD, and pan models, but improved spongiosis and involucrin expression in Th2 models.

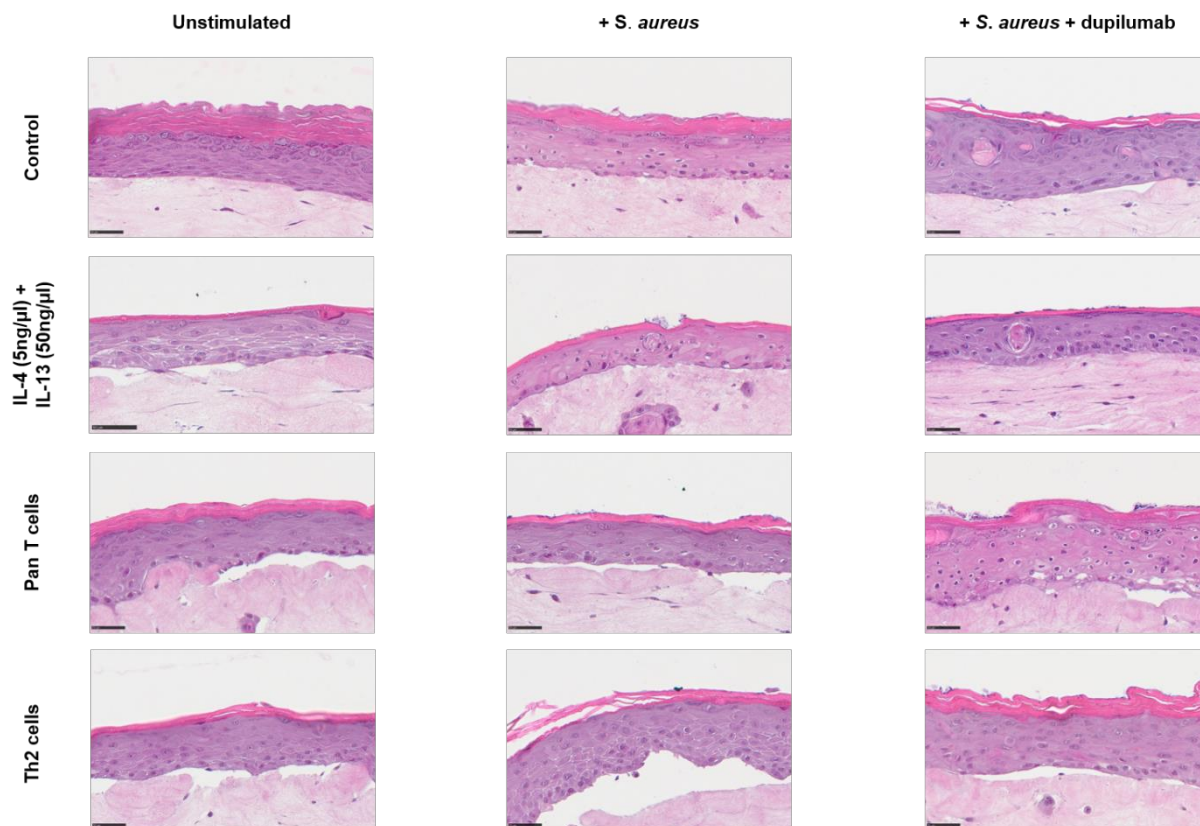


Figure 2: Representative H&E staining of formalin-fixed paraffin-embedded slides of skin models. Histological evaluation on H&E staining of 3D skin models was performed to confirm adequate differentiation and development as well as identify pathological changes due to different treatments. Scale bar= 50μm. *S. aureus* = *Staphylococcus aureus*; Th = T helper.

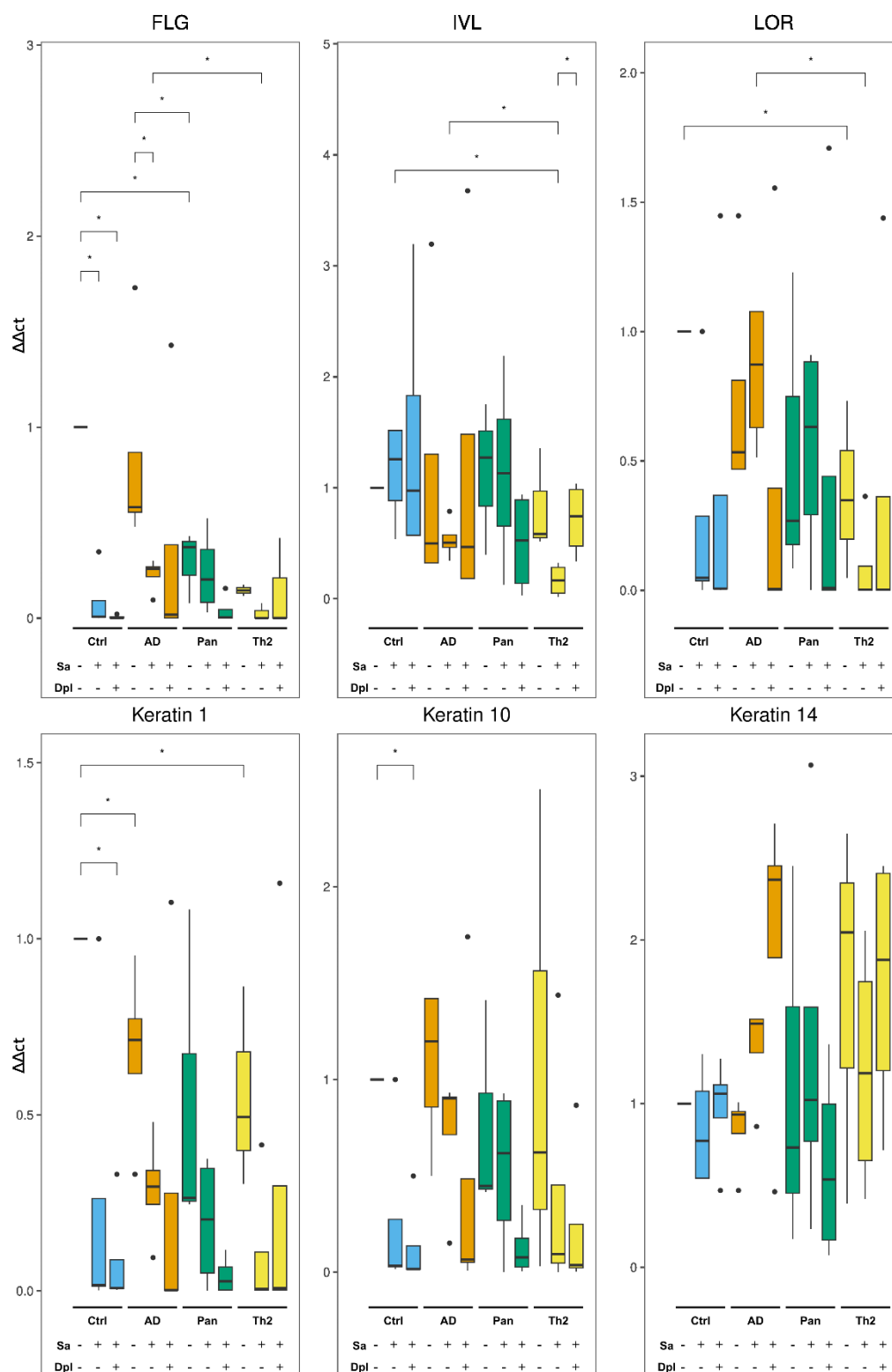


Figure 3: Analysis of skin barrier and keratinocyte differentiation 3D skin models. Relative gene expression of selected keratinocyte differentiation (keratin 1, keratin 10, keratin 14) and skin barrier (involucrin, loricrin, filaggrin) proteins was assessed in 3D skin models. $\Delta\Delta Ct$ values were calculated using RPL38 as housekeeping gene and normalized to unstimulated control models. Significant comparisons are shown for p -value $< 0.05 = *$, ($n=4$). Ctrl = control; AD = atopic dermatitis (IL-4 (5ng/ μ l) + IL-13 (50ng/ μ l); FLG = filaggrin; IVL = involucrin; LOR = loricrin; Sa = *Staphylococcus aureus*; Dpl = dupilumab.

Th2-driven 3D skin models show increased *S. aureus* growth

Elevated *S. aureus* colonization is a known feature of AD pathology that can *in vivo* be reverted by dupilumab treatment. Thus, we further assessed *S. aureus* growth following incorporation of Th2 and pan T cells, as well as dupilumab treatment. Real time PCR analysis and immunohistochemistry revealed a significant increase in *S. aureus* growth upon addition of Th2 cells to 3D skin models compared to pan T cell 3D skin models (Figure 4a, Figure 4c). This growth was reversed by dupilumab treatment, while dupilumab had no effect in pan T cell models. To elucidate whether this increase in *S. aureus* growth was primarily mediated by the key Th2 cytokines IL-4 and IL-13, we assessed *S. aureus* growth in simple AD skin and control models (Figure 4b, Figure 4c). Addition of IL-4 and IL-13 alone did not result in increased *S. aureus* growth when compared to control models and dupilumab treatment showed no significant effect on *S. aureus* growth in this simplified model (Figure 4b, Figure 4c).

Incorporation of Th2 cells into 3D skin models seems essential to replicate the observed increase in *S. aureus* growth seen *in vivo*. However, supplementation with the two key Th2 cytokines IL-4 and IL-13 alone is not adequate to significantly influence *S. aureus* growth in 3D skin models.

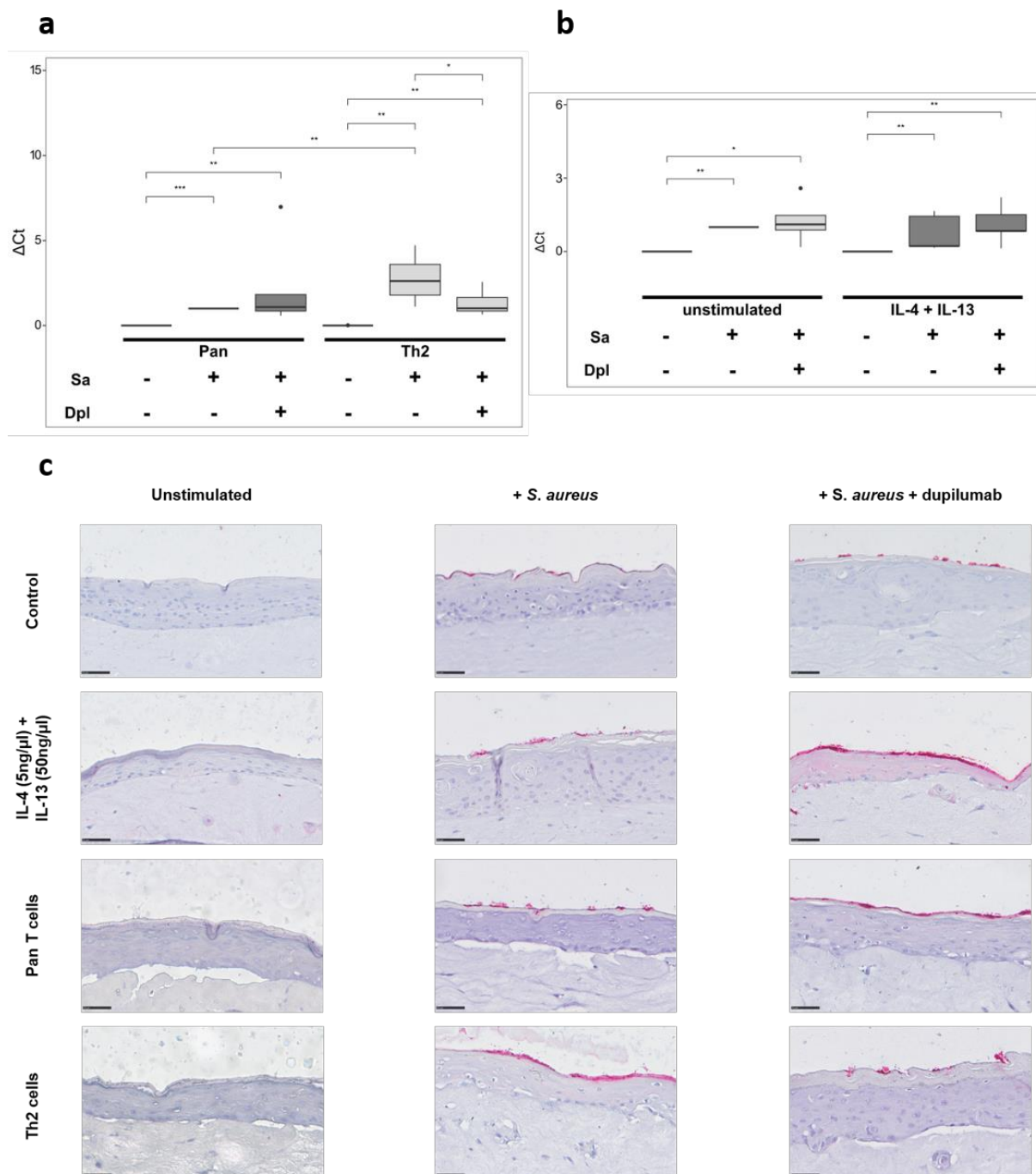


Figure 4: Th2 cells increase *S. aureus* growth which is abrogated by dupilumab treatment. Microbial DNA was isolated and *S. aureus* was quantified by qPCR in immunocompetent (a) and simple models (b). Values were normalized to *S. aureus* infected control models (pan or unstimulated). Results represent the means and s.e.m from at least 5 independent experiments. Significant comparisons are shown for p-value < 0.05 = *, p-value < 0.01 = **, p-value < 0.001 = *** Representative, supporting immunohistochemistry for *S. aureus* (pink) in immune competent and simple 3D skin models (c). Scale bar = 50 μ m. Dpl = Dupilumab; Sa = *Staphylococcus aureus*; Th = T helper; *S. aureus* = *Staphylococcus aureus*.

Discussion

In vitro human skin equivalents are an important tool to study epidermal barrier function, keratinocyte differentiation and skin microbiome. Through manipulation of culture medium, dermal matrix, and cellular constituents, different microenvironments can be generated to better imitate certain diseases^{25,26}. So far the integration of T cells was only successful using undifferentiated or Th1 polarized T cells²⁵, while Th2 associated skin models have not yet been successfully developed²². We here present the successful fabrication of a 3D skin model including Th2 cells and *S. aureus* creating an AD-like environment. By placing ionomycin/PMA-activated Th2 cells below the dermis, we induced a type-2 cytokine milieu with prominent IL-4 and IL-13 secretion. In our model, we did not observe migration of T cells into the dermis (data not shown), thus creating an indirect T cell 3D skin model. Indirect T cell cultivation in 3D skins is known to affect cytokine levels and can activate keratinocytes to produce chemokines but yet no change in skin morphology was observed²².

We compared our Th2 3D skin model to an unstimulated control model, a simple AD model, and a model including pan-activated T cells. The Th2 3D skin model is characterized and differentiates from the unstimulated control model by significant higher levels of IL-4, IL-13, IL-31, TSLP, IL-22, IL-17a, IL-1 α , IL-1 β , and IFN- γ in the basolateral medium, and a deficient skin barrier that is characterized by decreased involucrin and loricrin expression and development of spongiosis. Moreover, increased *S. aureus* growth was observed in Th2 3D skin models when compared to pan T cell 3D skin models. As a proof of principle, we treated our 3D skin models with dupilumab, a systemic treatment that is often used in clinical settings to treat patients with severe AD. In clinical settings, dupilumab not only ameliorates AD symptoms, but can also reduce pro-inflammatory cytokine levels and has been shown to be associated with reduced *S. aureus* skin colonization²⁷. Up to date, simple AD models were insufficiently complex to show expected dupilumab effects as observed in clinical settings. Introducing our new, Th2 cell model we can show for the first time significant effects of dupilumab resembling the mode of action known from clinical studies as we observed reduction in levels of different Th2, Th17, Th22 mediators and IFN- γ , improvement of spongiosis and most importantly, reduced *S. aureus* growth in Th2 3D skin models. However, dupilumab treatment did not significantly rescue expression of targeted skin integrity and barrier markers except for involucrin. This could be possibly explained by the limited incubation period (48h) of dupilumab. It could be possible that the beneficial effects of dupilumab treatment on epidermis requires a longer time span to induce skin restoration. *In vivo*, improvements in skin barrier function in AD patients have been observed after 2 weeks of dupilumab treatment²⁸. Still, treatment of Th2 3D skin with dupilumab resembles some effects of dupilumab observed in AD patient skin after successful treatment²⁷ showing that our model displays *in vivo* features.

Interestingly, levels of IFN- γ , a typical Th1 cell cytokine were also significantly higher in Th2 3D skin models compared to pan T cell models. Additionally, IFN- γ levels significantly increased after *S. aureus* cultivation and significantly decreased after additional dupilumab treatment. Keratinocytes have been shown to express IFN- γ in response to contact allergens²⁹. The presence of significantly higher IFN- γ levels in the basolateral medium of Th2 3D skin models compared pan T cell skin models could be due to increased expression of IFN- γ by keratinocytes when challenged with Th2 cells. Further investigation on the source of IFN- γ and its role in inducing *S. aureus* growth or epidermal damage would be of interest.

S. aureus was added to 3D skin models already co-cultured with either IL-4 and IL-13 stimulated, pan-activated or Th2-polarized T cells for 24h. Topical *S. aureus* application affected skin barrier and integrity in all models, but negative effects were most pronounced in Th2 3D skin models. Keratinocytes in a Th2 milieu seem to be more prone to *S. aureus* mediated barrier defects as the reduction in gene expression was most severe in Th2 models infected with *S. aureus*. *S. aureus* application had no significant effect on keratin 14 expression in all models, suggesting that *S. aureus* does not affect basal keratinocytes but keratinocytes in the suprabasal and granular layer, impairing expression of proteins of the cornified envelope, thus reducing the protective skin barrier. Keratin 1 and 10 are known to be downregulated in lesional AD skin compared to healthy control skin, and experiments in cultured keratinocytes indicate that this effect may be caused by IL-4 and IL-13^{30,31}. This substantiates that a Th2 milieu is essential for *S. aureus* mediated damage of epidermal organisation. In this study, we have also observed a significant reduction of keratin 1 expression after cultivation with IL-4 and IL-13. However, effects on were more pronounced in Th2 model than in simple AD model. Brauweiler et al. showed that *S. aureus*-derived lipoteichoic acid reduces filaggrin and involucrin and that this reduction is mediated via an IL-1 mediated pathway³². This induction of IL-1 α and IL-1 β by *S. aureus* is in concordance with previous studies²⁰ and we also observed a *S. aureus* mediated increase in IL-1 β , indicating that this pathway might play an important role in *S. aureus*-mediated impairment of the skin barrier.

We observed an increased *S. aureus* growth in models with Th2 compared to pan T cells. Filaggrin reduction in the epidermis has been shown to increase *S. aureus* attachment¹⁹ and might be one factor favouring *S. aureus* growth in the Th2 3D skin model. In our study, Th2 cell co-cultivation downregulated filaggrin which possibly made more bacteria adhere to the skin after removal of the filter paper¹⁹. Our data suggests that the Th2 milieu plays an essential role as *S. aureus* growth is only induced due to Th2 cell incorporation and inhibition of the IL-4 / IL-13 pathways by dupilumab can revert increased *S. aureus* growth. However, IL-4 and IL-13 alone are unlikely the key factors mediating *S. aureus* growth as in simplified 3D skin models the addition of IL-4 and IL-13 alone did not promote *S. aureus* growth. We observed

an additional significant increase in TSLP and IL-22 levels in Th2 3D skin models exposed to *S. aureus* but not in pan T cell or simplified 3D skin models. These cytokines are possible future targets to be analysed in simple AD models for further understanding the mechanisms of *S. aureus* growth^{24,33,34}.

Limitations of our study include the missing of additional immune cells known to contribute to AD pathology such as dendritic cells and other T cell populations. Moreover, we focused on *S. aureus* application in our model. The incorporation of different *Staphylococci* known to promote AD or contribute to a healthy skin microbiome would better mimic the *in vivo* situation. In general, we observe a high variability in data generated from 3D skins cultivated with T cells and *S. aureus* which is explained by the complexity of the experimental set up. Still, this model represents a first step in the development of complex skin models including microbial and immunological parameters with the potential for further enhancement by incorporation of different members of the skin microbiome and other immune players.

Supporting information

Appendix S1 Fabrication of 3-dimensional skin models

Human 3-dimensional skin equivalents were generated using a fibroblasts-collagen matrix seeded with 0.5×10^6 keratinocytes using a well-established protocol³³. Briefly, 0.5×10^6 fibroblasts in 250µl FCS were mixed with 2.5ml of 0.4% collagen G type I (Biochrom) mixed with Hank's Balanced Salt Solution (HBSS 10x, Gibco) and seeded onto filter inserts (3µm pore size, BD Bioscience) integrated into a 6 well deep well cell culture plate (BD Bio Coat, Corning). After 2h at 37°C w/o CO₂ the collagen solution was gelled and KGM medium with supplements was added (13ml to the surrounding external well and 2ml to the insert containing the gelled collagen matrix). After overnight incubation at 37°C and 5% CO₂, 0.5×10^6 keratinocytes were seeded on top of the matrix. After two more days, the keratinocyte layer was raised to an air-liquid interface by removing the apical media which initiates skin growth and differentiation. Skin equivalents were grown for further 5 days in supplemented keratinocyte defined medium (SKDM) consisting of KGM (without bovine pituitary extract and epinephrine) supplemented with 1.3mM calcium, 50µg/ml ascorbic acid (Sigma-Aldrich) and 0.1% bovine serum albumin (fatty acid-free, Roth). Medium was changed every second day.

Appendix S2 RNA isolation and qPCR

Total RNA of each 3D skin equivalent was isolated using the reagent Crystal RNAmagic according to the manufacturer's protocol (Biolabproducts). 0.5µg of the isolated RNA was digested and reverse transcribed to cDNA (PrimeScript RT Reagent Kit with gDNA Eraser (Perfect Real Time); TaKaRa Bio). cDNA corresponding to 10ng total RNA was used as the template in a real-time PCR. Real-time PCR was performed with the QuantStudio 3 System (BD Biosciences) using SYBR Premix Ex Taq II mix (TaKaRa Bio). The following primers were used: *filaggrin* (forward: GGCAAATCCTGAAGAATCCAGATG, reverse: GGTAATTCTCTTTTCTGGTAGACTC), *involucrin* (forward: CTGCCTCAGCCTTACTGTGA, reverse: GGAGGAGGAACAGTCTTGAGG), *loricrin* (forward: CTCTCCTCAC-TCACCTTCCT, reverse: AGGTCTTCACGCAGTCCAC), *keratin 1* (forward: CTTCTTCAGCCCCCTCAATGT, reverse: GTACCTGGTTCTGCTGCTCC), *keratin 10* (forward: TGAAAAGCATGGCAACTCAC, reverse: TGTCGATCTGAAGCAGGATG), *keratin 14* (forward: GGCCTGCTGAGATCAAAGAC, reverse: TCTGCAGAAGGACATTGGC). *RPL38* (forward: TCAAGGACTTCCTGCTCACA, reverse: AAAGGTATCTGCTGCATCGAA) was used as a housekeeping gene in order to calculate ΔC_t values.

Appendix S3 Bacterial DNA isolation and qPCR

Total bacterial DNA was isolated from each skin equivalent (3mm punch biopsy) using QIAamp DNA Microbiome Kit (Qiagen). Briefly, 3mm punch biopsy was directly transferred into a lysis tube and stored at -80°C. For bacterial DNA isolation, samples were thawed and 190µl RDD buffer + 2.5µl benzonase was added and incubated for 30min at 37°C at 600rpm. Afterwards 20µl proteinase k was added and samples were incubated for 30min at 56°C at 600rpm. 200µl ATL/DX was added and tissue was homogenized using a speedmill (2x 45s). Samples were centrifuged for 1min at 10.000xg and supernatant was transferred into a new tube containing 40µl proteinase k followed by 30min incubation at 56°C at 600rpm. After incubation, 200µl APL2 buffer was added and samples were incubated for 10min at 70°C. 100% ethanol was added, solution was mixed using a vortexer, and DNA was extracted using a column. 1µl of bacterial DNA was used for real-time PCR. Real-time PCR was performed with the QuantStudio 3 System (BD Biosciences) using SYBR Premix Ex Taq II mix (TaKaRa Bio). The following primer was used: forward: 5' tca ttt tgc cgg aag tta tgc 3', reverse: 5' aac ggt caa tgc cat gat tta at 3'.

Appendix S4 H&E staining

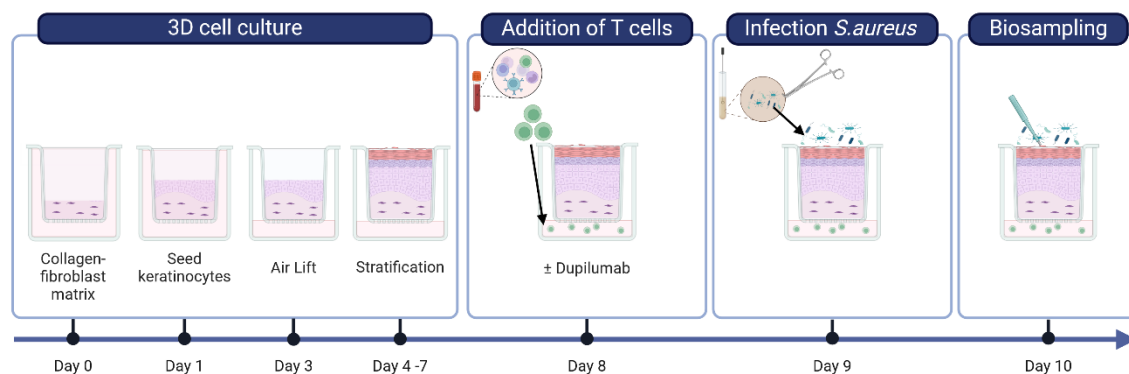
H&E staining was performed as previously reported ³⁴ starting with deparaffinization using xylene followed by hydration steps (100% ethanol, 96% ethanol, 70% ethanol, H₂O). Hematoxylin staining was performed using Shandon Gill 3 Gematoxylin (Thermo Fisher Scientific, Dreieich, Germany). Glacial acid was used for differentiation and eosin staining was performed using Shandon Eosin Y (Thermo Fisher Scientific, Dreieich, Germany). Finally, dehydration was performed (70% ethanol, 96% ethanol, 100% ethanol) and slides were placed into xylene providing compatible solvent for the mounting medium (Thermo Fisher Scientific, Dreieich, Germany).

Appendix S5 Immunohistochemistry

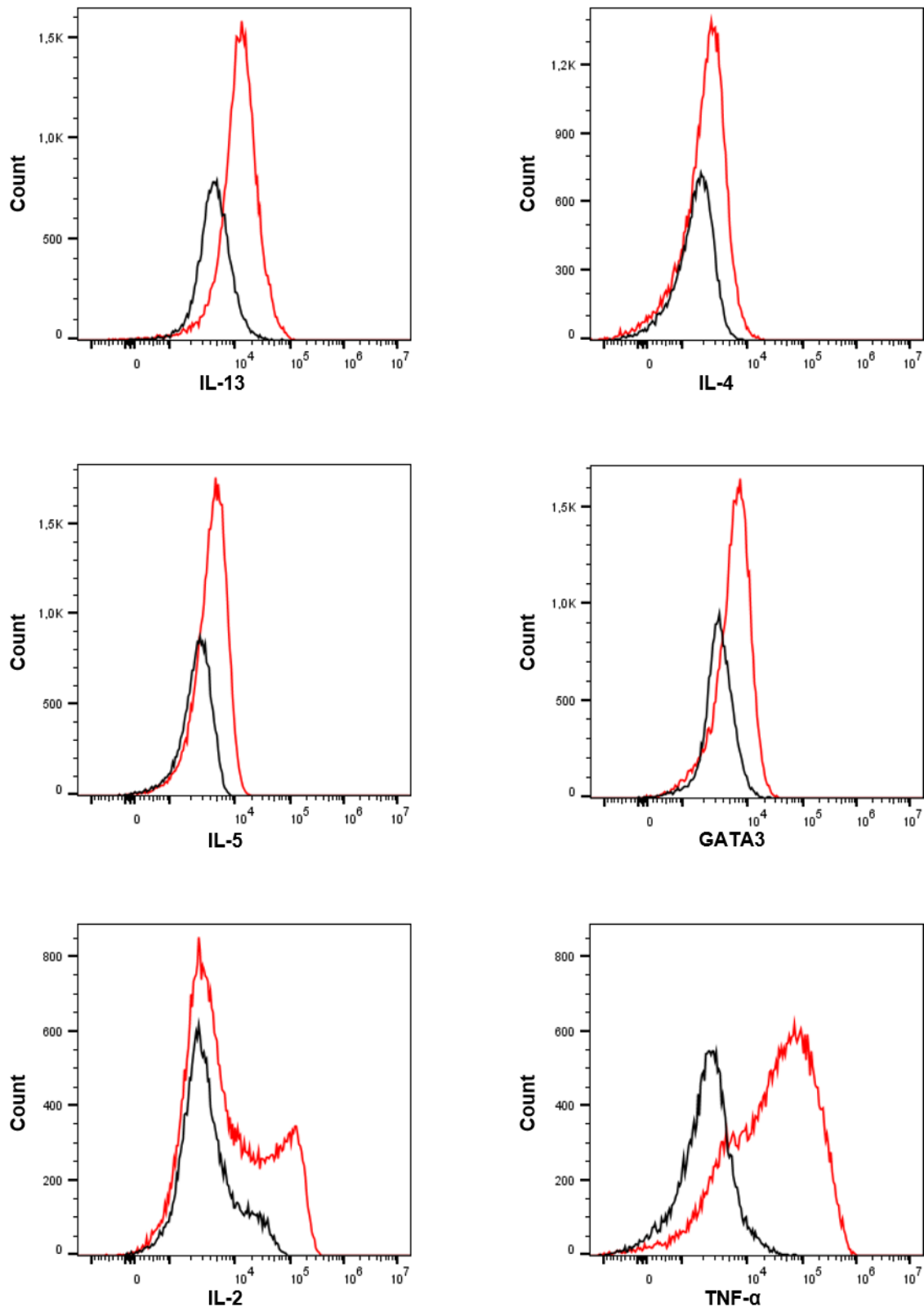
The organotypic 3D skin equivalents were fixed by formalin and embedded in paraffin. For immunostaining anti-*staphylococcus aureus* (Abcam, #ab20920) 1:500 diluted; anti-filaggrin (#sc66192), 1:50 diluted; anti-involucrin (Abcam, #ab53112), 1:300 diluted; and anti-loricrin (Invitrogen, #PA5-30583), 1:500 diluted; antibodies were used. Dilutions have been performed in tris-buffered saline (TBS)/1% bovine serum albumin (BSA). Biotinylated swine anti-rabbit (Dako) 1:300 diluted in TBS/1% BSA served as second antibody. Blocking was performed with TBS/12% BSA. For development, the Vectastain Elite ABC Komplex (PK-6100) followed by

the Vector Nova Red-Substrate (SK-4800; both Vector Laboratories, USA) was used. Slides were counterstained with hematoxylin and mounted using Cytoseal XYL (ThermoFisher Scientific).

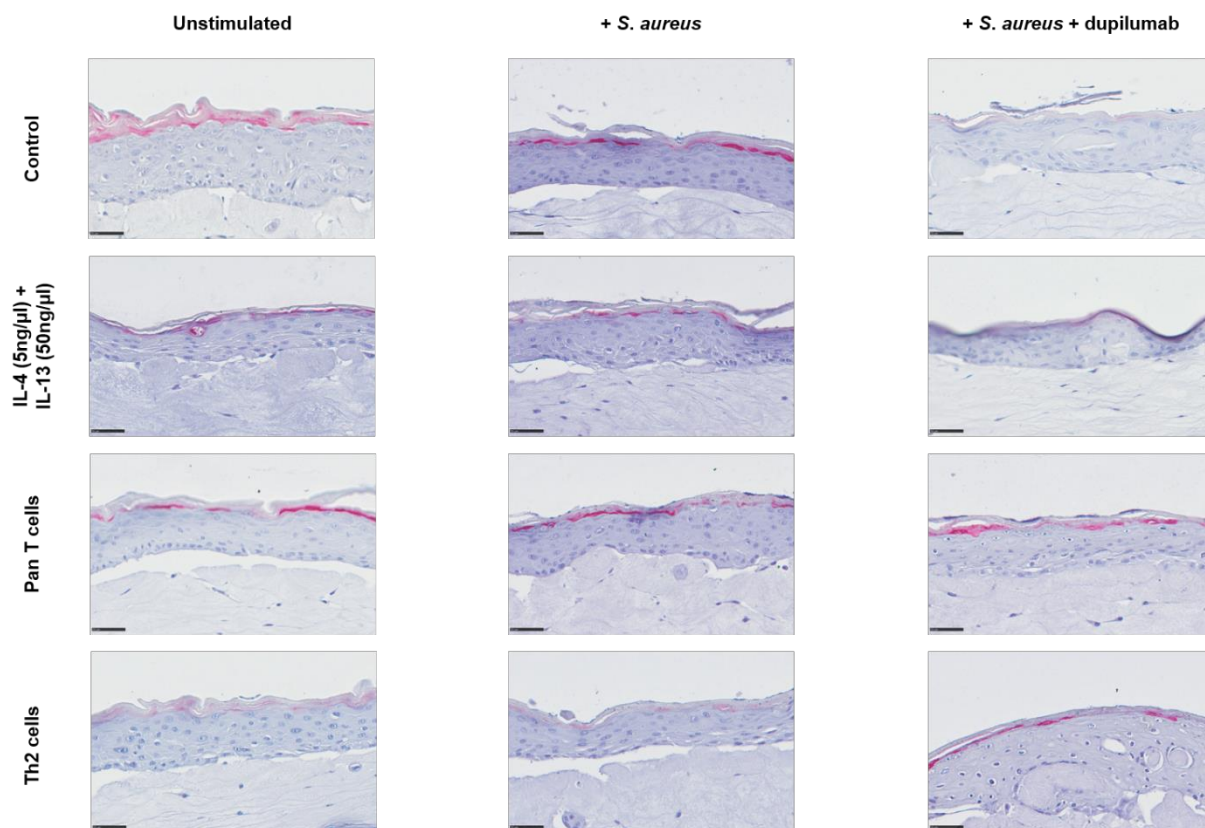
Supporting Figures



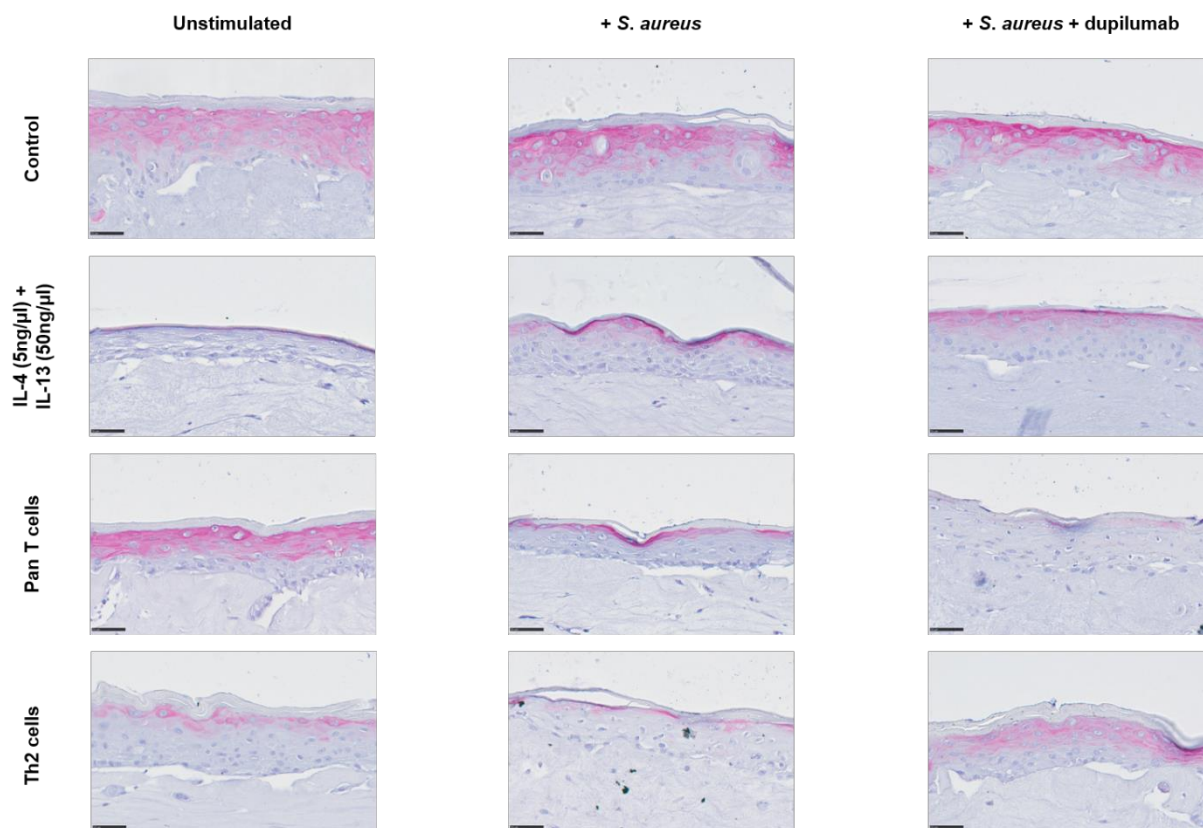
Supplemental Figure 1: Workflow of constructing immunocompetent 3D skin microbiome models. Th2 or pan T cells were placed directly under the dermis of the fully developed skin equivalents for 48h. *S. aureus* was applied by filter paper transfer for the last 24h of the experiment.



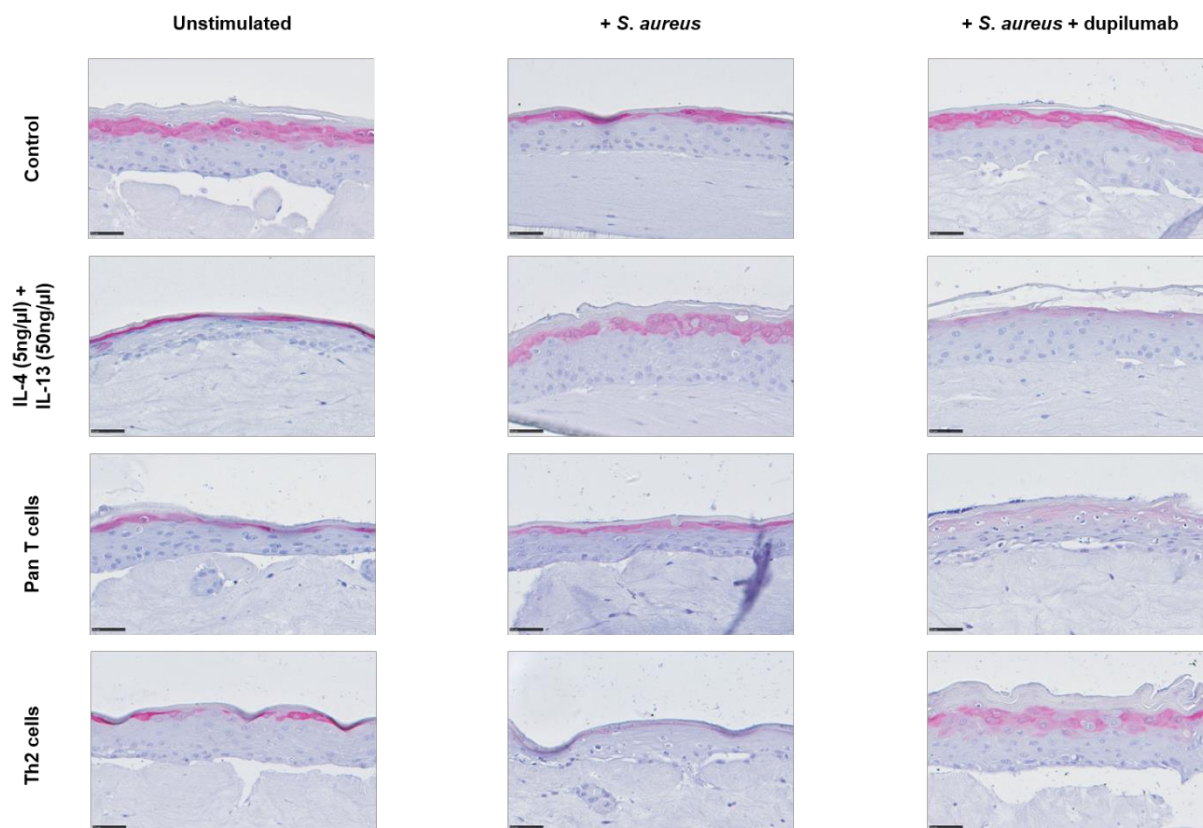
Supplemental Figure 2: Flow cytometric analysis of T cells after in vitro differentiation. T cells were either pan-activated (black) by anti-CD3 and anti-CD28 stimulation or differentiated into Th2 cells (red) by additional cultivation with IL-4 and anti-IFN- γ . Cytokine expression was analysed after PMA and ionomycin stimulation together with brefeldin A incubation after intracellular flow cytometry. Pictures show representative plots from 5 individual experiments.



Supplemental Figure 3a: Supporting immunohistochemistry for the skin barrier protein filaggrin (pink). Immunohistochemistry targeting filaggrin was performed on representative histological slides from different 3D skin models. Scale bar = 50μm.



Supplemental Figure 3b: Supporting immunohistochemistry for the skin barrier protein involucrin (pink). Immunohistochemistry targeting involucrin was performed on representative histological slides from different 3D skin models. Scale bar = 50μm.



Supplemental Figure 3c: Supporting immunohistochemistry for the skin barrier protein loricrin (pink). Immunohistochemistry targeting loricrin was performed on representative histological slides from different 3D skin models. Scale bar = 50μm.

References

- 1 Basu MN, Mortz CG, Jensen TK, *et al.* Natural moisturizing factors in children with and without eczema: Associations with lifestyle and genetic factors. *J Eur Acad Dermatol Venereol* 2022; **36**:255–62.
- 2 Batista DIS, Perez L, Orfali RL, *et al.* Profile of skin barrier proteins (filaggrin, claudins 1 and 4) and Th1/Th2/Th17 cytokines in adults with atopic dermatitis. *J Eur Acad Dermatol Venereol* 2015; **29**:1091–5.
- 3 Janssens M, Van Smeden J, Gooris GS, *et al.* Increase in short-chain ceramides correlates with an altered lipid organization and decreased barrier function in atopic eczema patients. *J Lipid Res* 2012; **53**:2755–66.
- 4 Kopfnagel V, Harder J, Werfel T. Expression of antimicrobial peptides in atopic dermatitis and possible immunoregulatory functions. *Curr Opin Allergy Clin Immunol* 2013; **13**:531–6.
- 5 Beck LA, Cork MJ, Amagai M, *et al.* Type 2 Inflammation Contributes to Skin Barrier Dysfunction in Atopic Dermatitis. *JID innovations : skin science from molecules to population health* 2022; **2**:100131.
- 6 Totté JEE, van der Feltz WT, Hennekam M, *et al.* Prevalence and odds of Staphylococcus aureus carriage in atopic dermatitis: a systematic review and meta-analysis. *Br J Dermatol* 2016; **175**:687–95.
- 7 Towell AM, Feuillie C, Vitry P, *et al.* Staphylococcus aureus binds to the N-terminal region of corneodesmosin to adhere to the stratum corneum in atopic dermatitis. *Proc Natl Acad Sci U S A* 2021; **118**. doi:10.1073/PNAS.2014444118.
- 8 Clausen ML, Slotved HC, Krogfelt KA, *et al.* In vivo expression of antimicrobial peptides in atopic dermatitis. *Exp Dermatol* 2016; **25**:3–9.
- 9 Williams MR, Nakatsuji T, Sanford JA, *et al.* Staphylococcus aureus Induces Increased Serine Protease Activity in Keratinocytes. *J Invest Dermatol* 2017; **137**:377–84.
- 10 Leung DYM, Bissonnette R, Kreimer S, *et al.* Dupilumab Inhibits Vascular Leakage of Blood Proteins Into Atopic Dermatitis Skin. *J Allergy Clin Immunol Pract* 2023; **11**:1421–8.
- 11 Schlievert PM, Gourronc FA, Leung DYM, Klingelutz AJ. Human Keratinocyte Response to Superantigens. *mSphere* 2020; **5**. doi:10.1128/MSPHERE.00803-20.
- 12 Tuffs SW, Haeryfar SMM, McCormick JK. Manipulation of Innate and Adaptive Immunity by Staphylococcal Superantigens. *Pathogens* 2018; **7**. doi:10.3390/PATHOGENS7020053.
- 13 De Vuyst E, Salmon M, Evrard C, *et al.* Atopic Dermatitis Studies through In Vitro Models. *Front Med (Lausanne)* 2017; **4**. doi:10.3389/FMED.2017.00119.
- 14 Morgner B, Tittelbach J, Wiegand C. Induction of psoriasis- and atopic dermatitis-like phenotypes in 3D skin equivalents with a fibroblast-derived matrix. *Sci Rep* 2023; **13**. doi:10.1038/S41598-023-28822-7.
- 15 Barker CL, McHale MT, Gillies AK, *et al.* The development and characterization of an in vitro model of psoriasis. *J Invest Dermatol* 2004; **123**:892–901.
- 16 Danso MO, Van Drongelen V, Mulder A, *et al.* TNF- α and Th2 cytokines induce atopic dermatitis-like features on epidermal differentiation proteins and stratum corneum lipids in human skin equivalents. *J Invest Dermatol* 2014; **134**:1941–50.

- 17 Pupovac A, Senturk B, Griffoni C, *et al.* Toward Immunocompetent 3D Skin Models. *Adv Healthc Mater* 2018; **7**. doi:10.1002/ADHM.201701405.
- 18 Emmert H, Rademacher F, Gläser R, Harder J. Skin microbiota analysis in human 3D skin models-“Free your mice”. *Exp Dermatol* 2020; **29**:1133–9.
- 19 van Drongelen V, Haisma EM, Out-Luiting JJ, *et al.* Reduced filaggrin expression is accompanied by increased Staphylococcus aureus colonization of epidermal skin models. *Clin Exp Allergy* 2014; **44**:1515–24.
- 20 Kohda K, Li X, Soga N, *et al.* An In Vitro Mixed Infection Model With Commensal and Pathogenic Staphylococci for the Exploration of Interspecific Interactions and Their Impacts on Skin Physiology. *Front Cell Infect Microbiol* 2021; **11**. doi:10.3389/FCIMB.2021.712360.
- 21 Rees B, Spiekstra SW, Carfi M, *et al.* Inter-laboratory study of the in vitro dendritic cell migration assay for identification of contact allergens. *Toxicol In Vitro* 2011; **25**:2124–34.
- 22 Van Den Bogaard EH, Tjabringa GS, Joosten I, *et al.* Crosstalk between keratinocytes and T cells in a 3D microenvironment: a model to study inflammatory skin diseases. *J Invest Dermatol* 2014; **134**:719–27.
- 23 Mildner M, Jin J, Eckhart L, *et al.* Knockdown of filaggrin impairs diffusion barrier function and increases UV sensitivity in a human skin model. *J Invest Dermatol* 2010; **130**:2286–94.
- 24 Breen EJ, Tan W, Khan A. The Statistical Value of Raw Fluorescence Signal in Luminex xMAP Based Multiplex Immunoassays. *Sci Rep* 2016; **6**. doi:10.1038/SREP26996.
- 25 Morin S, Bélanger S, Cortez Ghio S, Pouliot R. Eicosapentaenoic acid reduces the proportion of IL-17A-producing T cells in a 3D psoriatic skin model. *J Lipid Res* 2023; **64**:100428.
- 26 Pupovac A, Senturk B, Griffoni C, *et al.* Toward Immunocompetent 3D Skin Models. *Adv Healthc Mater* 2018; **7**:1701405.
- 27 Hartmann J, Moitinho-Silva L, Sander N, *et al.* Dupilumab but not cyclosporine treatment shifts the microbiome toward a healthy skin flora in patients with moderate-to-severe atopic dermatitis. *Allergy* 2023; **78**:2290–300.
- 28 Berdyshev E, Goleva E, Bissonnette R, *et al.* Dupilumab significantly improves skin barrier function in patients with moderate-to-severe atopic dermatitis. *Allergy* 2022; **77**:3388–97.
- 29 Howie SEM, Aldridge RD, McVittie E, *et al.* Epidermal keratinocyte production of interferon-gamma immunoreactive protein and mRNA is an early event in allergic contact dermatitis. *J Invest Dermatol* 1996; **106**:1218–23.
- 30 Totsuka A, Omori-Miyake M, Kawashima M, *et al.* Expression of keratin 1, keratin 10, desmoglein 1 and desmocollin 1 in the epidermis: possible downregulation by interleukin-4 and interleukin-13 in atopic dermatitis. *Eur J Dermatol* 2017; **27**:247–53.
- 31 Howell MD, Kim BE, Gao P, *et al.* Cytokine modulation of atopic dermatitis filaggrin skin expression. *J Allergy Clin Immunol* 2007; **120**:150–5.
- 32 Brauweiler AM, Goleva E, Leung DYM. Staphylococcus aureus Lipoteichoic Acid Damages the Skin Barrier through an IL-1-Mediated Pathway. *J Invest Dermatol* 2019; **139**:1753-1761.e4.
- 33 Mildner M, Ballaun C, Stichenwirth M, *et al.* Gene silencing in a human organotypic skin model. *Biochem Biophys Res Commun* 2006; **348**:76–82.

- 34 Arnold DL, Gold R, Kappos L, *et al.* Effects of delayed-release dimethyl fumarate on MRI measures in the Phase 3 DEFINE study. *J Neurol* 2014; **261**:1794–802.

6 General Discussion and Outlook

Advancements in disease models, biosampling techniques, and high throughput analyses are permanently enhancing our understanding of the molecular mechanisms underlying Atopic Dermatitis (AD) pathology. Nevertheless, several questions regarding AD pathology remain yet unanswered, necessitating future exploration. Therefore, my research has focused on characterizing the inflammatory milieu in AD, linking it to oxidative stress (OS), introducing minimally invasive biosampling techniques for enhanced patient material accessibility, and refining disease models that could be potentially used for biomarker validation and a deeper understanding of AD pathology.

Identification of signature cytokines at Atopic Dermatitis manifestation and their potential to predict disease manifestation in infants

I conducted a comprehensive assessment of the inflammatory environment in AD skin *ex vivo* using tape strips (Article II). Tape strips represent a crucial tool for minimally invasive biosampling on patient skin, and have the potential to supplement or even substitute conventional biosampling methods such as skin punch biopsies. The primary limitation of skin punch biopsies lies in their invasive nature, leading to reluctance of study participants to contribute biopsies. Furthermore, there is a higher frequency of biosampling from patients with severe AD and a lower participation of children. This imbalance has the potential to introduce bias in the data collected from skin punch biopsies. The quantity of publications examining *stratum corneum* protein levels through tape strips is growing, underscoring the significance of this field^{92,94,96,97}. However, there is still a scarcity of data on transcriptomic analyses conducted on material obtained from tape strips^{137–140}. AD typically manifests during childhood with the highest incidence occurring between three and six months of age¹⁴¹. Moreover, 15-20% of children worldwide are affected⁸⁴ underscoring the significance of understanding the underlying mechanisms that contribute to the manifestation of the disease in infants. Due to this early onset, there is a need to develop minimally invasive methods for monitoring immune responses in the skin of children. In my thesis, I established tape stripping as a minimally invasive method to measure pro-inflammatory cytokine levels in infants. In my work, I characterized the inflammatory environment in children shortly after birth, prior to AD manifestation, and at initial AD manifestation, comparing it to the protein signature of healthy children (Article II). Our study revealed elevated levels of pro-inflammatory cytokines such as IL-8, IL-18, IL-22, CCL2, CCL17/TARC, and VEGF α in the *stratum corneum* of children who later developed AD, could precede clinical manifestation (**Figure 9**). Previous studies have reported an association of *stratum corneum* CCL17/TARC and TSLP levels with later AD development¹⁴² as well as IL-

General Discussion and Outlook

IL-18 and IL-8 levels with later moderate to severe AD manifestation^{95,143} which is further supported by our findings. Notably, the majority of the identified cytokines potentially preceding childhood AD were reported to either directly damage skin barrier or positively correlated with skin barrier defects highlighting the role of cytokines in facilitating skin barrier deficiencies in AD pathology. For instance, elevated IL-22 concentrations are correlated with epidermal hyperplasia, acanthosis and skin barrier defects^{144–146}. IL-18 was found to be upregulated in the *stratum corneum* of AD skin lesions¹⁴⁷, with even higher levels in *S. aureus* colonized patients and additionally, strong associations between IL-18 levels and barrier deficiency have been reported^{147,148}. Furthermore, IL-18 increases IL-4, IL-13, and histamine levels by activating mast cells and basophils¹⁴⁹. Consequently, IL-18 indirectly facilitates skin barrier deficiency as IL-4 and IL-13 have been shown to downregulate FLG, LOR and IVL *in vitro*^{150,151} and histamine acts as an itch-inducing substance promoting scratching¹⁵².

These results could potentially support the inside-out hypothesis postulated in AD pathology that suggests that immune dysregulation may trigger skin barrier dysfunction¹⁵³. This indicates that various inflammatory cytokines present in AD skin lead to downregulation of different proteins necessary for maintaining the skin barrier such as epidermal differentiation and tight junctions. This barrier disruption could lead to skin penetration by allergens and pathogens, thus amplifying immune responses¹⁵⁴. Different studies have contributed data supporting the inside out hypothesis and several identified mutations in AD patients affect genes that facilitate systemic inflammations like mutations of IL4RA, CD14, SPINK5 and RANTES^{27,155,156}.

The outside in hypothesis however implies that the impaired skin barrier precedes AD manifestation and is required for the dysregulation of the immune system to occur¹⁵³. This hypothesis was mainly driven by the identification of a FLG mutation that was linked to almost 20% of AD cases in northern Europe populations^{25,29,153}. FLG is essential for skin barrier function and the skin barrier dysfunction resulting from a FLG mutation results in increased cutaneous and systemic Th2 responses that are characteristic for AD^{93,121,157,158}. However, FLG mutations do not always lead to AD manifestation¹⁵⁹.

Having identified various cytokines linked to AD prior to the manifestation of the disease, it could be inferred that these cytokines may compromise the skin barrier in infants, potentially serving as a triggering factor for the onset of the disease.

At AD onset several protein markers involved in AD pathology were upregulated including markers associated with Th2 immune responses¹⁴⁶, markers linked to Th1 and Th17/22 immune responses as well as key innate and adaptive immunity markers^{160,161}. The identified upregulated proteins at disease onset cover almost all known immune axes postulated to be involved in AD pathology. Article II therefore extends previous observations and highlights the

General Discussion and Outlook

feasibility of a non-invasive collection of skin biomarkers that characterize pediatric AD at onset, possibly even precede disease manifestation (**Figure 9**).

We hereby provide additional supporting data for CCL17/TARC as a key biomarker for childhood AD. CCL17/TARC mediates type 2 inflammation. It binds to C-C chemokine receptor type 4 which is expressed by Th2 cells, thereby serving as a Th2 chemoattractant ^{89,162}. CCL17/TARC was previously shown to correlate with AD severity ¹⁶³. Additionally, Halling *et al.* and Rinnoov *et al.* have shown that *stratum corneum* TARC predicts and precedes AD manifestation in children ^{143,164} and a Japanese study even identified differences in umbilical cord serum levels of CCL17/TARC between children that later manifested AD and those who did not ¹⁶⁵.

In summary, Article II of this thesis not only presents a distinct inflammatory protein signature preceding and characterizing AD but also demonstrates that tape strips provide a suitable alternative to skin biopsies for capturing the inflammatory environment in skin of AD patients. Tape strips can detect AD features and could be useful to identify novel biomarkers and therapeutic targets for AD treatment.

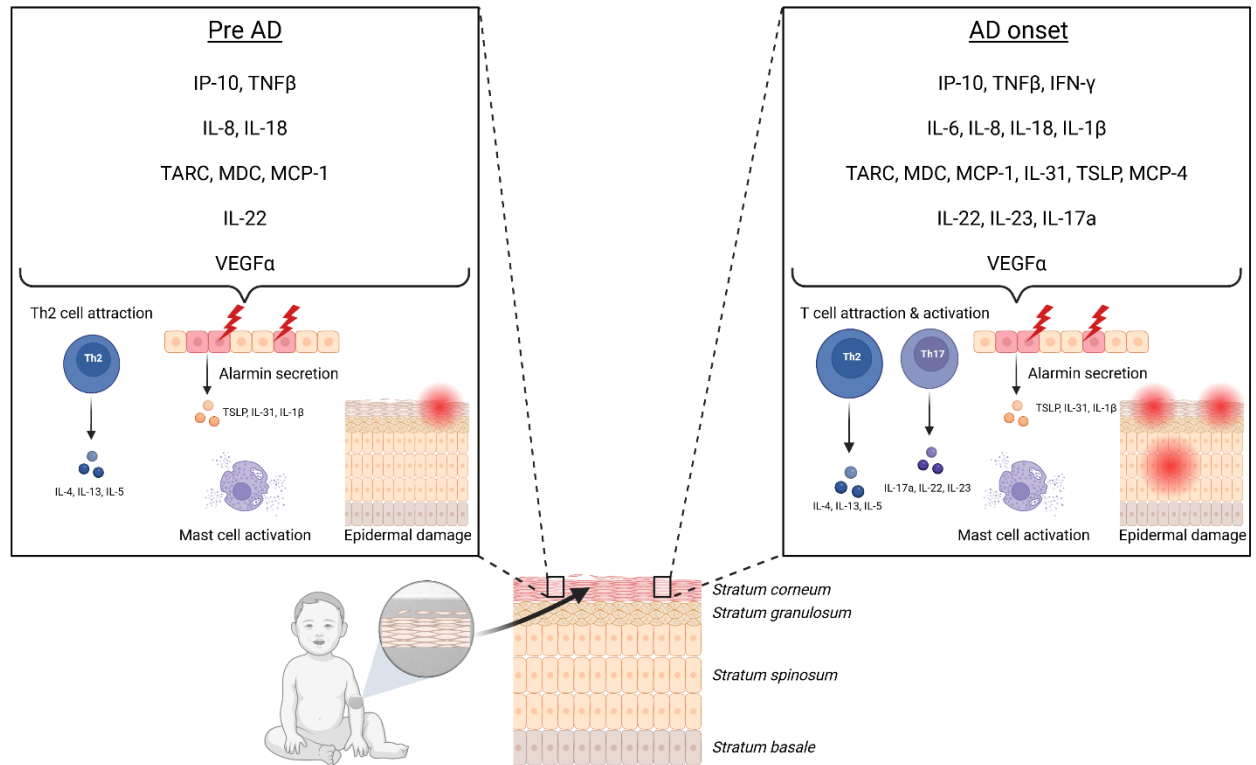


Figure 9: Molecular profiling of the inflammatory environment of the *stratum corneum* using tape strips.

Tape strips gently remove upper skin layers in a minimally invasive way. Analysis of proteins isolated from tape strips from infants at high risk of developing atopic dermatitis (AD) indicates elevated levels of various innate immunity markers, Th1 and Th2 mediators, and IL-22 preceding the manifestation of AD (pre AD). These proteins have the potential to compromise the skin barrier and foster skin inflammation. Upon AD onset, additional inflammatory mediators are measured in the *stratum corneum*, attracting and activating various T cell populations, activating mast cells, and causing damage to the skin barrier. AD = atopic dermatitis. Created with BioRender.com

The role of oxidative stress in inflammatory signaling – a vicious cycle

In addition to increased levels of pro-inflammatory mediators in both, serum and skin, various studies have highlighted elevated oxidative stress (OS) as an additional aspect of AD pathology. Given the understanding that the generation of reactive oxygen species (ROS) can trigger pro-inflammatory processes^{70,72}, I was interested in further investigating the interplay between inflammation and OS in primary skin cells, specifically keratinocytes and fibroblasts. Hence, I emphasized the link between cellular OS state and inflammation in AD in chapter 5.1. Furthermore, I demonstrated targeted NADPH oxidase (NOX) inhibition as a potential treatment approach to mitigate the harmful effects induced by high levels of pro-inflammatory cytokines in the skin.

General Discussion and Outlook

The AD model keratinocytes employed in this article (Article I) exhibited an increased oxidative stress state presented by high intracellular ROS levels that translated into DNA damage. In fact, ROS activates MAPKs like ERK, JNK, and p38 kinases resulting in the induction of several pro-inflammatory transcription factors and genes such as the recruitment of c-Fos and c-Jun to the nucleus that activate AP-1 and therefore amplify inflammation ¹⁶⁶. Activation of p38 signaling is further involved in NFκB activation, leading to transcription of several proinflammatory genes involved in AD pathology such as iNOS and COX-2 ¹⁶⁷.

Our study revealed that in addition to high ROS levels inducing inflammation, pro-inflammatory cytokines themselves stimulate ROS formation in keratinocytes. Moreover, we showed that keratinocytes serve as one major source of ROS, underlining their substantial contribution to skin inflammation. Elevated ROS levels in human keratinocytes can enhance EGFR phosphorylation activating ERK and JNK and thereby amplifying inflammation ¹⁶⁸. This could potentially lead to a vicious circle, in which pro-inflammatory cytokines and high levels of ROS mutually trigger the formation and release of each other, thus leading to a self-perpetuating inflammatory cycle (**Figure 10**). In Article III I demonstrated that treatment of cultured keratinocytes with AD signature cytokines additionally stimulates the secretion of various pro-inflammatory cytokines. Among them, IL-8 and IL-18 for instance, are known to be both regulated by and are capable of regulating intracellular ROS levels ^{169–171}. IL-8 was shown to be secreted by keratinocytes in response to UVB and following p38MAPK activation which is mediated by ROS ^{169,171}. IL-8 itself is involved in neutrophil recruitment ¹⁷² and IL-18 and IL-1β have been shown to induce the oxidative burst of neutrophils ¹⁷⁰. Taken together, these findings suggest that heightened pro-inflammatory and oxidative signaling jointly influence the severity of AD, underscoring sources of ROS as additional therapeutic targets in the treatment of AD.

Increased levels of measured ROS in AD can be explained via either impaired redox homeostasis mechanisms or due to increased ROS production ^{168,173,174}. Theoretically, supplementation with antioxidants either topical or systemic could help to decrease resulting ROS levels thereby preventing oxidative stress which could lead to the improvement of skin inflammation. However, most clinical trial results failed to show effectiveness which could be explained by missing bioavailability and solubility of the antioxidants ^{173,175–177}. Still, resveratrol which is a naturally produced phenol and phytoalexin, was reported to be efficient in AD treatment in AD like mice models ¹⁷⁸. Treatment has led to increasing loricrin and filaggrin levels and epithelial thickness with concurrent reduction of OS markers and AD like skin lesions ¹⁷⁹. Still, resveratrol lacks solubility and bioavailability and data from clinical trials in humans are missing ^{178,180}.

To further address the question whether the impaired redox homeostasis in inflammatory skin diseases results from increased ROS production or reduced antioxidant capacity, I have used the pan NOX inhibitor DPI which inhibits intracellular ROS production. Thereby I was able to

General Discussion and Outlook

show that elevated oxidative stress in our disease models arises from increased intrinsic ROS production rather than from impaired antioxidant capacity. DPI treatment successfully abolished high ROS levels in our experiments and still maintains basal ROS levels that are needed for physiological processes. Still, there are some drawbacks that lower the potential of DPI in AD treatment and that need to be discussed. DPI also inhibits CYP450, nitric oxide (NO) synthase and the mitochondrial chain, which all are important physiological producers of ROS making DPI unspecific leading to toxic side effects ^{173,181}. Our results show that DPI has some the toxic effects when cells are not in an oxidative stress state as the addition of DPI to un-stressed cells (without H₂O₂) reduced cell survival.

The identification of specific inhibitors would have the potential to offer a promising alternative for DPI in AD treatment as they would evade the unspecific toxic side effects of DPI and concurrently provide higher specificity. In keratinocytes NOX 1, 2 and 4 are expressed ^{77,78,81,182–184} and the specific inhibition of specific NOX could reduce off target effects and improve treatment effectiveness as compared to the pan inhibitor DPI ^{82,185,186}. Until today, NOX inhibitors are not approved for AD treatment but clinical trials (phase II) with 170 patients have demonstrated that the NOX1 and NOX1/4 inhibitors used in our experiments are well-tolerated and non-toxic therefore providing a promising future alternative for DPI ¹⁸⁵. In Article I, I could show that the specific inhibitors exhibited good results, presenting their effectiveness in 2D-cultured keratinocytes and offering a promising possibility for future treatment options. It would be of interest to further validate their effectiveness and safety in future *in vitro* and *in vivo* studies.

A noteworthy example presenting the potential of NOX inhibition in treatment of inflammatory skin diseases is gentian violet. Gentian violet is a triphenylmethane dye made of hexamethylrosaniline and has been used since the 19th century for the treatment of different dermatological conditions such as atopic dermatitis and burns ¹⁸⁷. It is known for its antimicrobial, antiviral, antifungal and anti-angiogenic properties ^{187,188}. Its efficacy for irritant atopic dermatitis was assessed in 18 subjects where a reduction of TEWL and improvement in skin hydration was observed when compared to placebo group after 14 days of application ¹⁸⁸. Moreover, a study including 38 atopic dermatitis patients colonized with *S. aureus* has shown that gentian violet treatment has led to decreased *S. aureus* colonization and improvements in SCORAD after four days of treatment ¹⁸⁹. Although gentian violet proved effective in topical treatment of AD, it fell out of favour as a topical sterilizing agent due to its skin-coloring properties. The rise of novel antibiotics and other colourless topical treatments might have also contributed to the decreased usage of gentian violet in treating atopic dermatitis.

Interestingly, gentian violet inhibits NOX2 resulting in a reduction of NO and superoxide levels ¹⁹⁰. While the effectiveness of gentian violet in treating AD has traditionally been attributed to its antimicrobial properties, the potential cause of these effects could be linked to NOX

General Discussion and Outlook

inhibition and the subsequent decrease in intracellular ROS. Given that gentian violet is an approved drug, it could serve as a promising candidate for additional clinical studies.

In summary, cellular ROS and cutaneous inflammation appear to be tightly linked processes reinforcing each other. AD key cytokines could potentially activate skin resident NOX, leading to an overproduction of ROS. These ROS, in turn, might trigger signalling cascades leading to induction of inflammatory processes. Inhibiting NOX activity could have the potential to reduce elevated levels of ROS, subsequently contributing to a decrease in skin inflammation.

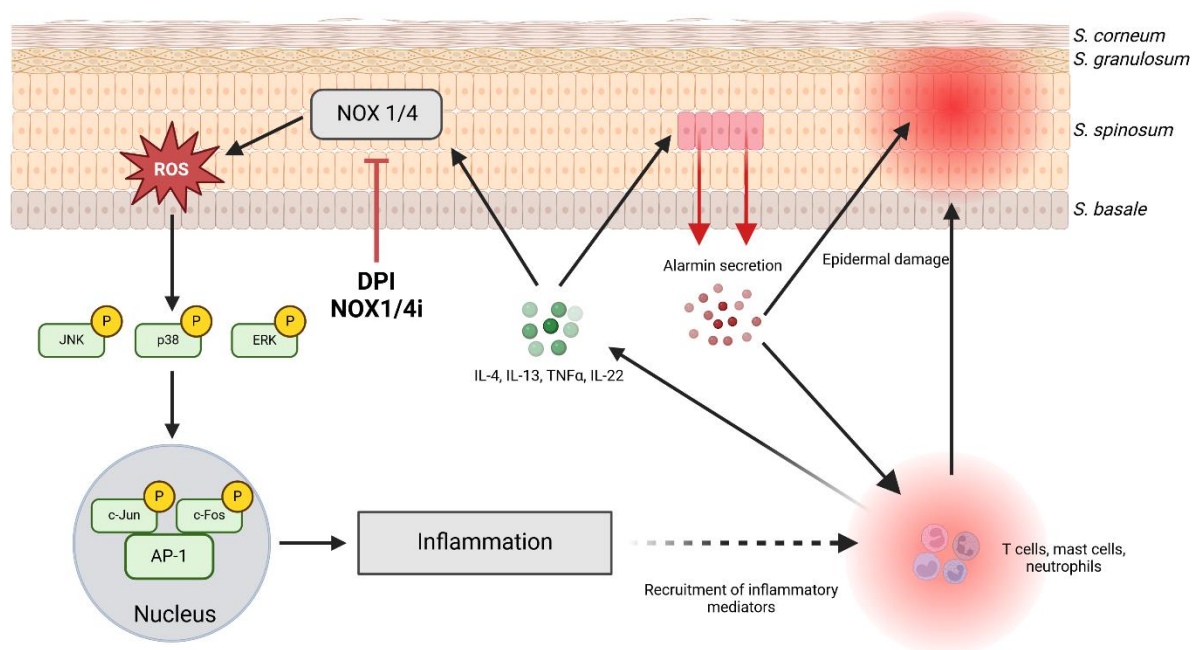


Figure 10: Vicious circle involving pro-inflammatory cytokines and production of reactive oxygen species by keratinocytes in atopic dermatitis. Cytokines known to be involved in AD pathology can induce NOX1/4 activity in human keratinocytes resulting in an excessive production of reactive oxygen species (ROS). These ROS, in turn, promote phosphorylation and activation of diverse pro-inflammatory pathways inducing inflammation. This cyclic process perpetuates additional ROS production and epidermal damage. AD = atopic dermatitis; NOX = NADPH oxidase; DPI = Diphenyleneiodonium; JNK = c-Jun N-terminal kinase; ERK = Extracellular signal-regulated kinase; c-Jun = Jun proto oncogene; c-Fos = Fos proto oncogene; AP-1 = Activator protein-1; ROS = reactive oxygen species. Created with BioRender.com

General Discussion and Outlook

The potential of complex 3-dimensional human skin models to address functional questions underlying AD pathology and validate new candidates for therapeutic targets

To characterize identified biomarkers, conduct adequate analyses of the pro-inflammatory milieu, assess functional effects, capture the detailed mechanisms of targeted therapies in AD, and, most importantly, to examine effects of different cell populations, compounds or antibodies on epidermal barrier, it is essential to establish and employ appropriate disease models. For this purpose, I have utilized and refined 3D skin models of atopic dermatitis.

I applied 3D skin models to explore the contribution of fibroblast- and keratinocyte-derived factors to epidermal dysfunction in AD pathology (Article III). I have identified several soluble factors that were secreted by fibroblasts and keratinocytes in response to stimulation with AD relevant cytokines. Of note, keratinocytes secreted higher levels of most of the targeted proteins (IL-1 α , IL-1 β , IL-1Ra, IL-16, IL-17a, IL-18, IL-22, IP-10 (CXCL10), CCL13, MDC, CCL17, TSLP, VEGF α , TNF α) underlining their major contribution to skin inflammation. Most of the detected proteins are known to be involved in AD pathology and could be already detected in the epidermis of AD patients in other parts of this thesis (Article II) highlighting their importance in disease manifestation and activity.

AD is typically characterized by a Th2-shifted immune dysregulation with IL-4 and IL-13 being major drivers of the disease ^{191,192}. Existing therapies mainly target the Th2 immune axis such as dupilumab (anti IL-4R α), tralokinumab (anti IL-13), nemolizumab (anti IL-31) or amltelimab (anti OX40L) ¹⁹³. However, the results of my thesis indicate that keratinocytes secrete high levels of cytokines associated with additional immune responses (e.g. IL-1 superfamily, Th17/22, Th1). Notably, the experiments in Article III demonstrated that dupilumab treatment alone is insufficient to counteract the pathological effects of keratinocyte-derived factors on 3D skin models emphasizing the involvement of additional immune axes in AD pathology. Therefore, the findings presented in my thesis could shift the view on multiple immune axes (both adaptive and innate) involved in AD pathology providing potential therapy targets that require further characterization and validation. The IL-1 superfamily becomes intriguing due to the abundant expression of all IL-1 superfamily cytokines in human skin ¹⁹⁴. Various inflammatory conditions such as psoriasis, alopecia and AD as well as other chronic diseases, including atherosclerosis and rheumatoid arthritis are associated with increased IL-1 family cytokine expression ¹⁹⁵. Most of the IL-1 family proteins are involved in detecting environmental threats invading the skin, such as pathogen-derived proteases or different pathogen associated patterns (PAMPs) and danger associated patterns (DAMPs) ¹⁹⁶. IL-18 secretion is induced by *S. aureus* colonization ¹⁹⁷ and IL-1 α is involved in development of chronic inflammation in filaggrin-deficient mice whereas IL-33 is triggered by different allergens. Keratinocytes strongly respond to IL-1 family proteins by releasing antimicrobial peptides (AMPs) like S100 proteins

General Discussion and Outlook

or human beta defensins as well as by secretion of IL-8, CCL2 and CCL20 which induce chemotaxis of neutrophils and myeloid cells^{198,199}. Several treatments targeting the IL-1 family have been developed and require further characterization and validation including bermekimab (anti IL-1 α), spesolimab (anti IL-36R), anakinra (recombinant IL-1Ra) and different anti IL-33 therapies¹⁹³. Still, many IL-33 targeting therapies failed to reach significance in clinical trials and are no longer considered for AD treatment¹⁹³. In general, there is a need for performing additional research on innate immunity as clinical research has mainly focused on adaptive immunity, in particular Th2, probably due to the success of Th2 targeting therapies (dupilumab, tralokinumab, upadacitinib) in recent years.

In Article III, I employed an advanced disease model that incorporates various cell types (fibroblasts and keratinocytes) and a functional skin barrier for assessment. However, further optimization could involve the inclusion of additional components of the human skin that play a role in AD pathology. To my knowledge, more complex models including bacteria and immune cells are still rare. It is of great interest to further improve 3D skin models as they provide powerful tools to study causative effects of disease pathologies and could improve personalized medicine. Therefore, I enhanced this model in Article IV introducing Th2 polarized CD4+ cells and *S. aureus* into 3D skin models, aiming for a more accurate representation of AD *in vivo* situation. As a proof of principle this model was treated with dupilumab, successfully mimicking the *in vivo* situation by reducing topical *S. aureus* load. A key observation of Article IV was that *S. aureus* load significantly increased only when 3D skin models were incubated with Th2 polarized CD4+ cells, and dupilumab was effective solely in Th2 models but not in simple AD models or in models incorporating pan T cells. In models including Th2-polarized T cells, inhibiting IL-4/IL-13 signaling might potentially counteracted the suppressive effects of IL-4 and IL-13 on AMPs leading to a reduction of *S. aureus* load. Additionally, various studies have reported a decrease in IL-17a levels after dupilumab treatment, which was also observed in our 3D skin model. Given these findings, further investigation into the role of IL-17a inducing *S. aureus* growth and its role in disease development would be of interest.

This model represents the first stage in the development of complex skin models, with the potential for further enhancement through the incorporation of even more sophisticated immune players such as dendritic cells, neutrophils or innate lymphoid cells^{101,200–202}. In addition, other members of the skin microbiome like *S. epidermidis*, *S. hominis* or *Malassezia spp.*²⁰³ could be included and combined in future in high complex 3D skin models. However, as complexity increases, achieving high-quality models becomes challenging due to elevated cellular stress from topical culture of bacteria and incorporation of cytokines and immune cells, potentially resulting in deficiencies in epidermal development. Reliable results on skin barrier or

General Discussion and Outlook

epidermal organization however require a well-developed epidermis to prevent potential artifacts from the experimental setup.

Article III emphasizes the crucial involvement of keratinocytes and fibroblasts in AD, as these cells produce diverse pro-inflammatory proteins that can impair the skin barrier in a Th2-independent fashion. Additionally, 3D skin models facilitate the simulation of both healthy and diseased skin states. Further incorporation of immune and microbiome components brings them closer to mimicking an *in vivo*-like scenario. In turn, this deepens our understanding of the molecular mechanisms underlying AD etiology and provides opportunities for investigating innovative therapeutic approaches in the future.

Future perspectives

In summary, this thesis highlights the role of increased oxidative stress in keratinocytes and its crosstalk in skin inflammation. The characterization of NOX1, 2, and 4 as well as effects of their inhibition on different skin cells and 3D skin models should be further investigated. Moreover, I applied a minimally invasive method that can be utilized to perform characterization of the inflammatory milieu in the epidermis of AD patients, potentially enhancing biomaterial quantity and thereby increasing the likelihood of discovering novel disease biomarkers and improving patient stratification. In this thesis, I have demonstrated the reliable analysis of *stratum corneum* proteins using tape strips. Nevertheless, there is an intriguing potential to explore additional -omic technologies through the use of tape strips. In AD research, transcriptomic analyses are currently conducted on skin punch biopsies. Tape strips offer the opportunity for RNA isolation and subsequent analyses, but this requires sampling a deeper layer of the skin, achievable by collecting up to 30 tape strips from the same sample site. Furthermore, a comprehensive comparison between results obtained from biopsies and tape strips from the same patients would be valuable to understand which questions could be better addressed with tape strips than with biopsies.

Finally, I applied and refined 3D skin models to better mimic AD conditions *in vitro*. The 3D skin model presented in chapter 5.4 of this thesis could be used to perform in-depth characterization and validation of results obtained throughout the thesis. First, cytokines preceding AD manifestation identified in children (Article II) could be assessed regarding their effects on skin barrier function and epidermal organization and antibodies targeting different identified cytokines could be functionally tested.

Second, inhibitors targeting NOX1, 2, and 4 could be tested in 3D skin models mimicking AD skin in order to expand our knowledge on mechanisms following NOX inhibition. The additional incorporation of the skin microbiome into 3D skin models would be valuable to further examine

General Discussion and Outlook

the role of NOX activity in microbial dysbiosis. Moreover, the identification of cytokines released by stimulated and unstimulated keratinocytes and fibroblast following treatment with DPI and specific NOX inhibitors would be of additional interest in order to get more insights into the crosstalk between oxidative stress and inflammatory response in the skin.

The presented 3D skin models could be further altered to address a variety of scientific questions: Throughout the *in vitro* experiments performed in this thesis neonatal primary keratinocytes without genetic alterations have been used. Different groups have identified different risk loci for AD development with a FLG loss of function mutation being the strongest known risk factor for AD development²⁹. Therefore, the introduction of different genetic alterations via e.g. gene silencing could further improve the understanding of the effects of distinct mutations¹²¹. Moreover, the use of patient-derived keratinocytes could improve the model, considering their distinct genetic background relevant for disease manifestation. Although protocols describing fabrication of 3D skin models using keratinocytes from different adult donors are available¹¹⁵, limited access to biomaterial, invasive biosampling methods and the risk of unwanted mutations during longer cultivation of keratinocytes present major drawbacks of this approach.

The AD skin models applied throughout this thesis are characterized by decreased barrier protein expression, increased spongiosis (Article III and Article IV), elevated *S. aureus* load, and a distinct inflammatory milieu (Article IV). In addition to that, there are several other characteristics of AD skin that could be addressed in downstream experiments of future studies such as epidermal hyperproliferation which could be assessed through histological examination or molecular analysis of K16 and Ki67 expression. Future experiments could also encompass analysis of tight junctions (gene expression or via immunohistochemistry), TEWL, and skin fatty acids and ceramides.

Finally, the presented 3D skin model could be applied to construct personalized 3D skin models by incorporating patient-derived keratinocytes (obtained from e.g. hair follicles²⁰⁴), patient's skin microbiome and immune cells. This approach would allow for the assessment of the distinct impact of each component within this model on disease manifestation. By performing heterologous stimulation, wherein "healthy" skin models are subjected to stimulation using skin microbiome or immune cells derived from AD patients, investigation of their respective impacts on factors like epidermal integrity and skin barrier function could be performed. Additionally, the presented 3D skin model could facilitate accurate personalized medicine and would allow for testing targeted therapies and thereby improving decision-making in clinical settings (**Figure 11**).

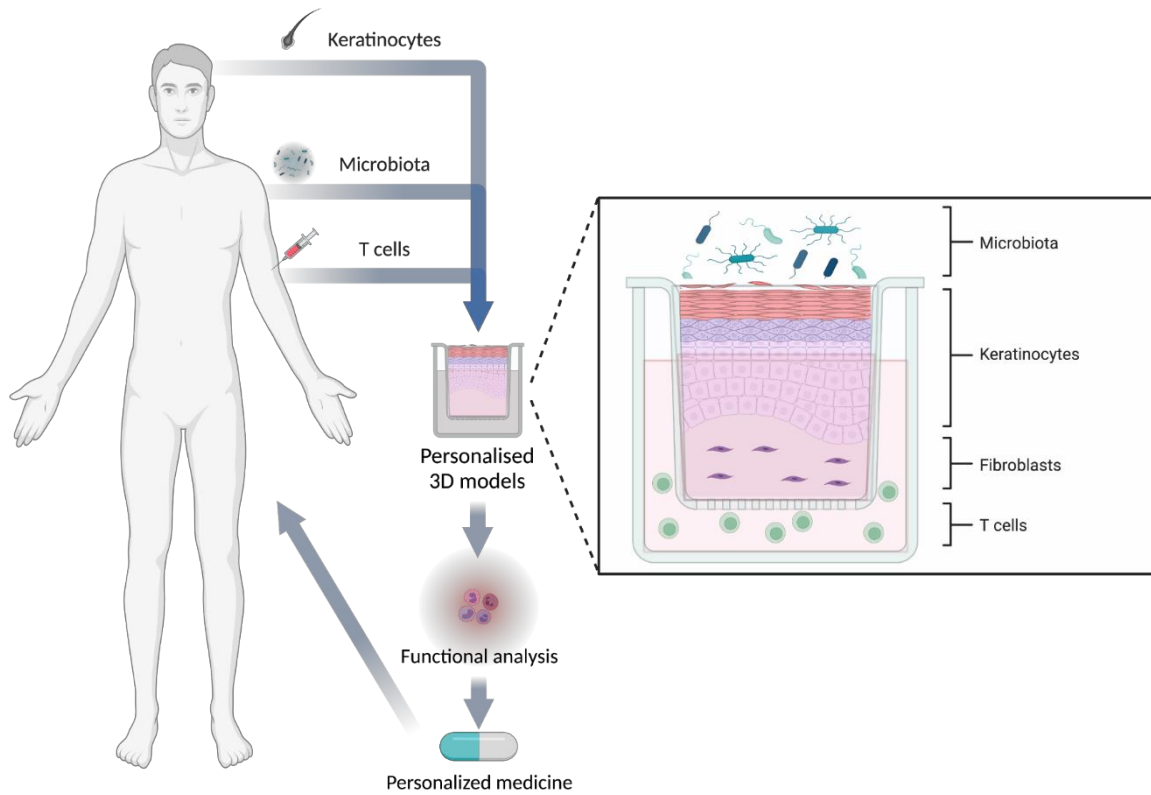


Figure 11: A hypothetical representation of a minimally invasive, personalized 3D skin model. Keratinocytes, obtained from hair follicles, could be employed to construct these specialized 3D skin models. The skin microbiome from patients could be obtained through skin rinsing and applied to the surface of the 3D skin models. Additionally, immune cells such as T cells, extracted from the patient's blood, could be incorporated into the skin model, establishing a distinctive and personalized *ex vivo* simulation of the patient's skin. This model could then be utilized to evaluate the effectiveness of various treatments, including monoclonal antibodies targeting specific cytokines, the topical application of antimicrobial peptides, or the use of NOX inhibitors. NOX = NADPH oxidase. Created with BioRender.com

7 References

1. Langan SM, Irvine AD, Weidinger S. Atopic dermatitis. *The Lancet*. 2020;396(10247):345-360.
2. Eichenfield LF, Hanifin JM, Luger TA, Stevens SR, Pride HB. Consensus Conference on Pediatric Atopic Dermatitis. *J Am Acad Dermatol*. 2003;49(6):1088-1095.
3. Weidinger S, Novak N. Atopic dermatitis. *The Lancet*. 2016;387(10023):1109-1122.
4. Weidinger S, Beck LA, Bieber T, Kabashima K, Irvine AD. Atopic dermatitis. *Nat Rev Dis Primers*. 2018;4(1).
5. Briggs E, Kamal MA, Kosloski MP, et al. Integrated Exposure-Response of Dupilumab in Children, Adolescents, and Adults With Atopic Dermatitis Using Categorical and Continuous Efficacy Assessments: A Population Analysis. *Pharm Res*. 2023;40(11):2653-2666.
6. Chopra R, Vakharia PP, Sacotte R, et al. Severity strata for Eczema Area and Severity Index (EASI), modified EASI, Scoring Atopic Dermatitis (SCORAD), objective SCORAD, Atopic Dermatitis Severity Index and body surface area in adolescents and adults with atopic dermatitis. *Br J Dermatol*. 2017;177(5):1316-1321.
7. Leshem YA, Hajar T, Hanifin JM, Simpson EL. What the Eczema Area and Severity Index score tells us about the severity of atopic dermatitis: an interpretability study. *Br J Dermatol*. 2015;172(5):1353-1357.
8. Silverberg JI, Hanifin JM. Adult eczema prevalence and associations with asthma and other health and demographic factors: a US population-based study. *J Allergy Clin Immunol*. 2013;132(5):1132-1138.
9. van der Hulst AE, Klip H, Brand PLP. Risk of developing asthma in young children with atopic eczema: a systematic review. *J Allergy Clin Immunol*. 2007;120(3):565-569.
10. Kapoor R, Menon C, Hoffstad O, Bilker W, Leclerc P, Margolis DJ. The prevalence of atopic triad in children with physician-confirmed atopic dermatitis. *J Am Acad Dermatol*. 2008;58(1):68-73.
11. Aw M, Penn J, Gauvreau GM, Lima H, Sehmi R. Atopic March: Collegium Internationale Allergologicum Update 2020. *Int Arch Allergy Immunol*. 2020;181(1):1-10.
12. Patel KR, Immaneni S, Singam V, Rastogi S, Silverberg JI. Association between atopic dermatitis, depression, and suicidal ideation: A systematic review and meta-analysis. *J Am Acad Dermatol*. 2019;80(2):402-410.
13. Wollenberg A, Barbarot S, Bieber T, et al. Consensus-based European guidelines for treatment of atopic eczema (atopic dermatitis) in adults and children: part II. *J Eur Acad Dermatol Venerol*. 2018;32(6):850-878.
14. Eczema (Atopic Dermatitis) Treatment | NIH: National Institute of Allergy and Infectious Diseases.
15. Shah S, Thomas Ginat D. Calcineurin Inhibitors. *Neuroimaging Pharmacopoeia, Second Edition*. 2022:173-183.
16. Eichenfield LF, Ahluwalia J, Waldman A, Borok J, Udkoff J, Boguniewicz M. Current guidelines for the evaluation and management of atopic dermatitis: A comparison of the Joint Task Force

References

- Practice Parameter and American Academy of Dermatology guidelines. *J Allergy Clin Immunol*. 2017;139(4S):49-57.
17. Topical corticosteroids - Systematic review of treatments for atopic eczema - NCBI Bookshelf.
18. Bieber T. Atopic dermatitis: an expanding therapeutic pipeline for a complex disease. *Nat Rev Drug Discov*. 2022;21(1):21-40.
19. Reich K, Thyssen JP, Blauvelt A, et al. Efficacy and safety of abrocitinib versus dupilumab in adults with moderate-to-severe atopic dermatitis: a randomised, double-blind, multicentre phase 3 trial. *The Lancet*. 2022;400(10348):273-282.
20. Kulthanan K, Tuchinda P, Nitiyaron R, et al. Allergy and Immunology Clinical practice guidelines for the diagnosis and management of atopic dermatitis. *Pac J Allergy Immunol*. 2021;39:145-155.
21. Harb H, Chatila TA. Mechanisms of Dupilumab. *Clin Exp Allergy*. 2020;50(1):5-14.
22. Stölzl D, Sander N, Heratizadeh A, et al. Real-world data on the effectiveness, safety and drug survival of dupilumab: an analysis from the TREATgermany registry. *Br J Dermatol*. 2022;187(6):1022-1024.
23. Wollenberg A, Blauvelt A, Guttman-Yassky E, et al. Tralokinumab for moderate-to-severe atopic dermatitis: results from two 52-week, randomized, double-blind, multicentre, placebo-controlled phase III trials (ECZTRA 1 and ECZTRA 2). *Br J Dermatol*. 2021;184(3):437-449.
24. Apfelbacher CJ, Diepgen TL, Schmitt J. Determinants of eczema: population-based cross-sectional study in Germany. *Allergy*. 2011;66(2):206-213.
25. Elmoose C, Thomsen SF. Twin Studies of Atopic Dermatitis: Interpretations and Applications in the Filaggrin Era. *J Allergy (Cairo)*. 2015;2015:1-7.
26. Kim JE, Kim JS, Cho DH, Park HJ. Molecular Mechanisms of Cutaneous Inflammatory Disorder: Atopic Dermatitis. *Int J Mol Sci*. 2016;17(8).
27. Budu-Aggrey A, Kilanowski A, Sobczyk MK, et al. European and multi-ancestry genome-wide association meta-analysis of atopic dermatitis highlights importance of systemic immune regulation. *Nat Commun*. 2023;14(1).
28. Thyssen JP, Kezic S. Causes of epidermal filaggrin reduction and their role in the pathogenesis of atopic dermatitis. *Journal of Allergy and Clinical Immunology*. 2014;134(4):792-799.
29. Palmer CNA, Irvine AD, Terron-Kwiatkowski A, et al. Common loss-of-function variants of the epidermal barrier protein filaggrin are a major predisposing factor for atopic dermatitis. *Nat Genet*. 2006;38(4):441-446.
30. Manolio TA, Collins FS, Cox NJ, et al. Finding the missing heritability of complex diseases. *Nature*. 2009;461(7265):747-753.
31. Proksch E, Fölster-Holst R, Jensen JM. Skin barrier function, epidermal proliferation and differentiation in eczema. *J Dermatol Sci*. 2006;43(3):159-169.
32. Lee AY. Molecular Mechanism of Epidermal Barrier Dysfunction as Primary Abnormalities. *Int J Mol Sci*. 2020;21(4).
33. Elias PM. Skin barrier function. *Curr Allergy Asthma Rep*. 2008;8(4):299-305.

References

34. Nemes Z, Steinert PM. Bricks and mortar of the epidermal barrier. *Exp Mol Med*. 1999;31(1):5-19.
35. Quiroz FG, Fiore VF, Levorse J, et al. Liquid-liquid phase separation drives skin barrier formation. *Science*. 2020;367(6483).
36. Harding CR, Aho S, Bosko CA. Filaggrin – revisited. *Int J Cosmet Sci*. 2013;35(5):412-423.
37. Pellerin L, Henry J, Hsu CY, et al. Defects of filaggrin-like proteins in both lesional and non-lesional atopic skin. *Journal of Allergy and Clinical Immunology*. 2013;131(4):1094-1102.
38. Flohr C, England K, Radulovic S, et al. Filaggrin loss-of-function mutations are associated with early-onset eczema, eczema severity and transepidermal water loss at 3 months of age. *British Journal of Dermatology*. 2010;163(6):1333-1336.
39. Kezic S, O'Regan GM, Lutter R, et al. Filaggrin loss-of-function mutations are associated with enhanced expression of IL-1 cytokines in the stratum corneum of patients with atopic dermatitis and in a murine model of filaggrin deficiency. *J Allergy Clin Immunol*. 2012;129(4).
40. Yuki T, Komiya A, Kusaka A, Kuze T, Sugiyama Y, Inoue S. Impaired tight junctions obstruct stratum corneum formation by altering polar lipid and profilaggrin processing. *J Dermatol Sci*. 2013;69(2):148-158.
41. Baurecht H, Rühlemann MC, Rodríguez E, et al. Epidermal lipid composition, barrier integrity, and eczematous inflammation are associated with skin microbiome configuration. *J Allergy Clin Immunol*. 2018;141(5):1668-1676.e16.
42. Howell MD, Kim BE, Gao P, et al. Cytokine modulation of atopic dermatitis filaggrin skin expression. *J Allergy Clin Immunol*. 2007;120(1):150-155.
43. Zaniboni MC, Samorano LP, Orfali RL, Aoki V. Skin barrier in atopic dermatitis: beyond filaggrin. *An Bras Dermatol*. 2016;91(4):472-478.
44. Yang G, Seok JK, Kang HC, Cho YY, Lee HS, Lee JY. Skin barrier abnormalities and immune dysfunction in atopic dermatitis. *Int J Mol Sci*. 2020;21(8):1-14.
45. Furue M. Regulation of Skin Barrier Function via Competition between AHR Axis versus IL-13/IL-4–JAK–STAT6/STAT3 Axis: Pathogenic and Therapeutic Implications in Atopic Dermatitis. *J Clin Med*. 2020;9(11):1-24.
46. Buddenkotte J, Steinhoff M. Pathophysiology and therapy of pruritus in allergic and atopic diseases. *Allergy*. 2010;65(7):805-821.
47. Oh MH, Oh SY, Lu J, et al. TRPA1-dependent pruritus in IL-13-induced chronic atopic dermatitis. *J Immunol*. 2013;191(11):5371-5382.
48. Cevikbas F, Wang X, Akiyama T, et al. A sensory neuron-expressed IL-31 receptor mediates T helper cell-dependent itch: Involvement of TRPV1 and TRPA1. *J Allergy Clin Immunol*. 2014;133(2).
49. Dainichi T, Kitoh A, Otsuka A, et al. The epithelial immune microenvironment (EIME) in atopic dermatitis and psoriasis. *Nat Immunol*. 2018;19(12):1286-1298.
50. Leung DYM. Role of IgE in atopic dermatitis. *Curr Opin Immunol*. 1993;5(6):956-962.

References

51. Wollenberg A, Thomsen SF, Lacour JP, Jaumont X, Lazarewicz S. Targeting immunoglobulin E in atopic dermatitis: A review of the existing evidence. *World Allergy Organ J.* 2021;14(3):100519.
52. Liu YJ. Thymic stromal lymphopoietin and OX40 ligand pathway in the initiation of dendritic cell-mediated allergic inflammation. *J Allergy Clin Immunol.* 2007;120(2):238-244.
53. Tanei R, Hasegawa Y. Immunological Pathomechanisms of Spongiotic Dermatitis in Skin Lesions of Atopic Dermatitis. *Int J Mol Sci.* 2022;23(12).
54. Humeau M, Boniface K, Bodet C. Cytokine-Mediated Crosstalk Between Keratinocytes and T Cells in Atopic Dermatitis. *Front Immunol.* 2022;13.
55. Chieosilapatham P, Kiatsurayanon C, Umehara Y, et al. Keratinocytes: innate immune cells in atopic dermatitis. *Clin Exp Immunol.* 2021;204(3):296-309.
56. Suárez-Fariñas M, Tintle SJ, Shemer A, et al. Nonlesional atopic dermatitis skin is characterized by broad terminal differentiation defects and variable immune abnormalities. *J Allergy Clin Immunol.* 2011;127(4).
57. Mack MR, Brestoff JR, Berrien-Elliott MM, et al. Blood natural killer cell deficiency reveals an immunotherapy strategy for atopic dermatitis. *Sci Transl Med.* 2020;12(532).
58. Grice EA, Kong HH, Conlan S, et al. Topographical and Temporal Diversity of the Human Skin Microbiome. *Science.* 2009;324(5931):1190.
59. Paller AS, Kong HH, Seed P, et al. The microbiome in patients with atopic dermatitis. *J Allergy Clin Immunol.* 2019;143(1):26.
60. Geoghegan JA, Irvine AD, Foster TJ. Staphylococcus aureus and Atopic Dermatitis: A Complex and Evolving Relationship. *Trends Microbiol.* 2018;26(6):484-497.
61. Alsterholm M, Strömbeck L, Ljung A, et al. Variation in Staphylococcus aureus Colonization in Relation to Disease Severity in Adults with Atopic Dermatitis during a Five-month Follow-up. *Acta Derm Venereol.* 2017;97(7):802-807.
62. Hülpmusch C, Tremmel K, Hammel G, et al. Skin pH-dependent Staphylococcus aureus abundance as predictor for increasing atopic dermatitis severity. *Allergy.* 2020;75(11):2888-2898.
63. Cho SH, Strickland I, Boguniewicz M, Leung DYM. Fibronectin and fibrinogen contribute to the enhanced binding of Staphylococcus aureus to atopic skin. *J Allergy Clin Immunol.* 2001;108(2):269-274.
64. Nakatsuji T, Chen TH, Two AM, et al. Staphylococcus aureus exploits epidermal barrier defects in atopic dermatitis to trigger cytokine expression. *J Invest Dermatol.* 2016;136(11):2192.
65. Fyhrquist N, Muirhead G, Prast-Nielsen S, et al. Microbe-host interplay in atopic dermatitis and psoriasis. *Nature Communications* 2019 10:1. 2019;10(1):1-15.
66. Nakatsuji T, Chen TH, Narala S, et al. Antimicrobials from human skin commensal bacteria protect against Staphylococcus aureus and are deficient in atopic dermatitis. *Sci Transl Med.* 2017;9(378).
67. Chin D, Goncheva MI, Flannagan RS, et al. Coagulase-negative staphylococci release a purine analog that inhibits Staphylococcus aureus virulence. *Nature Communications* 2021 12:1. 2021;12(1):1-12.

References

68. Edslev SM, Agner T, Andersen PS. Skin Microbiome in Atopic Dermatitis. *Acta Derm Venereol*. 2020;100(12):358-366.
69. Clausen ML, Agner T, Lilje B, Edslev SM, Johannesen TB, Andersen PS. Association of Disease Severity With Skin Microbiome and Filaggrin Gene Mutations in Adult Atopic Dermatitis. *JAMA Dermatol*. 2018;154(3):293.
70. Sivaranjani N, Venkata Rao S, Rajeev G. Role of reactive oxygen species and antioxidants in atopic dermatitis. *Journal of Clinical and Diagnostic Research*. 2013;7(12):2683-2685.
71. Prasad A, Duchová H, Manoharan RR, Rath D, Pospíšil P. Imaging and Characterization of Oxidative Protein Modifications in Skin. *Int J Mol Sci*. 2023;24(4).
72. Borgia F, Li Pomi F, Vaccaro M, Alessandrello C, Papa V, Gangemi S. Oxidative Stress and Phototherapy in Atopic Dermatitis: Mechanisms, Role, and Future Perspectives. *Biomolecules*. 2022;12(12).
73. Niwa Y, Sumi H, Kawahira K, Terashima T, Nakamura T, Akamatsu H. Protein oxidative damage in the stratum corneum: Evidence for a link between environmental oxidants and the changing prevalence and nature of atopic dermatitis in Japan. *Br J Dermatol*. 2003;149(2):248-254.
74. Omata N, Tsukahara H, Ito S, et al. Increased oxidative stress in childhood atopic dermatitis. *Life Sci*. 2001;69(2):223-228.
75. Furue M. Regulation of Filaggrin, Loricrin, and Involucrin by IL-4, IL-13, IL-17A, IL-22, AHR, and NRF2: Pathogenic Implications in Atopic Dermatitis. *Int J Mol Sci*. 2020;21(15):1-25.
76. Chung J, Oh SY, Shin YK. Association of glutathione-S-transferase polymorphisms with atopic dermatitis risk in preschool age children. *Clin Chem Lab Med*. 2009;47(12):1475-1481.
77. Rudolf J, Raad H, Taieb A, Rezvani HR. NADPH Oxidases and Their Roles in Skin Homeostasis and Carcinogenesis. *Antioxid Redox Signal*. 2018;28(13):1238-1261.
78. Panday A, Sahoo MK, Osorio D, Batra S. NADPH oxidases: an overview from structure to innate immunity-associated pathologies. *Cell Mol Immunol*. 2015;12(1):5-23.
79. Bedard K, Krause KH. The NOX family of ROS-generating NADPH oxidases: physiology and pathophysiology. *Physiol Rev*. 2007;87(1):245-313.
80. Riganti C, Gazzano E, Polimeni M, Costamagna C, Bosia A, Ghigo D. Diphenyleneiodonium inhibits the cell redox metabolism and induces oxidative stress. *J Biol Chem*. 2004;279(46):47726-47731.
81. Geiszt M, Leto TL. The Nox family of NAD(P)H oxidases: Host defense and beyond. *Journal of Biological Chemistry*. 2004;279(50):51715-51718.
82. Teixeira G, Szyndralewicz C, Molango S, et al. Therapeutic potential of NADPH oxidase 1/4 inhibitors. *Br J Pharmacol*. 2017;174(12):1647-1669.
83. Kim BE, Goleva E, Kim PS, et al. Side-by-side Comparison of Skin Biopsies and Skin Tape Stripping Highlights Abnormal Stratum Corneum in Atopic Dermatitis. *J Invest Dermatol*. 2019;139(11):2387.
84. Tokura Y, Hayano S. Subtypes of atopic dermatitis: From phenotype to endotype. *Allergol Int*. 2022;71(1):14-24.

References

85. Olesen CM, Fuchs CSK, Philipsen PA, Hædersdal M, Agner T, Clausen ML. Advancement through epidermis using tape stripping technique and Reflectance Confocal Microscopy. *Sci Rep*. 2019;9(1):1-6.
86. Simon K, Oberender G, Roloff A. Continuous removal of single cell layers by tape stripping the stratum corneum - a histological study. *Eur J Pharm Biopharm*. 2023;188:48-53.
87. Clausen ML, Slotved HC, Krogfelt KA, Agner T. Tape Stripping Technique for Stratum Corneum Protein Analysis. *Sci Rep*. 2016;6(Table 2):1-8.
88. Hughes AJ, Tawfik SS, Baruah KP, O'Toole EA, O'Shaughnessy RFL. Tape strips in dermatology research. *British Journal of Dermatology*. Published online 2021:1-10.
89. Andersson AM, Sølberg J, Koch A, et al. Assessment of biomarkers in pediatric atopic dermatitis by tape strips and skin biopsies. *Allergy*. 2022;77(5):1499-1509.
90. Pavel AB, Renert-Yuval Y, Wu J, et al. Tape strips from early-onset pediatric atopic dermatitis highlight disease abnormalities in nonlesional skin. *Allergy*. 2021;76(1):314-325.
91. Guttman-Yassky E, Diaz A, Pavel AB, et al. Use of Tape Strips to Detect Immune and Barrier Abnormalities in the Skin of Children With Early-Onset Atopic Dermatitis. *JAMA Dermatol*. 2019;155(12):1358-1370.
92. Sølberg JBK, Quaade AS, Drici L, et al. The Proteome of Hand Eczema Assessed by Tape Stripping. *J Invest Dermatol*. 2023;143(8):1559-1568.e5.
93. Kezic S, Kemperman PMJH, Koster ES, et al. Loss-of-function mutations in the filaggrin gene lead to reduced level of natural moisturizing factor in the stratum corneum. *Journal of Investigative Dermatology*. 2008;128(8):2117-2119.
94. De Boer FL, Van Der Molen HF, Kezic S. Epidermal biomarkers of the skin barrier in atopic and contact dermatitis. *Contact Dermatitis*. 2023;89(4):221-229.
95. Berdyshev E, Kim J, Kim BE, et al. Stratum Corneum Lipid and Cytokine Biomarkers at Two Months of Age Predict the Future Onset of Atopic Dermatitis. *Journal of Allergy and Clinical Immunology*. 2023;151(5):1307-1316.
96. He H, Bissonnette R, Wu J, et al. Tape strips detect distinct immune and barrier profiles in atopic dermatitis and psoriasis. *Journal of Allergy and Clinical Immunology*. 2021;147(1):199-212.
97. Berekméri A, Latzko A, Alase A, et al. Detection of IL-36 γ through noninvasive tape stripping reliably discriminates psoriasis from atopic eczema. *J Allergy Clin Immunol*. 2018;142(3):988-991.e4.
98. Emmert H, Rademacher F, Gläser R, Harder J. Skin microbiota analysis in human 3D skin models-"Free your mice". *Exp Dermatol*. 2020;29(11):1133-1139.
99. Gerber PA, Buhren BA, Schrumpf H, Homey B, Zlotnik A, Hevezi P. The top skin-associated genes: a comparative analysis of human and mouse skin transcriptomes. *Biol Chem*. 2014;395(6):577-591.
100. Harder J, Schröder JM, Gläser R. The skin surface as antimicrobial barrier: present concepts and future outlooks. *Exp Dermatol*. 2013;22(1):1-5.

101. Pasparakis M, Haase I, Nestle FO. Mechanisms regulating skin immunity and inflammation. *Nature Reviews Immunology* 2014 14:5. 2014;14(5):289-301.
102. Emmert H, Fonfara M, Rodriguez E, Weidinger S. NADPH oxidase inhibition rescues keratinocytes from elevated oxidative stress in a 2D atopic dermatitis and psoriasis model. *Exp Dermatol*. 2020;29(8):749-758.
103. Niebuhr M, Heratizadeh A, Wichmann K, Satzger I, Werfel T. Intrinsic alterations of pro-inflammatory mediators in unstimulated and TLR-2 stimulated keratinocytes from atopic dermatitis patients. *Exp Dermatol*. 2011;20(6):468-472.
104. Anton D, Burckel H, Josset E, Noel G. Three-dimensional cell culture: A breakthrough in vivo. *Int J Mol Sci*. 2015;16(3):5517-5527.
105. van den Bogaard E, Ilic D, Dubrac S, et al. Perspective and Consensus Opinion: Good Practices for Using Organotypic Skin and Epidermal Equivalents in Experimental Dermatology Research. *Journal of Investigative Dermatology*. 2021;141(1):203-205.
106. Niehues H, Bouwstra JA, El Ghalbzouri A, Brandner JM, Zeeuwen PLJM, van den Bogaard EH. 3D skin models for 3R research: The potential of 3D reconstructed skin models to study skin barrier function. *Exp Dermatol*. 2018;27(5):501-511.
107. De Vuyst E, Salmon M, Evrard C, de Rouvroit CL, Poumay Y. Atopic Dermatitis studies through in vitro models. *Front Med (Lausanne)*. 2017;4(JUL):119.
108. Randall MJ, Jüngel A, Rimann M, Wuertz-Kozak K. Advances in the Biofabrication of 3D Skin in vitro: Healthy and Pathological Models. *Front Bioeng Biotechnol*. 2018;6(OCT):154.
109. Leman G, Moosbrugger-Martinez V, Blunder S, Pavel P, Dubrac S. 3D-Organotypic Cultures to Unravel Molecular and Cellular Abnormalities in Atopic Dermatitis and Ichthyosis Vulgaris. *Cells*. 2019;8(5):489.
110. Hennies HC, Poumay Y. Skin Disease Models In Vitro and Inflammatory Mechanisms: Predictability for Drug Development. *Handb Exp Pharmacol*. 2021;265:187-218.
111. Huet F, Severino-Freire M, Chéret J, et al. Reconstructed human epidermis for in vitro studies on atopic dermatitis: A review. *J Dermatol Sci*. 2018;89(3):213-218.
112. Moon S, Kim DH, Shin JU. In Vitro Models Mimicking Immune Response in the Skin. *Yonsei Med J*. 2021;62(11):969.
113. Michaelidou M, Redhu D, Kumari V, Babina M, Worm M. IL-1 α / β and IL-18 profiles and their impact on claudin-1, loricrin and filaggrin expression in patients with atopic dermatitis. *J Eur Acad Dermatol Venereol*. 2023;37(9):e1141-e1143.
114. Morgner B, Tittelbach J, Wiegand C. Induction of psoriasis- and atopic dermatitis-like phenotypes in 3D skin equivalents with a fibroblast-derived matrix. *Scientific Reports* 2023 13:1. 2023;13(1):1-17.
115. Kamsteeg M, Bergers M, De Boer R, et al. Type 2 Helper T-Cell Cytokines Induce Morphologic and Molecular Characteristics of Atopic Dermatitis in Human Skin Equivalent. *Am J Pathol*. 2011;178(5):2091-2099.

References

116. Van Den Bogaard EH, Tjabringa GS, Joosten I, et al. Crosstalk between keratinocytes and T cells in a 3D microenvironment: A model to study inflammatory skin diseases. *Journal of Investigative Dermatology*. 2014;134(3):719-727.
117. Mildner M, Ballaun C, Stichenwirth M, et al. Gene silencing in a human organotypic skin model. *Biochem Biophys Res Commun*. 2006;348(1):76-82.
118. Smits JPH, van den Brink NJM, Meesters LD, et al. Investigations into the FLG Null Phenotype: Showcasing the Methodology for CRISPR/Cas9 Editing of Human Keratinocytes. *J Invest Dermatol*. 2023;143(8):1520-1528.e5.
119. van den Bogaard EH, Elias PM, Goleva E, et al. Targeting skin barrier function in atopic dermatitis. *J Allergy Clin Immunol Pract*. 2023;11(5):1335-1346.
120. De Vuyst E, Salmon M, Evrard C, de Rouvroit CL, Poumay Y. Atopic Dermatitis studies through in vitro models. *Front Med (Lausanne)*. 2017;4(JUL):119.
121. Pendaries V, Malaisse J, Pellerin L, et al. Knockdown of Filaggrin in a Three-Dimensional Reconstructed Human Epidermis Impairs Keratinocyte Differentiation. *Journal of Investigative Dermatology*. 2014;134(12):2938-2946.
122. van Drongelen V, Haisma EM, Out-Luiting JJ, Nibbering PH, El Ghalbzouri A. Reduced filaggrin expression is accompanied by increased Staphylococcus aureus colonization of epidermal skin models. *Clin Exp Allergy*. 2014;44(12):1515-1524.
123. Niehues H, Schalkwijk J, van Vlijmen-Willems IMJJ, et al. Epidermal equivalents of filaggrin null keratinocytes do not show impaired skin barrier function. *Journal of Allergy and Clinical Immunology*. 2017;139(6):1979-1981.e13.
124. Emmert H, Culley J, Brunton VG. Inhibition of cyclin-dependent kinase activity exacerbates H2O2-induced DNA damage in Kindler syndrome keratinocytes. *Exp Dermatol*. 2019;28(9):1074-1078.
125. Emmert H, Patel H, Brunton VG. Kindlin-1 protects cells from oxidative damage through activation of ERK signalling. *Free Radic Biol Med*. 2017;108:896-903.
126. Walter S, Rademacher F, Kobinger N, Simanski M, Gläser R, Harder J. RNase 7 participates in cutaneous innate control of *Corynebacterium amycolatum*. *Scientific Reports* 2017 7:1. 2017;7(1):1-7.
127. Feldman AT, Wolfe D. Tissue processing and hematoxylin and eosin staining. *Methods Mol Biol*. 2014;1180:31-43.
128. Stange EL, Rademacher F, Drerup KA, et al. Staphylococcus aureus Activates the Aryl Hydrocarbon Receptor in Human Keratinocytes. *J Innate Immun*. 2022;14(6):582-592.
129. Hartmann J, Moitinho-Silva L, Sander N, et al. Dupilumab but not cyclosporine treatment shifts the microbiome toward a healthy skin flora in patients with moderate-to-severe atopic dermatitis. *Allergy*. 2023;78(8):2290-2300.
130. Harder I, Stölzl D, Sander N, et al. Effects of Early Emollient Use in Children at High Risk of Atopic Dermatitis: A German Pilot Study. *Acta Derm Venereol*. 2023;103:adv5671.

References

131. Straub D, Blackwell N, Langarica-Fuentes A, Peltzer A, Nahnsen S, Kleindienst S. Interpretations of Environmental Microbial Community Studies Are Biased by the Selected 16S rRNA (Gene) Amplicon Sequencing Pipeline. *Front Microbiol.* 2020;11:550420.
132. Straub D, Peltzer A, Lundin D, et al. nf-core/ampliseq: Ampliseq Version 2.1.0 “Gray Steel Boa.” Published online September 14, 2021.
133. Ewels PA, Peltzer A, Fillinger S, et al. The nf-core framework for community-curated bioinformatics pipelines. *Nature Biotechnology* 2020 38:3. 2020;38(3):276-278.
134. Quast C, Pruesse E, Yilmaz P, et al. The SILVA ribosomal RNA gene database project: improved data processing and web-based tools. *Nucleic Acids Res.* 2013;41(Database issue).
135. Kopp M V., Muche-Borowski C, Abou-Dakn M, et al. S3 guideline Allergy Prevention. *Allergol Select.* 2022;6(3):153-194.
136. Fischer AH, Jacobson KA, Rose J, Zeller R. Hematoxylin and eosin staining of tissue and cell sections. *CSH Protoc.* 2008;2008(5).
137. Tam I, Hill KR, Park JM, Yu J De. Skin tape stripping identifies gene transcript signature associated with allergic contact dermatitis. *Contact Dermatitis.* 2021;84(5):308-316.
138. Tsoi LC, Xing X, Xing E, et al. Noninvasive Tape-Stripping with High-Resolution RNA Profiling Effectively Captures a Preinflammatory State in Nonlesional Psoriatic Skin. *Journal of Investigative Dermatology.* 2022;142(6):1587-1596.e2.
139. Dyjack N, Goleva E, Rios C, et al. Minimally invasive skin tape strip RNA sequencing identifies novel characteristics of the type 2-high atopic dermatitis disease endotype. *J Allergy Clin Immunol.* 2018;141(4):1298-1309.
140. Hu T, Todberg T, Andersen D, et al. Profiling the Atopic Dermatitis Epidermal Transcriptome by Tape Stripping and BRB-seq. *Int J Mol Sci.* 2022;23(11).
141. Gilaberte Y, Pérez-Gilaberte JB, Poblador-Plou B, Bliet-Bueno K, Gimeno-Miguel A, Prados-Torres A. Prevalence and Comorbidity of Atopic Dermatitis in Children: A Large-Scale Population Study Based on Real-World Data. *J Clin Med.* 2020;9(6).
142. Halling AS, Rinno MR, Ruge IF, et al. Skin TARC/CCL17 increase precedes the development of childhood atopic dermatitis. *J Allergy Clin Immunol.* 2023;151(6).
143. Rinno MR, Halling AS, Gerner T, et al. Skin biomarkers predict development of atopic dermatitis in infancy. *Allergy: European Journal of Allergy and Clinical Immunology.* 2023;78(3):791-802.
144. Boniface K, Bernard FX, Garcia M, Gurney AL, Lecron JC, Morel F. IL-22 Inhibits Epidermal Differentiation and Induces Proinflammatory Gene Expression and Migration of Human Keratinocytes. *The Journal of Immunology.* 2005;174(6):3695-3702.
145. Prignano F, Donetti E. Looking at Interleukin-22 from a New Dermatological Perspective: From Epidermal Homeostasis to Its Role in Chronic Skin Diseases. *Dermatology.* 2022;238(5):829-836.
146. Gittler JK, Shemer A, Suárez-Fariñas M, et al. Progressive activation of T(H)2/T(H)22 cytokines and selective epidermal proteins characterizes acute and chronic atopic dermatitis. *J Allergy Clin Immunol.* 2012;130(6):1344-1354.

References

147. Inoue Y, Aihara M, Kirino M, et al. Interleukin-18 is elevated in the horny layer in patients with atopic dermatitis and is associated with *Staphylococcus aureus* colonization. *Br J Dermatol*. 2011;164(3):560-567.
148. Wang X, Wang L, Wen X, Zhang L, Jiang X, He G. Interleukin-18 and IL-18BP in inflammatory dermatological diseases. *Front Immunol*. 2023;14:955369.
149. Yoshimoto T, Tsutsui H, Tominaga K, et al. IL-18, although antiallergic when administered with IL-12, stimulates IL-4 and histamine release by basophils. *Proc Natl Acad Sci U S A*. 1999;96(24):13962-13966.
150. Kim BE, Leung DY, Boguniewicz M, al. et. Loricrin and involucrin expression is down-regulated by Th2 cytokines through STAT-6. *Clin Immunol*. 2008;126:332-337.
151. Furue M. Regulation of Filaggrin, Loricrin, and Involucrin by IL-4, IL-13, IL-17A, IL-22, AHR, and NRF2: Pathogenic Implications in Atopic Dermatitis. *International Journal of Molecular Sciences* 2020, Vol 21, Page 5382. 2020;21(15):5382.
152. Fukasawa T, Yoshizaki-Ogawa A, Enomoto A, Miyagawa K, Sato S, Yoshizaki A. Pharmacotherapy of Itch—Antihistamines and Histamine Receptors as G Protein-Coupled Receptors. *Int J Mol Sci*. 2022;23(12).
153. Silverberg NB, Silverberg JL. Inside Out or Outside In: Does Atopic Dermatitis Disrupt Barrier Function or Does Disruption of Barrier Function Trigger Atopic Dermatitis? *Cutis*. 2015;96:359.
154. Beck LA, Cork MJ, Amagai M, et al. Type 2 Inflammation Contributes to Skin Barrier Dysfunction in Atopic Dermatitis. *JID Innov*. 2022;2(5):100131.
155. Gupta J, Johansson E, Bernstein JA, et al. Resolving the etiology of atopic disorders by using genetic analysis of racial ancestry. Published online 2016.
156. Paternoster L, Standl M, Waage J, et al. Multi-ancestry genome-wide association study of 21,000 cases and 95,000 controls identifies new risk loci for atopic dermatitis. *Nature Genetics* 2015 47:12. 2015;47(12):1449-1456.
157. Mildner M, Jin J, Eckhart L, et al. Knockdown of filaggrin impairs diffusion barrier function and increases UV sensitivity in a human skin model. *Journal of Investigative Dermatology*. 2010;130(9):2286-2294.
158. Smits JPH, van den Brink NJM, Meesters LD, et al. Investigations into the FLG Null Phenotype: Showcasing the Methodology for CRISPR/Cas9 Editing of Human Keratinocytes. *Journal of Investigative Dermatology*. 2023;143(8):1520-1528.e5.
159. Moosbrugger-Martinez V, Leprince C, Méchin MC, et al. Revisiting the Roles of Filaggrin in Atopic Dermatitis. *Int J Mol Sci*. 2022;23(10).
160. Humeau M, Boniface K, Bodet C. Cytokine-Mediated Crosstalk Between Keratinocytes and T Cells in Atopic Dermatitis. *Front Immunol*. 2022;13.
161. Giustizieri ML, Mascia F, Frezzolini A, al. et. Keratinocytes from patients with atopic dermatitis and psoriasis show a distinct chemokine production profile in response to T cell-derived cytokines. *J Allergy Clin Immunol*. 2001;107:871-877.
162. Saeki H, Tamaki K. Thymus and activation regulated chemokine (TARC)/CCL17 and skin diseases. *J Dermatol Sci*. 2006;43(2):75-84.

References

163. Kakinuma T, Nakamura K, Wakugawa M, et al. Thymus and activation-regulated chemokine in atopic dermatitis: Serum thymus and activation-regulated chemokine level is closely related with disease activity. *J Allergy Clin Immunol.* 2001;107(3):535-541.
164. Halling AS, Rinno MR, Ruge IF, et al. Skin TARC/CCL17 increase precedes the development of childhood atopic dermatitis. *Journal of Allergy and Clinical Immunology.* 2023;151(6):1550-1557.e6.
165. Miyahara H, Okazaki N, Nagakura T, Korematsu S, Izumi T. Elevated umbilical cord serum TARC/CCL17 levels predict the development of atopic dermatitis in infancy. *Clin Exp Allergy.* 2011;41(2):186-191.
166. Son Y, Kim S, Chung HT, Pae HO. Reactive oxygen species in the activation of MAP kinases. *Methods Enzymol.* 2013;528:27-48.
167. Liu T, Zhang L, Joo D, Sun SC. NF- κ B signaling in inflammation. *Signal Transduct Target Ther.* 2017;2:17023.
168. Bickers DR, Athar M. Oxidative Stress in the Pathogenesis of Skin Disease. *Journal of Investigative Dermatology.* 2006;126(12):2565-2575.
169. Kang JS, Kim HN, Jung DJ, et al. Regulation of UVB-Induced IL-8 and MCP-1 Production in Skin Keratinocytes by Increasing Vitamin C Uptake via the Redistribution of SVCT-1 from the Cyto-sol to the Membrane. *Journal of Investigative Dermatology.* 2007;127(3):698-706.
170. Elbim C, Guichard C, Dang PMC, et al. Interleukin-18 Primes the Oxidative Burst of Neutrophils in Response to Formyl-Peptides: Role of Cytochrome b558 Translocation and N-Formyl Pep-tide Receptor Endocytosis. *Clin Diagn Lab Immunol.* 2005;12(3):436.
171. Zhang QS, Maddock DA, Chen JP, et al. Cytokine-induced p38 activation feedback regulates the prolonged activation of AKT cell survival pathway initiated by reactive oxygen species in response to UV irradiation in human keratinocytes. *Int J Oncol.* 2001;19(5):1057-1061.
172. Hwang YS, Jeong M, Park JS, et al. Interleukin-1 β stimulates IL-8 expression through MAP kinase and ROS signaling in human gastric carcinoma cells. *Oncogene.* 2004;23(39):6603-6611.
173. Forman HJ, Zhang H. Targeting oxidative stress in disease: promise and limitations of antioxi-dant therapy. *Nature Reviews Drug Discovery* 2021 20:9. 2021;20(9):689-709.
174. Alfadda AA, Sallam RM. Reactive Oxygen Species in Health and Disease. *J Biomed Biotechnol.* 2012;2012:14.
175. Sivaranjani N, Venkata Rao S, Rajeev G. Role of reactive oxygen species and antioxidants in atopic dermatitis. *Journal of Clinical and Diagnostic Research.* 2013;7(12):2683-2685.
176. Baek J, Lee MG. Oxidative stress and antioxidant strategies in dermatology. *Redox Report.* 2016;21(4):164-169.
177. Dunaway S, Odin R, Zhou L, Ji L, Zhang Y, Kadekaro AL. Natural antioxidants: Multiple mecha-nisms to protect skin from solar radiation. *Front Pharmacol.* 2018;9(APR).
178. Casagrande R, Marko M, Pawliczak R. Resveratrol and Its Derivatives in Inflammatory Skin Dis-orders-Atopic Dermatitis and Psoriasis: A Review. *Antioxidants (Basel).* 2023;12(11):1954.
179. Shen Y, Xu J. Resveratrol Exerts Therapeutic Effects on Mice With Atopic Dermatitis. *Wounds.* 2019;31(11):279-284.

References

180. Carlucci CD, Hui Y, Chumanevich AP, et al. Resveratrol Protects against Skin Inflammation through Inhibition of Mast Cell, Sphingosine Kinase-1, Stat3 and NF- κ B p65 Signaling Activation in Mice. Published online 2023.
181. Massart C, Giusti N, Beauwens R, Dumont JE, Miot F, Sande J Van. Diphenyleneiodonium, an inhibitor of NOXes and DUOXes, is also an iodide-specific transporter. *FEBS Open Bio*. 2014;4(1):55-59.
182. Lambeth JD. NOX enzymes and the biology of reactive oxygen. *Nat Rev Immunol*. 2004;4(3):181-189.
183. Lambeth JD. Nox/Duox family of nicotinamide adenine dinucleotide (phosphate) oxidases. *Curr Opin Hematol*. 2002;9(1):11-17.
184. Raad H, Serrano-Sanchez M, Harfouche G, et al. NADPH Oxidase-1 Plays a Key Role in Keratinocyte Responses to UV Radiation and UVB-Induced Skin Carcinogenesis. *Journal of Investigative Dermatology*. 2017;137(6):1311-1321.
185. Elbatreek MH, Mucke H, Schmidt HHHW. NOX Inhibitors: From Bench to Naxibs to Bedside. *Handb Exp Pharmacol*. 2021;264:145-168.
186. Augsburger F, Filippova A, Rasti D, et al. Pharmacological characterization of the seven human NOX isoforms and their inhibitors. *Redox Biol*. 2019;26.
187. Maley AM, Arbiser JL. Gentian Violet: A 19th Century Drug Re-Emerges in the 21st Century. *Exp Dermatol*. 2013;22(12):775.
188. Pona A, Quan EY, Cline A, Feldman SR. Review of the use of gentian violet in dermatology practice. *Dermatol Online J*. 2020;26(5).
189. Brockow K, Grabenhorst P, Abeck D, et al. Effect of Gentian Violet, Corticosteroid and Tar Preparations in Staphylococcus-aureus-Colonized Atopic Eczema. *Dermatology*. 1999;199(3):231-236.
190. Mukawera E, Chartier S, Williams V, Pagano PJ, Lapointe R, Grandvaux N. Redox-modulating agents target NOX2-dependent IKK ϵ oncogenic kinase expression and proliferation in human breast cancer cell lines. *Redox Biol*. 2015;6:9.
191. Akdis CA, Arkwright PD, Brüggen MC, et al. Type 2 immunity in the skin and lungs. *Allergy: European Journal of Allergy and Clinical Immunology*. 2020;75(7):1582-1605.
192. Li H, Zhang Z, Zhang H, Guo Y, Yao Z. Update on the Pathogenesis and Therapy of Atopic Dermatitis. *Clin Rev Allergy Immunol*. 2021;61(3):324-338.
193. Facheris P, Jeffery J, Duca E Del, Guttman-Yassky E. The translational revolution in atopic dermatitis: the paradigm shift from pathogenesis to treatment.
194. Jensen LE. Targeting the IL-1 family members in skin inflammation. *Curr Opin Investig Drugs*. 2010;11(11):1211.
195. Yano S, Banno T, Walsh R, Blumenberg M. Transcriptional responses of human epidermal keratinocytes to cytokine interleukin-1. *J Cell Physiol*. 2008;214(1):1-13.
196. Sims JE, Smith DE. The IL-1 family: regulators of immunity. *Nat Rev Immunol*. 2010;10(2):89-102.

References

197. Syed AK, Reed TJ, Clark KL, Boles BR, Kahlenberg JM. Staphylococcus aureus Phenol-Soluble Modulins Stimulate the Release of Proinflammatory Cytokines from Keratinocytes and Are Required for Induction of Skin Inflammation. *Infect Immun*. 2015;83(9):3428.
198. Macleod T, Berekmeri A, Bridgewood C, Stacey M, McGonagle D, Wittmann M. The Immunological Impact of IL-1 Family Cytokines on the Epidermal Barrier. *Front Immunol*. 2021;12:808012.
199. Jiang Y, Tsoi LC, Billi AC, et al. Cytokines: the diverse contribution of keratinocytes to immune responses in skin. *JCI Insight*. 2020;5(20).
200. Chambers ES, Vukmanovic-Stejić M. Skin barrier immunity and ageing. *Immunology*. 2020;160(2):116.
201. Guttman-Yassky E, Krueger JG, Lebwohl MG. Systemic immune mechanisms in atopic dermatitis and psoriasis with implications for treatment. *Exp Dermatol*. 2018;27(4):409-417.
202. Werfel T. The role of leukocytes, keratinocytes, and allergen-specific IgE in the development of atopic dermatitis. *J Invest Dermatol*. 2009;129(8):1878-1891.
203. Byrd AL, Belkaid Y, Segre JA. The human skin microbiome. *Nature Reviews Microbiology* 2018 16:3. 2018;16(3):143-155.
204. Wagner T, Gschwandtner M, Strajner A, et al. Establishment of keratinocyte cell lines from human hair follicles. *Sci Rep*. 2018;8(1):13434-13434.

8 Acknowledgements

I would like to thank all the people who supported me during my PhD studies. First of all, I would like to express my deep and sincere gratitude to my supervisor Hila Emmert for her trust, advice (personal and professional) and great support during my PhD journey. I am truly thankful for your supervision!

I would also like to express my thanks to Stephan Weidinger for providing me with the opportunity to engage in research within such a captivating field. I am grateful for the chance to work in his excellent lab and to contribute to studies of the highest quality.

Special acknowledgments go to my colleagues who shared the path of my PhD studies: Nicole, Jan, Irene, Rashmi, and Sina. Your presence in the office made the working environment doubly enjoyable. I also want to extend my gratitude to Inken, Elke, Steffi, Matthias, and Rob for fostering a pleasant working atmosphere.

A special note of thanks to Anke and Britta for their exceptional assistance in the lab and their unwavering moral support. I would also like to appreciate Ina Suhrkamp for sharing her knowledge and offering support.

I am deeply thankful to my family for their moral and financial support throughout my academic journey. Without you, this path would likely have been possible.

A heartfelt and special thanks to Moritz, Laura, Marta, Lena, and all my other close friends. Your unwavering support means the world to me, and I am truly grateful for your constant backing. Thank you all!